Exploring human skin explant models for inflammation and impaired wound healing

By Kelly Rebekah Arekion BSc (hons)

Supervised by: Dr Jelena Gavrilovic, Dr Damon Bevan

The degree of Master of Science by Research in Biomolecular Science
The University of East Anglia
School of Biological Sciences

November 2022
Word Count: 22,369

Table of Contents

Acknowledgements

Foremost, I wish to show my appreciation to the extensive support and guidance provided by Dr Jelena Gavrilovic throughout the course of my research, for her motivation, enthusiasm and continuous encouragement during the highs and lows of the difficult months. I would also like to thank Dr Damon Bevan for your patience and guidance throughout the completion of the practical components of my project and for sharing his advanced knowledge with me.

I am hugely grateful for the companionship provided by my fellow students: Ruby Driver, Maduri Satkunabalan, Oliver Dillon and Katie Griffiths. Our time together which although limited due to circumstances of the pandemic, was still greatly appreciated.

Lastly, a special thanks goes towards my partner Elie-André Pagna-Disso for his emotional support and encouragement, which made completion of this project possible.

Abstract

Diabetic foot ulcers (DFUs) are a leading cause of non-traumatic limb amputations and can have a severe negative impact on the quality of life of diabetic patients. The main cause of DFUs is inefficient wound healing which is a result of a combination of a number of characteristic symptoms of diabetes mellitus, including chronic inflammation, hyperglycaemia and decreased immune function. This project utilises a human skin *ex vivo* model to investigate the genes which may be differentially expressed in diabetic patients compared to healthy patients and their subsequent effects on wound healing of the skin. This could help to obtain a further understanding of the deregulation of the wound healing cascade that can occur as a result of the various abnormalities in homeostasis of the body in a diabetic patient. Through subjecting human skin explants to various stimulants that mimic diabetic conditions (chronic inflammation, hyperglycaemia and bacterial infection) microarray analysis, immunohistochemistry and qRT-PCR methods were used to investigate differential gene/protein expression in the stimulated skin compared to unstimulated controls. Various genes were found to be up/downregulated in this model. In particular, the genes indoleamine 2,3-dioxygenase (*IDO1*) and tryptophan 2,3-dioxygenase (*TDO2*) – which were selected as the main focus of this study, were found to be upregulated. The protein products of these genes; TDO2 and IDO1 are enzymes that are essential for the metabolism of the essential amino acid tryptophan through the kynurenine pathway. Through further analysis via literature mining, a potential correlation between these genes and wound healing was found. This was then tested using the TDO2 inhibitor 680C91 in a scratch wound healing assay using 3T3 mouse cells, which suggested that inhibition of TDO2 substantially decreases the rate of wound healing with an additional effect of altering glucose concentrations. These data suggest a possible correlation between TDO2 and diabetic wound healing.

Chapter 1: Introduction

1.1 Skin structure/function overview

Background

As the largest single organ, the skin is a vital component of the human body, providing both physical and physiological mechanisms which are essential for homeostasis. The skin is the body's primary defence barrier between the external and internal environment, protecting the body from UV radiation, pathogens, chemicals, mechanical injury and loss of important substances (Sahle et al., 2015; Yousef et al., 2020). It is also essential in protection from infection and regulation of temperature and water content (Boer et al., 2016). Once the skin is ruptured, the body becomes highly vulnerable to infection, thus the complex process of wound healing is essential to rebuild the skin's barrier function, defend against invading pathogens and eliminate foreign particles from the environment (Dąbrowska et al., 2018). The skin is composed of three layers; the epidermis, dermis and subcutaneous tissue (Figure 1-1). The epidermis is further subdivided into four layers of rapidly dividing keratinocytes which rise to the surface; where they are shed (Gordon, 2013). The underlying dermis provides nutrients and support for the epidermis. It is also where the hair follicles, fibroblasts and various glands reside. The blood vessels and nerves in this area allow sensation of touch and pain (Watkins, 2013). The lowermost layer is the subcutaneous tissue, where there is storage of adipose tissue (fat) as well as larger blood vessels, nerves and connective tissue. Here, body temperature is regulated, and the tissue acts as a cushioning for shock absorption to prevent injury (Gordon, 2013).

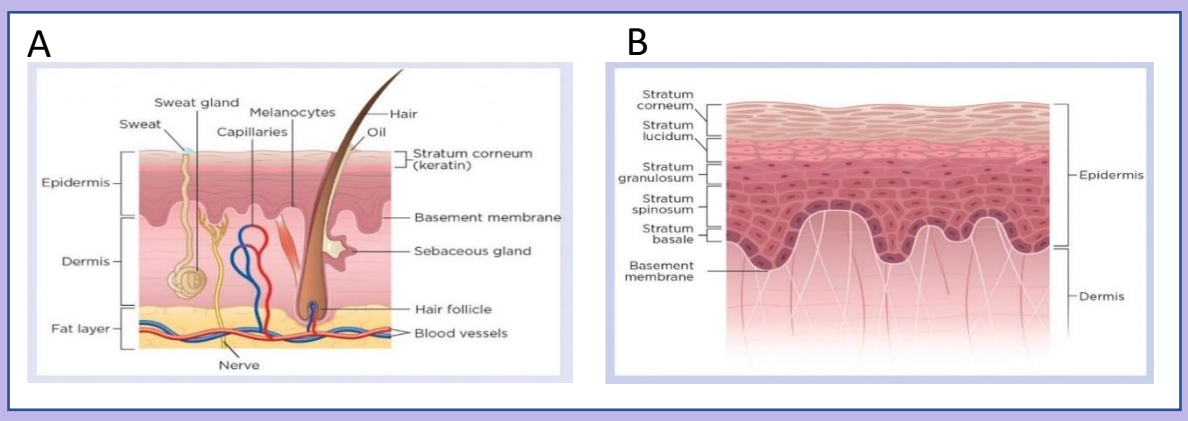

Figure 1-1*: Structure of the skin. (A) Cross-section through the skin showing 3 main layers – epidermis, dermis and subcutaneous tissue/fat layer. (B) Sub-layers of the epidermis. Images taken from* (Lawton, 2019).

Epidermis

The epidermis is composed of four sublayers: the stratum corneum, stratum granulosum, stratum spinosum and stratum basale (Figure 1-1A). The stratum corneum, which is important for skin barrier function is composed of lipid bilayers with embedded corneocytes. Lipid bilayers are made up of ceramides, free fatty acids and cholesterol (loss of these components is thought to contribute to the loss of barrier function). Desquamation (shedding of cells) occurs here, as it is the outermost layer (Sahle et al., 2015). Overall, the skin epidermis is a stratified epithelium that continuously renews itself, mostly made up of keratinocytes (90-95%), Merkel cells and melanocytes (Kanitakis, 2002). It is also home to various haematopoeitic lineages (Kobayashi et al., 2019).

Dermis

The dermis accounts for the majority of the thickness (3-5mm) of the skin, providing the skin's elasticity and tensile strength (Sahle et al., 2015) (Kolarsick et al., 2011). It is an amorphous connective tissue; a collagen/elastin matrix embedded with collagen-producing fibroblasts as the major cell type, but also consisting of macrophages, mast cells and other blood cells which enter via the vascular network within the tissue (Sahle et al., 2015) (Kolarsick et al., 2011). The function of this layer of the skin is to support the epidermis nutritionally and structurally (Powell, 2006).

Subcutaneous Tissue

The subcutaneous tissue, sometimes referred to as the hypodermis, is the layer of fat that lies beneath the dermis. This layer is made up of lobules of fat cells called lipocytes which have fibrous septa, large blood vessels and collagen running between them. The thickness of this layer varies depending on the area of the body. It also functions as an endocrine organ, producing the hormone leptin and converting hormones such as androstenedione into estrone by aromatase (Kolarsick et al., 2011). In addition, it acts as a storehouse of energy in the form of fatty acids and acts as an insulator for the body (Nguyen and Soulika, 2019).

1.2 Skin wound healing

In the instances wherein the skin barrier is compromised i.e., injury, the wound healing pathway is triggered to repair the laceration and the immune system is activated to fight infection from invading pathogens from the external environment.

There are four stages of wound healing: haemostasis, inflammation, proliferation and remodelling (Figure 1-2). These stages are overlapping but intricately timed, resulting in a dynamic, organised process in healthy conditions. Deregulation of this process in a diseased state leads to a cascade of events leading to delayed wound healing and thereafter formation of chronic wounds.

Haemostasis

Haemostasis is necessary for the preliminary closure of the wound to prevent blood loss and protect the vascular system (Velnar et al., 2009). This is achieved by vasoconstriction of the blood vessels surrounding the area of injury, to divert blood flow away from the wound and reduce the amount of blood loss (Phillips, 2000). Upon exposure to collagen from the damaged tissue, platelets in the blood are activated, and then aggregate and adhere to the damaged endothelium at the wound site (Baltzis et al., 2014). Activated platelets and damaged tissue also initiate the activation of the intrinsic and extrinsic coagulation pathways, respectively (Bass and Ellis, 2002). These pathways in conjunction facilitate the stabilisation of the fibrin clot (thrombus). The resulting thrombus is formed with the provisional extracellular matrix (ECM) as inactive fibrinogen which is converted into active fibrin (Baltzis et al., 2014; Bass and Ellis, 2002). The insoluble thrombus is composed of erythrocytes, leukocytes, activated platelets and the fibrin matrix (Walton et al., 2015). This provides scaffolding for infiltrating inflammatory cells in later stages (Gurtner et al., 2008; Zhao et al., 2016). In addition, the formation of a scab on the surface of the skin by dehydrated proteins in the serum temporarily provides protection from contaminants in the external environment. It also helps sustain internal homeostasis and creates a surface for cell migration upon wound closure in later stages (Phillips, 2000).

Inflammation

The inflammatory phase is essential for preventing infection, providing nutrients to the wound site and providing stimuli for wound healing (Phillips, 2000; Young and McNaught, 2011). Initiation of this phase begins with activation of the innate immune system. Nearby platelets and resident mast cells degranulate, inducing recruitment and adherence of leukocytes such as neutrophils and monocytes to the wound site (Baltzis et al., 2014; Koh and DiPietro, 2011). Platelets and leukocytes secrete pro-inflammatory cytokines, such as interleukin 1 (IL-1) and oncostatin M (OSM), which further prolong the inflammatory stage, (Baltzis et al., 2014; Zhao et al., 2016). These are the cytokines used in the work described in this thesis to mimic inflammation in the *ex vivo* models.

Initially, the recruitment of leukocytes is dominated by neutrophils (Zhao et al., 2016). Neutrophils enter the wound via diapedesis and secrete growth factors stimulating cell division and ECM degradation (Baltzis et al., 2014). In addition, they help kill invading bacteria by generating free radicals via the myeloperoxidase pathway, and subsequently phagocytose dead bacteria and matrix debris (Zhao et al., 2016).

Around 48 hours after the initial injury, the recruitment of monocytes into the wound site via nearby blood vessels is increased, and they mature into macrophages (Cristina De Oliveira Gonzalez et al., 2016). Macrophages can be classified into M1 and M2 classes. M1 macrophages are proinflammatory as they secrete cytokines that amplify inflammation, and they are primarily infiltrated into the wound in early stages of inflammation (Krzyszczyk et al., 2018). These macrophages debride the wound by phagocytosis of bacteria, debris, apoptotic cell fragments and damaged tissue components (Baltzis et al., 2014). Whereas M2 macrophages, which are subdivided into several different types, are anti-inflammatory cells which aid various healing processes such as angiogenesis and contribute to the resolution of inflammation (Krzyszczyk et al., 2018).

It is crucial for acute inflammation to undergo resolution to prevent further digression into the damaging effects of chronic inflammation. In healthy conditions, resolution of inflammation is well managed, consisting of termination of inflammatory processes such as cell infiltration and cytokine production as well as removal of present inflammatory cells and mediators through dilution of chemokines and apoptosis of immune cells. Abnormalities

that may arise in this highly controlled process may lead to the onset of chronic inflammation which can then trigger development of a range of diseases including type 2 diabetes (Chen et al., 2018).

In addition, in the late inflammatory phase, T-lymphocytes enter the wound site, modulating the activity of tissue remodelling (Baltzis et al., 2014).

Proliferation

This stage of wound repair occurs 2-10 days after the initial injury (Gurtner et al., 2008). The granulation tissue is formed in this phase while the skin's barrier function is restored (Demidova-Rice et al., 2012). The cellular activity in this stage is in response to the cytokines epidermal growth factor (EGF), vascular endothelial growth factor (VEGF) and transforming growth factor beta (TGF-β) (Zhao et al., 2016). These cytokines are produced by the anti-inflammatory M2 macrophages to resolve the inflammatory phase (Baltzis et al., 2014). Growth factors also activate fibroblasts which use the provisional matrix as a scaffold to

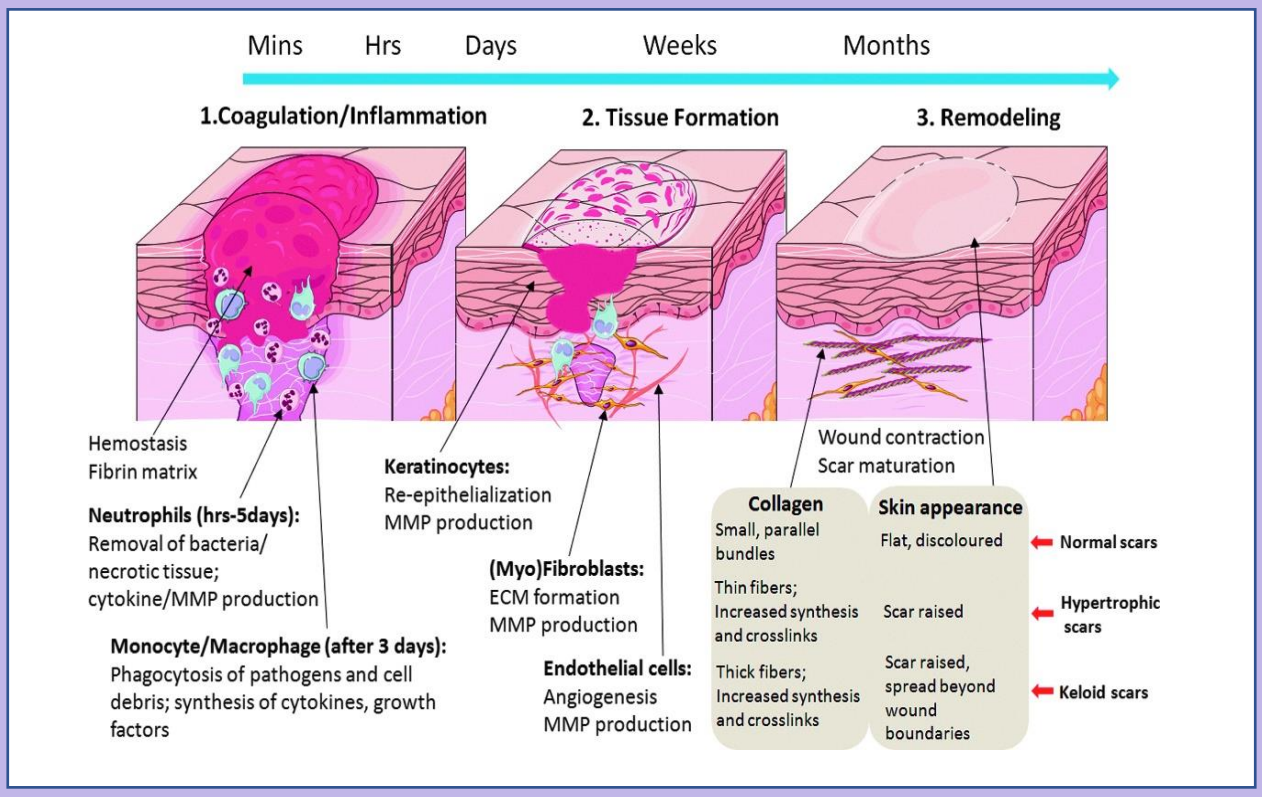

Figure 1-2: Wound healing pathway. Initial phases consist of coagulation/haemostasis phase, which overlaps with the inflammatory phase. This is followed by the tissue formation/remodelling phase and finally the remodelling phase. Image taken from (Xue and Jackson, 2015).

migrate into the wound where they produce collagen and ECM molecules (Baltzis et al., 2014). To begin the reepithelialisation process, the keratinocytes and epithelial stem cells proliferate and migrate over the injured dermis on top of a fibrin/fibronectin-rich provisional ECM (Gurtner et al., 2008; Zhao et al., 2016). This process requires sufficient blood supply for delivery of nutrients, therefore an efficient sprouting of capillaries from the existing vasculature into the wound site (angiogenesis) is necessary (Demidova-Rice et al., 2012). Angiogenesis and *de novo* formation of blood vessels from endothelial progenitor cells (EPCs) to re-vascularise the wound area is induced in response to tissue hypoxia and growth factors (such as hypoxia inducible factor (HIF) and VEGF) (Baltzis et al., 2014).

Remodelling

The last stage of wound healing is the remodelling stage, which occurs 2-3 weeks after the initial injury and can last for as long as one year (Gurtner et al., 2008). This phase comprises of wound contraction and matrix remodelling. Contraction of the wound is mediated by myofibroblasts which are contractile fibroblast cells that bring the wound edges together through the expression of smooth muscle actin–containing stress fibres (Zhao et al., 2016). These cells also interact with fibroblasts to organise the ECM which is mostly composed of collagen, forming the remaining scar tissue (Gurtner et al., 2008). Matrix-remodelling enzymes, particularly matrix metalloproteinases (MMPs) then break down the disorganised collagen so that the newly synthesised collagen can take its place (Demidova-Rice et al., 2012). The newly organised collagen is more closely bound so cross-linking between fibres is more efficient and the tensile strength of the wound is increased (Baltzis et al., 2014).

1.3 Impaired wound healing

There are various local and systemic factors that can lead to impaired wound healing. A few examples of these factors include the presence of reactive oxygen species (ROS), infection and chronic inflammation. All of these factors contribute to the development of chronic wounds due to negative impacts on the rate of wound healing.

Oxygen levels and ROS

One of the factors that can impair the wound healing process is the level of oxygen present in the wound area. It is critical for the wound to receive sufficient oxygen for effective wound healing since it is needed for cell metabolism through the production of adenosine triphosphate (ATP) (Guo and Dipietro, 2010). This factor is essential for most of the processes involved in wound healing, including protection from infection, angiogenesis, fibroblast proliferation, re-epithelialisation and wound contraction (Bishop, 2008). Therefore, if oxygen supply is limited e.g. due to defective angiogenesis, the wound healing efficacy is perturbed. There is also the critical effect of ROS such as hydrogen peroxide and superoxide in wound healing, which are useful cellular messengers involved in regulation of cell behaviour and angiogenesis (Guo and Dipietro, 2010). On the other hand, in chronic inflammatory conditions, an overproduction of ROS can be damaging to the local cellular environment, negatively impacting the rate of wound closure (Dunnill et al., 2015). This is a common observation in diabetic patients (Krishna Kolluru et al., 2012).

Hyperglycaemia

Hyperglycaemia has been shown to be correlated with poor prognosis in critically ill patients. Insulin is the only glucose-lowering hormone in the body, and it alleviates the detrimental effects of hyperglycaemia through its metabolic regulation, it also directly modulates inflammatory mediators and acts upon immune cells to enhance immunocompetence (Sun et al., 2014). Hyperglycaemic conditions in addition to lipid toxicity leads to the activation of protein kinase C which is regulated by calcium, diacylglycerol, hydrogen peroxide, phosphatidylserine and superoxide which are also all upregulated in response to hyperglycaemia (Park et al., 2019). The increase in production of ROS such as superoxide leads to prolonged inflammation in diabetic patients (Park et al., 2019). In addition, hyperglycaemia results in the non-enzymatic glycation of collagen and

other proteins, leading to the formation of advanced glycation end products (AGEs). Furthermore, AGEs decrease the solubility of the ECM and contributes to decreased levels of EPCs, impairing angiogenesis and vasculogenesis, which are key processes in wound healing (Baltzis et al., 2014). Importantly, AGEs induce the secretion of pro-inflammatory cytokines from inflammatory cells, leading to chronic inflammation (Pierce, 2001).

Infection

Another factor that can impact the rate of wound closure is infection. Persistent infections can slow down the wound healing pathway, therefore proper wound care is required to prevent this (Frykberg and Banks, 2015). Upon rupture of the skin following injury, exposure of the external environment can lead to invasion of pathogens which in turn triggers the activation of the immune response. This is known as inflammation.

The initial line of defence following infection is referred to as innate immunity. This consists of various nonspecific reactions which involve detection of highly conserved structures that are commonly found on the surfaces of micro-organisms e.g., pathogen-associated molecular patterns (PAMPs) or molecules released by host cells which are damaged i.e., damage-associated molecular patterns (DAMPs) (Strbo et al., 2014). Most DAMPs consist of cytosolic and nuclear proteins (Strbo et al., 2014). An example of a PAMP is the glycolipid known as lipopolysaccharide (LPS) (also known as endotoxin). This is a structural protein found in the outer membrane of most Gram-negative bacteria, acting as a permeability barrier while protecting the bacteria from environmental stresses (e.g., antimicrobial stresses) (Bertani and Ruiz, 2018). LPS stimulates the immune system since it is a common component of bacteria whereas it is not produced by cells of the host. There are several other examples of PAMPs, including double stranded RNA, and peptidoglycan, however LPS was used in the current study. The subsequent phase of the immune response is known as adaptive immunity. This is a more specific response consisting of humoral and cell-mediated responses, including activation of various leukocytes and production of antibodies (Strbo et al., 2014). Inflammation is therefore important for functional wound healing in healthy patients, however, it poses a risk when the inflammation becomes prolonged and chronic (Pahwa et al., 2021).

Chronic Inflammation

A chronic low-grade inflammatory state is a common feature in patients suffering from a wide range of diseases, including diabetes. Diabetic patients have the tendency to have a raised circulating level of inflammatory cells, which secrete pro- inflammatory cytokines, further increasing the infiltration of leukocytes such as neutrophils (Baltzis et al., 2014; Zhao et al., 2016). This excessive infiltration of neutrophils plays a major role in the pathophysiology of diabetic wound healing, due to their production of ROS. Excessive production of ROS eventually causes damage to the ECM and cell membrane. As a result, cell senescence occurs prematurely and the ECM breakdown further inhibits the wound healing while further promoting inflammation, ultimately leading to a self-sustaining cycle of inflammatory, inept wound healing (Zhao et al., 2016). Inflammatory conditions also induce the migration of monocytes into adipose tissue and polarisation of these cells into M1 pro-inflammatory macrophages instead of M2, which again, further increases the inflammatory state by inhibiting resolution of inflammation (Furuya et al., 2019). These effects may be the link between diabetes and impaired wound healing. Also, a previous study showed that inhibiting the IL-1β pathway in diabetic mice blocked proinflammatory cytokine upregulation and increased production of pro-healing factors and also caused proinflammatory macrophages to switch to healing-associated macrophage phenotypes (Mirza et al., 2013). Inflammatory cytokines also pay a large role; in healthy conditions they are important to facilitate modulation of the immune response by triggering a complex cascade of interactions, however in excessive amounts, cytokines can damage surrounding tissue and impair the wound healing process even further (Chen et al., 2018). Therefore, prolonged inflammation, which in part is caused by hyperglycaemia, results in delayed wound healing, eventually leading to development of diabetic foot ulcers (DFUs).

Diabetic Foot Ulcers

DFUs are a leading cause of non-traumatic limb amputation and one of the most devastating complications of diabetes (Alexiadou and Doupis, 2012). Worldwide, the percentage of DFU patients is 1.7%-11.9%, and the subsequent percentage of amputations is 1.3%-6.7% (Zhang et al., 2020) The onset of DFUs occurs due to neuropathy, which many diabetic patients suffer from, leading to absence of the protective sensation of pain in the feet (Wu et al., 2014). Thus, acute wounds in the skin often go unnoticed, so in combination with the

inefficient skin wound healing and defective immune system associated with diabetes, the patient becomes vulnerable to a major risk of infection (Brem and Tomic-Canic, 2007). The slow healing wound can become so severely infected, that the only solution is limb amputation (Zhang et al., 2020). The inability to metabolise glucose leads to a hyperglycaemic state in diabetic patients, which is a major causative factor to the impaired wound healing (Patel et al., 2019). Hyperglycaemia leads to prolonged inflammation; a key stage in the process of wound healing (Gao et al., 2015). In diabetes, each step can be dysfunctional in various ways (Patel et al., 2019).

Diabetic Impaired Wound Healing

DFUs usually originate from acute wounds that gradually become chronic wounds due to inefficient wound healing caused by various complications of diabetes (Baltzis et al., 2014). These chronic wounds often remain in a locked inflammatory state, preventing the next stage, proliferation, from taking place (Zhao et al., 2016). Some examples of diabetic complications that affect wound healing are hyperglycaemia, chronic inflammation, micro-/macrocirculatory dysfunction, hypoxia, autonomic and sensory neuropathy and impaired neuropeptide signalling (Baltzis et al., 2014). This study focuses on chronic inflammation.

1.4 The Kynurenine Pathway

The Kynurenine Pathway is a metabolic pathway that breaks down the amino acid tryptophan into kynurenine. It is the route by which the majority of this particular amino acid is decomposed, and it also pays a role in a variety of different physiological mechanisms, however some recent research has also revealed that deregulation of the pathway may contribute to the pathogenesis of multiple different diseases, such as liver disease and cancer (Ye et al., 2019).

Tryptophan

Tryptophan is an essential amino acid that is used to build proteins and also acts as a precursor for neurological compounds such as serotonin and melatonin. The kynurenine pathway is the pathway through which 95% of the essential amino acid tryptophan is metabolised (Davis and Liu, 2015). This pathway is also fundamental in the production of cellular energy through the biogenesis of NAD+ (Savitz, 2020). Furthermore, it is a key regulator of the immune system during an inflammatory response, as energy requirements are heightened in these instances (Savitz, 2020). There are several catabolic products of the kynurenine pathway (kynurenines), these are all diverse, performing different biological functions (Wardhani et al., 2019) including an anti-inflammatory role.

Kynurenines

Many of the kynurenines are neuroactive, so involved in inflammatory psychiatric illnesses (Savitz, 2020). Therefore, dysregulation or overstimulation of the kynurenine pathway may lead to activation of the immune system and build-up of neurotoxic compounds (Davis and Liu, 2015). Cytokines can elevate IDO1 expression (Baumgartner et al., 2019; Robinson et al., 2005). Upregulated metabolism of tryptophan through the kynurenine pathway leads to elevated levels of kynurenines, which inhibit T cell responses, leading to formation of tolerogenic dendritic cells (Bandeira et al., 2015). A study showed that although activation of the kynurenine pathway (via IFN-α) had no significant difference on tryptophan levels in cerebrospinal fluid, it led to inflammation as a result of the upregulation in levels of kynurenine, kynurenic acid and QUIN (Raison et al., 2010). Generation of QUIN is thought to be the link between the inflammatory response and the kynurenine pathway (Davis and Liu,

2015). The kynurenines are also involved in various physiological mechanisms, neuron excitability, host–microbiome signalling and the immune cell response (Ciapała et al., 2021).

TDO2, IDO1 and IDO2

The enzymes that catalyse the first rate-limiting step of this pathway are TDO2 and IDO1. These proteins were selected because TDO2 was the second most upregulated gene in response to inflammatory cytokines in the microarray, and IDO1 performs the same function as TDO2. There is also a third enzyme that catalyses this step - indoleamine 2,3-dioxygenase (IDO2), however, due to time restrictions as a result of the COVID-19 pandemic, this study will only focus on TDO2 and IDO1. In addition, very little is known about IDO2 and it was not listed as a gene up/downregulated in the microarray by >1.5 fold in either donor. Although, further research around the function of this protein would be useful.

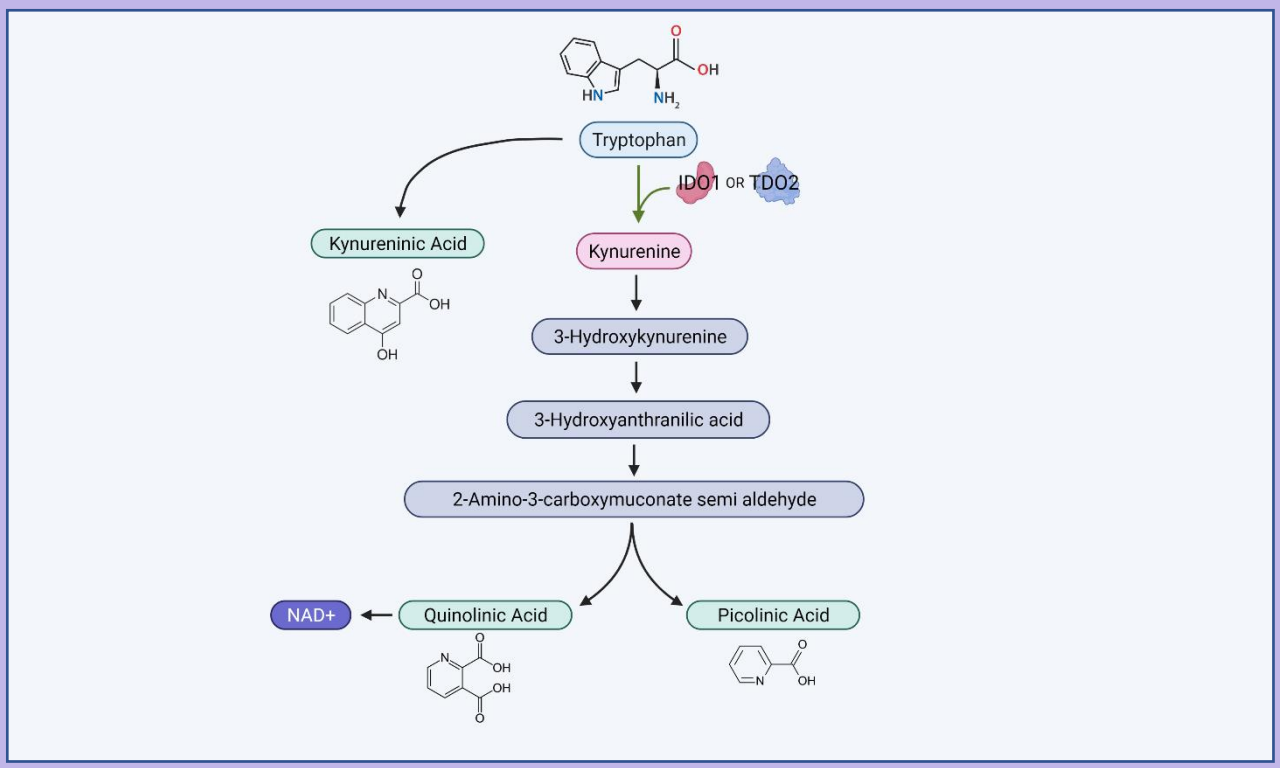

***Figure 1-3**: This pathway catalyses the metabolism of the amino acid tryptophan into kynurenine. The first, rate limiting, step of the pathway is catalysed by either TDO2 or IDO1 depending on the context. The remaining steps are catalysed by different enzymes. This pathway usually occurs in the liver. Created with BioRender.com with information from Davis and Liu (2015).*

The Pathway

The first step of the kynurenine pathway (Figure 1-3) is the TDO2/IDO1 mediated oxygenation of tryptophan, leading to the production of N-formyl-kynurenine. After the subsequent hydrolysation of N-formyl-kynurenine to kynurenine, the following enzymatically mediated steps of the pathway varies depending on the tissue type (Davis and Liu, 2015). In certain cell types such as in microglial cells (macrophages of the central nervous system), kynurenine is fed into the tricarboxylic acid cycle (Davis and Liu, 2015). Alternatively, in astrocytes (neuronal support cells) and other cell types, kynurenine is converted into kynurenic acid (Davis and Liu, 2015). A second dioxygenase is then used to open the aromatic ring (which came from the original tryptophan molecule) (Davis and Liu, 2015). Quinolinic acid (QUIN) is generated subsequently and another enzyme then determines whether QUIN will be used to form nicotinamide adenine dinucleotide (NAD) or undergo further metabolism. Both its substrate and product are unstable (Davis and Liu, 2015). The next enzyme in the pathway is α-aminomuconate-ε-semialdehyde dehydrogenase (AMSDH). Although very little is known about this enzyme, it is thought to separate further metabolism from the formation of picolinic acid (Davis and Liu, 2015). AMSDH is an aldehyde dehydrogenase and catalyses the first energy producing step of the pathway through production of NAD (Davis and Liu, 2015).

The Kynurenine Pathway and DFUs

Since the kynurenine pathway and its metabolites are linked to inflammation, and inefficient wound healing in diabetic wound healing is caused by chronic inflammation as a main factor, it was hypothesised that the enzymes IDO1 and TDO2 could be involved in the pathology of DFUs (Figure 1-6). In addition, since studies have linked lower tryptophan levels to slower wound healing (Bandeira et al., 2015) and higher kynurenine and QUIN levels to increased risk of infection and neurotoxicity (Savitz, 2020), the kynurenine pathway could contribute to the many factors that slow down wound healing in diabetic patients, leading to DFUs. Thus, using these enzymes as targets could potentially lead to development of new therapies for DFU patients.

1.5 TDO2

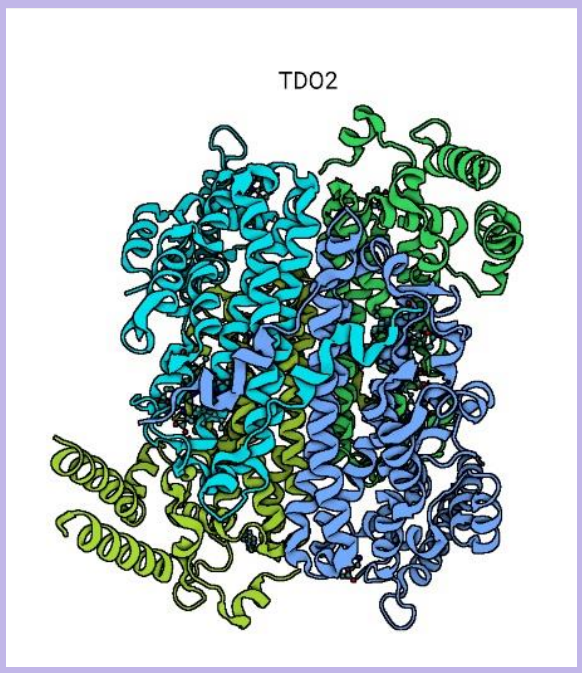

Figure 1-4: *Crystal structure of human TDO2 in complex with Tryptophan, Northeast Structural Genomics Consortium Target HR6161. PBD ID: 5TIA. PDB DOI: 10.2210/pdb5TIA/pdb.*

TDO2 is a 167 kDa homotetramer of four subunits each containing one heme group (Figure 1-4). It is primarily expressed in the liver to regulate tryptophan homeostasis and was formerly known as tryptophan pyrrolase (Davis and Liu, 2015). While previous literature on the role of TDO2 in wound healing is lacking, there have been a few studies that have shown a role for TDO2 in this aspect. Several studies have reported that TDO2 expression is correlated with cancer prognosis, these studies may also highlight the effect of TDO2 on wound healing since many of the processes involved in cancer metastasis are also important in wound healing, e.g. cell proliferation and migration (Novikov et al., 2016).

1.6 IDO1

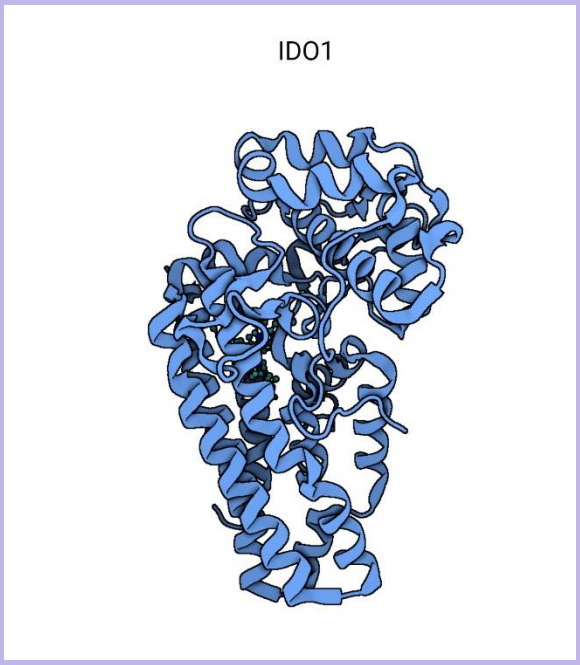

Figure 1-5: *Crystal structure of human indoleamine 2,3-dioxygenase 1 (IDO1) in complex with ferrous heme and tryptophan. PDB ID: 6E46. PDB DOI: 10.2210/pdb6E46/pdb.*

IDO1 is a 37 kDa heme-binding cytosolic enzyme that catalyses the oxidation of tryptophan as part of the first step of the kynurenine pathway (Song et al., 2018)(Sari et al., 2019). It exists as a monomer formed of two subunits connected by an interconnecting loop (Figure 1-5) (Orabona et al., 2012). IDO1 harbours a more relaxed specificity in comparison to TDO2, with the ability to act upon several substrates; L-tryptophan, D-tryptophan, D-5-hydroxytryptophan and several indoleamines (Davis and Liu, 2015) (Hayaishi, 1993). Induction of tryptophan catabolism in several tissues by IDO1 is often in response to bacterial products e.g. LPS and pro-inflammatory mediators e.g. TNF-α, IFN-γ (Bandeira et al., 2015). In particular, IFN-γ transcriptionally controls the expression of IDO1 by binding to the IDO1 promoter region (Fallarino et al., 2003) (Sorgdrager et al., 2019). Although the exact role of this enzyme is not yet entirely understood, it is increasingly being recognised as the link between the kynurenine pathway and the immune system (Davis and Liu, 2015). This stems from the effect of IDO1 on immune cells. For example, the IFN-γ effect on IDO1 is well understood in macrophages and dendritic cells (Sorgdrager et al., 2019). Dendritic cells that express IDO1 fail to undergo antigen presentation, differentiation into effector cells and clonal expansion as usual, but instead activated T cells undergo apoptosis, become anergic, or differentiate into T regulatory cells (Pakyari et al., 2019). However, in the presence of IDO1, the strong immunoregulatory phenotype is initiated and this stimulates multiple pathways within adaptive and innate immunity including the regulatory T responses. Ultimately, IFN-γ/IDO1 assists in the inhibition of micro-organism replication and protects against harmful chronic inflammatory responses.

1.7 Models for skin inflammation & Microarray experiment

The current study utilised human skin explants as an experimental model. There are many benefits of this model, and its use is continuing to improve since its first use dating back around 50 years ago (Reaven and Cox, 1965). Various recent studies have demonstrated the use of this model system today, as it is a good representation of the human response to various stimuli, which is a drawback of animal *in-vivo* models, and it does not present risks of in-human clinical trials (Orzalli, 2019; Khalil, 2018). However, one drawback of this model system is the inability to recruit immune cells to inflammatory sites due to the absence of the vascular system, and other organ systems. While it is an inexpensive model since the skin is donated by the hospital, it is rather difficult to obtain, and usually arrive in small sections, making large replications of experiments difficult. Receipt of new tissue is also unpredictable as it relies on patients having surgery in which excess skin is produced, which can be irregular, especially during the pandemic. However, overall, it is a well-recognised model for analysis of skin diseases.

Oncostatin M (OSM) is a pleiotropic inflammatory cytokine belonging to the gp130 (or IL-6/LIF) family of cytokines, which are all multifunctioning proteins involved in processes such as cell differentiation, proliferation, and immunology (Richards, 2013). OSM regulates activation of MAPK and JAK/STAT signal transduction pathways, which is induced via the only functioning receptor expressed on keratinocytes – the type II OSM-receptor (Simonneau et al., 2018). Due to the known functioning of OSM within keratinocytes of the skin as well as a previous experiment performed in the Gavrilovic lab which showed that human skin explants respond to OSM in combination with IL-1α (Bevan and Gavrilovic, unpublished data), this cytokine was selected as a cytokine in conjunction with IL-1α to mimic skin inflammation in experiments in this study.

Prior to this project, Dr Damon Bevan from Dr Jelena Gavrilovic's lab performed various experiments using this model which generated results that were used as a basis for this project (described in more detail in Chapter 2, Methods). Data generated from a microarray experiment comparing the gene expression of human skin explants with and without stimulation with inflammatory cytokines led to the selection of two key genes which are the main focus of this study. IL-1 and OSM were selected to act as inflammatory stimulants, and

differential gene expression was observed through comparison to unstimulated controls. This microarray was performed on donors with the anonymous identity codes “SLPL003” and “SPL004”. In particular, the inflammatory cytokines significantly up-regulated the expression of these genes, tryptophan 2,3-dioxygenase (TDO2) and (to a much lesser extent) indoleamine 2,3-dioxygenase (IDO1) which have key roles in the kynurenine pathway (Table 1-1).

Table 1-1: Microarray results obtained prior to this study, human skin explants from two donors caused increased expression of TDO2 and IDO1

DONOR	SPL003		SPL004	
Gene	Fold change	P value	Fold change	P value
TDO2	20.59	3.25×10^{-11}	8.97	7.74×10^{-11}
IDO1	1.71	0.00051	1.28	0.02

1.8 Hypothesis

The hypothesis of this study is that TDO2 and/or IDO1 is negatively correlated with chronic inflammatory wound healing (Figure 1-6).

This hypothesis that formed the basis of this study was conceived through literature mining. Firstly, it is a well-known fact that diabetic patients are characterised with a low-grade inflammatory state (Baltzis et al., 2014). Additionally, previous research on the enzymes of interest, TDO2 and IDO1 indicate that under inflammatory conditions TDO2 and IDO1 are upregulated, and this is consistent with the data obtained in the initial microarray experiment as well as previous research (Murakami et al., 2013). This could suggest that in diabetic patients, due to chronic inflammation, TDO2 (and IDO1 by association) would be more highly expressed (Tsalamandris et al., 2019). This upregulation could increase the activity of the kynurenine pathway, since these enzymes catalyse the first rate-limiting step of the cascade. As a result, since the pathway catalyses tryptophan, levels of this amino acid will be depleted. Some studies have shown that tryptophan accelerates the rate of wound healing, thus lower levels of tryptophan could (in theory) lead to a slower rate of healing (Bandeira et al., 2015). This could then be a contributing factor to the development of DFUs. At the same time, upregulation of the kynurenine pathway would lead to increased levels of kynurenines and QUIN – metabolites of the pathway. These have been previously linked to neurotoxicity and increased risk of infection by suppression of T cell response, both of which would eventually contribute to the development of chronic wounds and subsequent DFUs (Birner et al., 2017) (Terness et al., 2002). This is because infection of wounds impedes the wound healing process, and neurotoxicity could impact neuropathy which already exists amongst diabetic patients and leads to ignorance of wound's presence due to loss of pain, which would result in poor/absence of proper wound care (Baltzis et al., 2014).

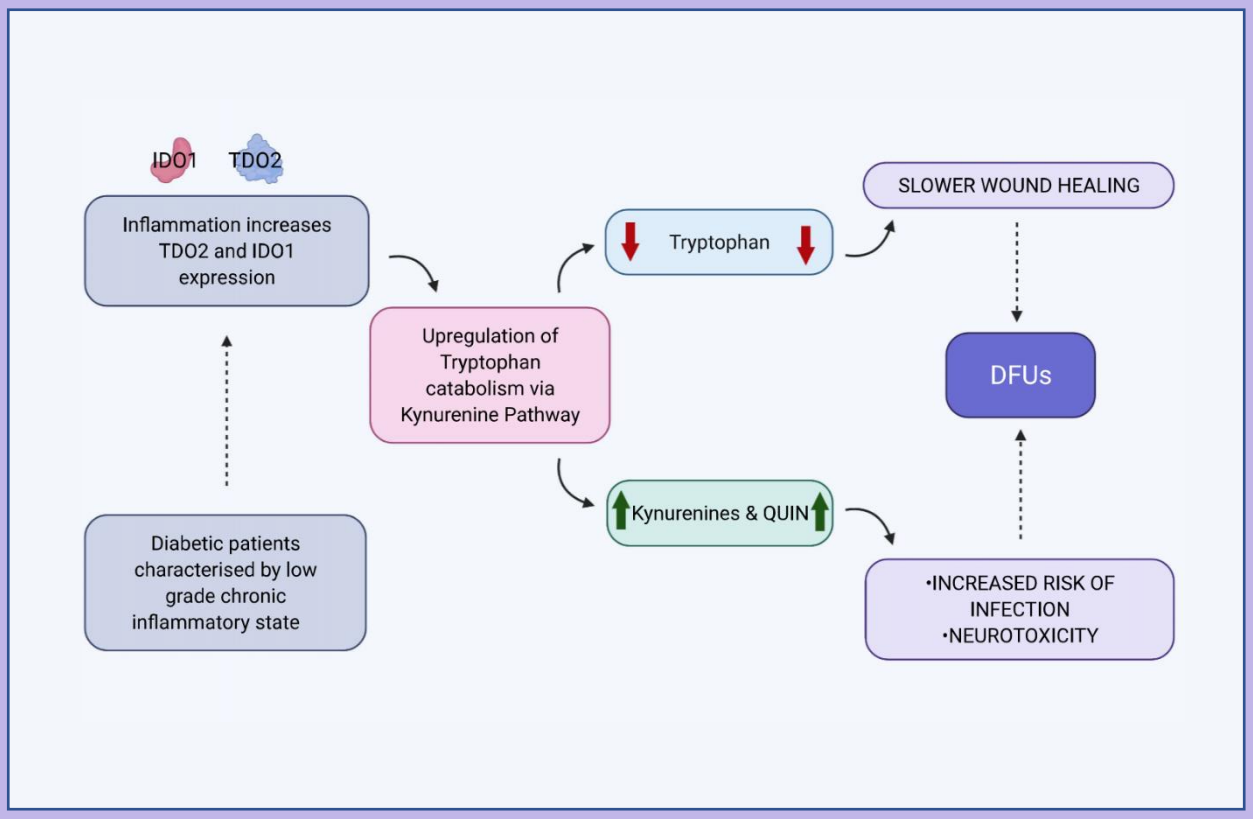

***Figure 1-6**: Hypothesis showing proposed connection between the kynurenine pathway and diabetic wound healing. Since diabetic patients are characterised by a low-grade inflammatory state* (Baltzis et al., 2014). *this would lead to an upregulation of TDO2 and IDO1 – as shown in the microarray and based on previous research* (Murakami et al., 2013). *This will then lead to an upregulation in the kynurenine pathway since these enzymes catalyse the first rate-limiting step of the pathway, depleting tryptophan levels and increasing levels of kynurenines and QUIN (Davis and Liu, 2015). Tryptophan has been linked to acceleration of wound healing in mice (Bandeira et al., 2015) and kynurenines/QUIN has been linked to increased risk of infection and neurotoxicity*(Feksa et al., 2008). *Lower tryptophan levels therefore may slow wound healing and the negative effects of kynurenines and QUIN could contribute to development of DFUs (Baltzis et al., 2014). Figure created with biorender.com.*

1.9 Aims of the study

The aims of the present study were to elucidate whether there is a role for TDO2 and IDO1 in aspects of skin wound healing due to the results of the microarray which revealed that TDO2 is highly upregulated in inflammatory conditions. Subjection of human explants to different conditions that mimic biological factors which cause impaired wound healing and subsequent analysis of differential gene expression can reveal novel mechanisms which could be potential targets for therapeutics.

Specific Thesis Aims:

- To analyse an existing microarray data set from Gavrilovic group's Norwich Skin Platform model in conjunction with the literature, with a focus on the kynurenine pathway
- To explore expression of key kynurenine pathway genes and proteins in skin explant models of inflammation and of impaired skin wound healing
- To explore the roles of IDO1/TDO2 in a model of fibroblast wound healing using a pharmacological approach

Chapter 2: Materials and Methods

2.1 Preparation of skin explants

Human abdominal skin tissue surplus to surgery (donated with ethical approval) was obtained with our clinical collaborators led by Prof Marc Moncrieff (NNUH). Each donor was given a code with the prefix SPL (skin platform) followed by three numbers for anonymity (see Appendix 2 for donor age information, some donor ages were unavailable due to reasons beyond our control). The following procedure was performed by Dr Damon Bevan prior to this study. The tissue was prepared for biopsy collection inside a sterile cabinet with sterile dissecting implements which were occasionally washed in 70% ethanol solution. To prepare for the dissection, the fat tissue was removed from the human skin tissue and placed on a board, epidermis side facing up. The tissue was stretched out as far as physiologically possible and pinned down to the board and the top of the tissue was wiped down clean with a sterile alcohol wipe. Biopsies of 6 mm diameter were then generated, which were subsequently washed in sterile PBS solution and transferred to EpiLife growth media supplement in individual wells of a 48-well plate. The biopsies were then left to equilibrate overnight in explant culture. The EpiLife growth media supplement contains the exact amount of growth factors and hormones essential for the growth of human epidermal keratinocytes. Furthermore, each bottle contains purified bovine serum, purified bovine transferrin, hydrocortisone, recombinant human insulin-like growth factor type-1 (rhIGF-1), prostaglandin E2 (PGE2), and recombinant human epidermal growth factor (rhEGF), although the concentrations of each growth factor are not provided by the manufacturer ("Thermo Fisher Scientific - UK", 2022).

2.2 Treatment of biopsies in varying conditions

Sterility was maintained at all times.

Explants from donors were then stimulated with various treatments to mimic different aspects of diabetes that affects wound healing i.e. chronic inflammation and bacterial infection in experiments “NSPinflam” (Table 2-1) and “NSPinfex” (Table 2-2), respectively (Figure 2-1). Diabetic conditions were also mimicked using differing levels of glucose, in which mannitol was used as an osmotic control (outlined in Table 2-3). This experiment was performed in line with the wound healing experiment, therefore EGF was incorporated as a positive control for wound healing. The blood glucose concentration in diabetic patients is usually approximately 2g/L ("NICE", 2020). This model uses a slightly higher concentration of 4.5g/L (25mM) to achieve maximum effect as has been described by others (Nowak et al., 2018). Mannitol was used as an osmotic control for glucose. Since the ‘high glucose’ treatment of the samples may alter the osmotic gradient, the ‘low glucose’ samples were treated with mannitol to mimic this effect, ensuring that any changes in gene expression were due to the stimulant rather than changes in the osmotic gradient. The tissue was then fixed in 4% paraformaldehyde and stored at 4°C until ready for wax embedding. To perform this, the tissue was transferred to individual embedding cassettes clearly labelled with corresponding experiment number and sample details. These were then processed through the following solutions with sufficient agitation throughout the process to ensure thorough mixing: 45 mins PBS, 45 mins PBS, 45 mins 50% EtOH, 45 mins 70% EtOH, 45 mins 95% EtOH, 45 mins 100% EtOH, 45 mins 100% EtOH, 45 mins Clearene, 45 mins Clearene, 45 mins paraffin wax, overnight paraffin wax. Once this is complete, the samples were embedded in disposable molds (15mm x 15mm x 5mm) and stored until sectioning.

To a 48-well plate, 500µL of supplemented EpiLife media to the required number of wells was added. Previously prepared biopsies were obtained and using fine tipped forceps carefully removed and transferred to the wells (one biopsy per well). This was repeated until the required number of biopsies had been added to the plate. The biopsies were incubated overnight at 37°C, 5% CO_2.

The stimulant in question (cytokine, glucose etc.) was then made up to the required concentration by dilution in EpiLife media (Table 2-1, 2-2 and 2-3) and used to replace existing media surrounding the biopsies and the plate was returned to the incubator. This is day 0.

1-day incubation protocol

After incubation for 24 hours after initial stimulation with stimulant, the biopsies were collected and processed the tissue biopsies ready for wax embedding as previously described to allow for further analysis.

5-day incubation protocol

For analysis at the 5-day period, the biopsies were re-stimulated with fresh media on day 3 and incubated until day 5 (120 hours post initial stimulation) when the tissue was collected and processed (Figure 2-1).

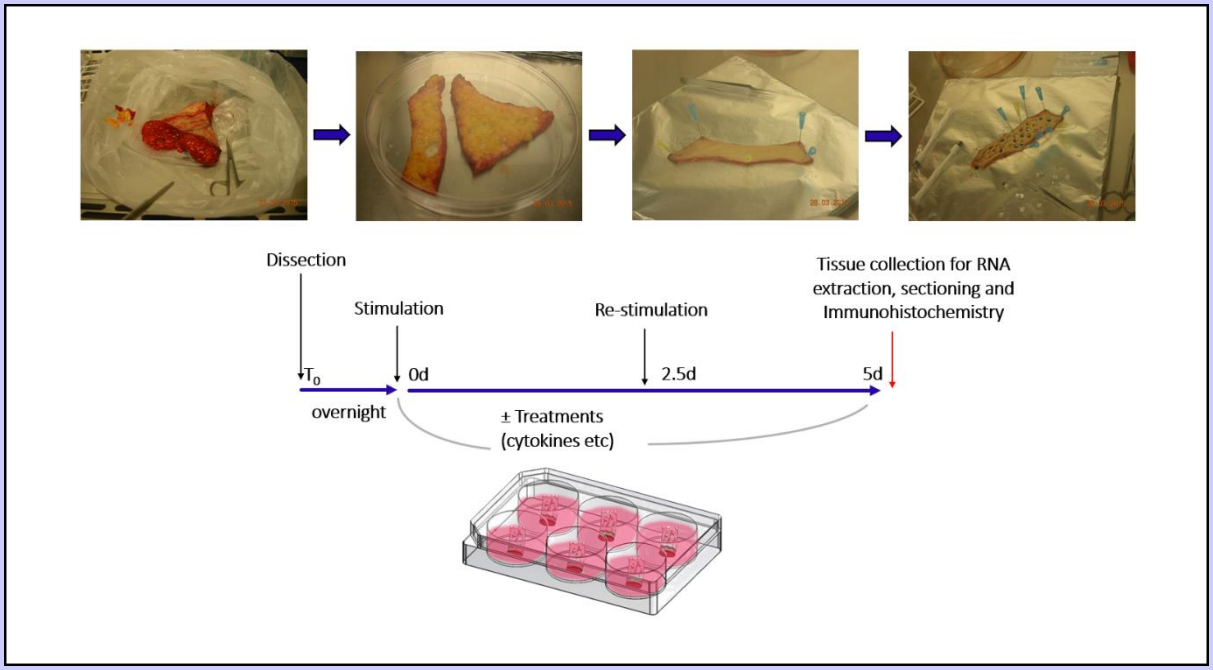

Figure 2-1: Preparation of human skin explants into 6 mm biopsies and subsequent treatment of the biopsies in different conditions to mimic different aspects of diabetes before performance of microarray. (Slide and procedure by Dr Bevan).

Table 2-1: "NSPinflam". Treatment conditions of the biopsies and their respective purposes for the inflammatory treated biopsies.

Treatment conditions	**To mimic:**
Control (unstimulated)	Healthy person
IL-1/OSM (conc) (IL-1 - 35ng/ml and OSM-100ng/ml)	Chronic inflammation as seen in diabetes

Table 2-2: "NSPinfex" Treatment conditions of the biopsies and their respective purposes for the LPS treated biopsies.

Treatment conditions	**To mimic:**
Control (unstimulated)	Healthy person
LPS (5µg/ml)	Infected wound
Bacteria	Infected wound

Table 2-3: Treatment conditions of the biopsies and their respective purposes for the hyperglycaemia conditioned biopsies.

Treatment conditions	**To mimic:**
Low glucose (1g/L)	Healthy person
High glucose (4.5g/L)	Hyperglycaemia as seen in diabetes
Low glucose (1g/L) + Mannitol (3.5g/L)	Healthy + Osmotic control
Low glucose (1g/L) + EGF (5µg/ml)	Healthy + Wound healing positive control
High glucose (4.5g/L) + EGF (5µg/ml)	Hyperglycaemia + Wound healing positive control
Low glucose (1g/L) + Mannitol (3.5g/L) + EGF (5µg/ml)	Healthy + Osmotic control + Wound healing positive control

2.3 Microarray

As mentioned previously, prior to this study, a microarray was performed on selected donors that were treated with/without inflammatory cytokines (IL-1 and OSM) as previously described. The donors used for this experiment were SPL003 and SPL004. The RNA extracted from the explants were taken from storage at -20°C and sent for microarray analysis at SourceBioscience.

The microarray data was collected and generated into a list of some thousands of genes which were up/downregulated in the samples in the inflammatory conditions, further research was then required to investigate these genes. This formed the foundation of this study, as this is where the two main genes of interest were selected. These two genes are *TDO2* and *IDO1*. *TDO2* was selected due to the large fold change seen between inflammatory cytokine treated skin compared to unstimulated skin - it had the second largest upregulation. *IDO1* was then selected following further literature research revealing that its protein IDO1 performs the same function as the TDO2 protein. qRT-PCR was used to confirm the results of the microarray. The expression of the protein product of these genes in the skin was then further investigated using immunohistochemistry (IHC) to confirm their potential involvement in diabetic wound healing.

The microarray results were analysed using string analysis ("STRING: functional protein association networks", 2022) and subsequent cluster analysis using The Markov Cluster algorithm (MCL clustering). The online software Genomatix was also used to find links between the up/downregulated genes in the microarray data and diabetes ("Genomatix Software Suite - Scientific Analysis of genomic data", 2022).

2.4 RNA extraction

RNA extraction from skin tissue samples was performed by Dr Damon Bevan in some cases. To extract the RNA from the tissue samples, the 6 mm biopsies were cut into small ~2 mm pieces and homogenised in 600 µL Trizol solution (in tissue lyser 2 x 8 mins @30 Hz). Rotation of the tube holder between the two stages ensured equal shaking. The homogenate was centrifuged at 14,000 g at 4 °C for 10 mins. The supernatant was then added to 200 µL chloroform, vortexed for 15 seconds and left at room temperature for 3-5 minutes. To separate the phases, the sample was centrifuged again for 15 minutes at 14,000g. The upper aqueous layer was removed and added to a tube containing 200 µL of 95% EtOH. The sample was mixed well and added to the RNeasy mini kit column and the column was spun for 30 seconds at 8,000 g. DNase digestion was then performed following Qiagen DNase kit instructions. This was then washed with 700 µL RW1 buffer from the Qiagen RNeasy kit and spun for 30 seconds 8,000g. Subsequently, 500 µL of RPE buffer was used to wash the sample twice before spinning again for 30 seconds at 8,000 g. The spin column was then replaced with a fresh collection tube and spun for 2 minutes at 8,000 g. The RNA was eluted from the column using 30 µL of RNase free water. The 30 µL of water was left for 3-5 minutes, allowing the water to be fully absorbed. Finally, the RNA content was measured using nanodrop and the samples were stored at -20 °C.

2.5 qRT-PCR

To validate the results obtained from the microarray, and to investigate expression of genes selected through literature analysis, qRT-PCR was performed, essentially as described in Bevan et al., (2016) on selected genes (Table 2-4) as it is a more accurate way of quantifying gene expression. RNA was extracted from skin explants from various other experiments that were performed prior to this study, comparing gene expression in skin explants treated with different stimulants to unstimulated controls. TaqMan qRT-PCR analysis was then performed on cDNA from reverse-transcribed mRNA from the samples to measure the changes in gene expression of the seven shortlisted genes in the different conditions generated. Analysis of 18s mRNA levels was used as a standard and was made up to 390 µL to generate 24 samples of 15 µL. The samples were made up to 360 µL for 24 samples of 15 µL. To each sample, TaqMan master mix, forward and reverse primers, the probe and water was added.

Donor explants included in this study were; SPL003, SPL004, SPL005 and SPL030. Data was collected at time points day 1 for SPL004 and SPL005 and day 5 for SPL003 and SPL004. All data was standardised to the average expression of TDO2 in the control samples to calculate the fold change relative to the unstimulated controls. SPL030 was treated with different concentrations of IL-1/OSM (high, medium and low) and data was collected at both time points (day 1 and day 5).
For SPL030, the "high IL-1/OSM" treatment was the same concentration as the treatment subjected to explants from donors SPL003, SPL004, SPL005 thus this data was combined with data from these donors to generate a graph of overall TDO2 expression at day 1 and day 5.

Table 2-4: Genes selected for qRT-PCR analysis and respective functions and UPL probes used.

Gene	UPL probe
Tryptophan 2,3-dioxygenase (TDO2)	#47
Indoleamine 2,3- dioxygenase (IDO1)	#42
Aryl Hydrocarbon Receptor (AhR)	#83
Interleukin 10 (IL-10)	#37
Suppressor Of Cytokine Signaling 3 (SOCS3)	#55
Solute Carrier Family 7 Member 7 (SLC7A7)	#55
Signal transducer and activator of transcription 3 (STAT3)	#43

2.6 Immunohistochemistry

The following method was performed on paraffin embedded skin sections that were sectioned to 5 µm slices using the HM 355S microtome and transferred onto a glass slide.

Initially, optimal antigen retrieval methods were tested in a preliminary experiment which compared the use of citrate buffer pH6, basic buffer pH9 and proteinase K. This revealed that the basic buffer pH9 produced the best results for the TDO2 secondary antibody. For IDO1, EDTA buffer at pH8 produced optimal results. Determination of the required concentration of secondary antibody was then established through trial and error using varying concentrations. This resulted in selection of the following concentrations of secondary antibodies: TDO2 – 1:200, IDO1 – 1:100.

To prepare the sections, the slides were dewaxed in clearene for 10 minutes, twice. Rehydration of the sections was performed in graded EtOH for 5 minutes each, followed by 5 minutes in 70% EtOH. The sections were then washed in PBS twice for 5 minutes each before addition to preheated antigen retrieval buffer in a water bath set at 95°C for 10 minutes. They were then left to cool for 20-30 minutes. The sections were then transferred into PBS to wash for another 5 minutes. Hydrophobic immedge pen was then used to outline the sections, before addition of 10% serum (diluted in PBS) which was left for 30 minutes at room temperature. The primary antibody was then diluted in the 10% serum in aliquots and vortexed. For all sections except the 'no primary antibody controls' , the 10% serum was removed and replaced with the primary antibody at 1:500 dilution. Subsequently, all sections were incubated overnight in a humidity chamber at 4°C. Afterwards, the slides were then washed three times in PBS for 5 minutes each. The secondary antibody at the desired concentration (diluted in PBS) was then added to the corresponding slides and left for 60 minutes at room temperature. After 45 minutes, the ABC kit was made up and allowed to stand for 30 minutes. Slides were then washed in PBS at the 60 minute mark, three times for 5 minutes each. ABC kit was then added to slides for 30 minutes at room temperature followed by three further washes in PBS for 5 minutes each. The alkaline phosphatase solution was then made up, which consisted of 2.5ml TRIS-HCl (100nM, pH8.2) + 25µL Levamisole (Vector) + 25µL TWEEN20 (10%) + 1 drop of reagents

1,2 and 3 from kit. The sections were then incubated in darkness for 20-30 minutes. One final wash in PBS was performed for 5 minutes followed by tap water for 1 minute to stop the reaction. The sections were then counterstained with 1:5 haematoxylin (diluted with distilled water) and rinsed in running water until the water ran clear. To dehydrate the sections, they were added to 70% and 100% EtOH for 2 minute each. DePex media was then used to mount the coverslips which were left to dry overnight before viewing under light microscope and images being taken on Axioplan 2 microscope.

2.7 Scratch Wound Healing Assay

Scratch wound healing assays were performed essentially as described previously (Martinotti and Ranzato, 2020). Mouse skin fibroblast cell line 3T3 was cultured in T75 flask and grown in Dulbecco's modified Eagles' medium (DMEM), low glucose DMEM was also used to grow a subset of cells. All cells were maintained at 37°C, 5% CO_2 and supplemented with 2% fetal calf serum (FCS). The cells were then transferred to a 24 well plate - 200,000 cells per well.

Dimethyl sulfoxide (DMSO) was used as a solvent to dissolve the TDO2 inhibitor 680C91 (as recommended by the manufacturer) to make up a 50mM stock which was subsequently used to make 3 different concentrations of the inhibitor. An intermediate solution at 2mM concentration was made by adding 8µL of the 50mM stock to 200µL of DMEM. The final concentrations (10µM, 20µM and 40µM) were made up by adding 20µL, 40µL and 80µL, respectively, to 4mls of media. To make the vehicle control (equivalent to the DMSO percentage contained in 20µM and 40µM inhibitor concentrations), 1.6µL or 3.2 µL (respectively) of pure DMSO was added to 4mls media.

To perform the scratch assay, 1ml of each treatment, in triplicate, were added to the wells of the previously prepared 24 well plate containing the confluent 3T3 cells. A 200µL pipette tip was then used to manually scratch down the centre of the well, creating a "scratch wound" which would then be left overnight under a timelapse microscope to analyse wound closure in a period of 24 hours.

Image J (Rasband, 1997-2018) was used to measure the wound areas by tracing the scratch wound area at each interval. The starting image was used as point 0, here the area of the wound is represented as 100%, this was then used as a basis for all subsequent images, whereas the area reduced in size as the scratch wound closed, the remaining area would be measured then represented as a percentage of the initial wound area. This was to prevent anomalies since the scratch wounds were performed by hand therefore the starting wound area varied from well to well.

2.8 Diabetic wounds

The following explant wound healing procedure was performed essentially as described previously (Brem and Tomic-Canic, 2007) with some modifications by Dr Damon Bevan. To prepare the PBS wash solution, 40 ml of PBS was transferred to a sterile 50 ml tube supplemented with 500 µL Gentamycin (final concentration 125 µg/ml) and 300 µL Amphotericin B (final concentration 1.87 µg/ml) to protect against contamination. All dissecting equipment was then sterilised (and occasionally washed in 70% ethanol throughout the process) and tissue was prepared for biopsy collection according to "Chapter 2, 2.1 Preparation of skin explants", generating biopsies with a diameter of 8 mm. To create the "wounds" in these biopsies, a fresh sterile 3 mm punch biopsy was used to make a partial full thickness biopsies, using gentle pressure and rotation in one direction to produce a shallow cut. Next, the skin biopsy was removed from the end of the punch and discarded. Residual fat tissue was removed from the remaining base of the biopsy, ensuring a flat dermal surface and this was transferred to a small bijou containing the PBS wash solution which was prepared previously. This was repeated with 6-8 biopsies which were then ready for "diabetic" treatments outlined in Table 2-5.

Table 2-5: Treatment conditions of the biopsies and their respective purposes for the hyperglycaemia conditioned biopsies

Treatment conditions	**To mimic:**
Low glucose (1g/L)	Healthy person
High glucose (4.5g/L)	Hyperglycaemia as seen in diabetes
Low glucose (1g/L) + Mannitol (3.5g/L)	Healthy + Osmotic control
Low glucose (1g/L) + EGF (5µg/ml)	Healthy + Wound healing positive control
High glucose (4.5g/L) + EGF (5µg/ml)	Hyperglycaemia + Wound healing positive control
Low glucose (1g/L) + Mannitol (3.5g/L) + EGF (5µg/ml)	Healthy + Osmotic control + Wound healing positive control

2.9 NSPinfex – proof-of-concept experiment

This proof-of-concept (PoC) experiment was unrelated to the main hypothesis.
It was hypothesised that the human skin explant model could be used as a surface to grow bacteria, which could be useful for various types of future experiments for example testing viability of different antiseptics. However, a method of growth, retrieval and counting bacteria must be established before any experiments could commence. Due to circumstantial events, i.e., the COVID-19 pandemic, these experiments never surpassed the PoC phase.

In order to investigate whether bacteria could grow on the skin explants and determine the optimal method of retrieval and quantifying the bacteria for future experiments; the following procedures were performed.

Growth of bacteria

Initially, to prepare the bacteria that would be added to the explants, an inoculation loop of growing *Staphylococcus epidermidis (S.epidermidis,* a gram-positive bacteria commonly found on the skin) was taken and added to 5ml of Tryptic Soy Broth (TSB). This was then incubated overnight at 37°C with shaking. The optical density (OD) of the bacteria was then measured using a spectrophotometer to ensure there were enough cells for $2x10^9$ cells per ml, equivalent to 10^7 cells per 5µL - an OD reading of at least 0.1 was therefore required. The exact OD of the culture was then used to calculate the volume needed for the required concentration. The aliquot was then spun down for 2 minutes at 6000rpm to pellet cells, the supernatant was removed, and the cells were resuspended in sterile PBS (or TSB in later experiments). Subsequently, the bacteria was serially diluted and plated in triplicate onto agar plates to verify the number of cells grown. The plates were incubated at 37°C and retrieved after 24 hours. In order to estimate the number of bacteria, the number of colony forming units (cfu) was counted by eye and recorded.

Retrieval of Bacteria

Growth of bacteria on the human skin explants and method of subsequent retrieval of bacteria was tested in order to elucidate practicality of further experiments. Previously cultured *S.epidermidis* was diluted to different concentrations and added to the surface of the explants, and left to grow overnight in the incubator at 37°C. The bacteria was then transferred to agar plates by two different methods; swab and vortex to assess which method of retrieval was optimal. This was then left to grow overnight and analysed at the 24-hour time mark. A total of twelve 8mm diameter biopsies were cut from the donated human skin explants with a biopsy tool as previously described (Chapter 2.1). The ability of skin explant surfaces to support the growth of added bacteria (10^7 bacteria/5µL drop). Initially, two different methods of bacterial retrieval from skin explants were evaluated: a 'swab', which consisted of using a cotton swab to swipe the bacteria off the surface of the explant and subsequently vortexing the cotton swab in an eppendorf tube filled with PBS; and 'vortex', which consisted of adding the whole explant into an eppendorf tube filled with PBS and vortexing the tube as detailed below. The bacteria retrieved in PBS samples from each explant were then measured by agar plate analysis. Three skin explants were plated in each of four separate wells, with or without added bacteria as indicated in Figure 2-2.

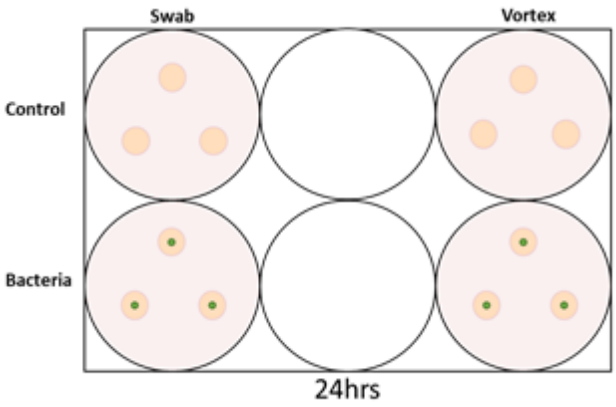

Figure 2-2: Experimental explant plate layout. 6 explants were cultured without were bacteria controls and 6 explants had 5µL of bacterial suspension (green dots) added to the centre of the epidermal surface.

A baseline swab was performed to quantify the amount of bacteria present on the explants prior to any addition of bacteria. This was obtained by swabbing the epidermis of the entire skin tissue with a damp swab dipped in 500µL aliquot sterile PBS. The end of the swab was then snapped off and added to the PBS aliquot. After vortexing the aliquot for 1 min, this was plated onto agar using 5µL neat and at 10-1 dilution (in triplicates) (incubated overnight at 37°C). The biopsies were then cut and arranged in wells containing 2ml EpiLife media (containing amphotericin B + CaCl2) as previously described. To bacteria explants, 5µL of bacterial suspension (containing approx. 10^7 cells) was added to the centre of epidermis, to control samples 5µL sterile PBS (or TSB in later experiments) was added. The explants were incubated for 24hrs at 37°C. A duplicate plate was incubated for 48hrs at 37°C.

For the 'swab' method, the explants were swabbed with a damp swab approximately 20 times each, the swab was snapped off and added to 500µL sterile PBS. This was then vortexed for 1 minute, serially diluted and dilutions 10^{-2} – 10^{-5} were plated in triplicate. For the 'vortex' method, each explant was placed in 500µL aliquot of sterile PBS and vortexing for 1min. After serial dilution, each sample was plated in triplicate dilutions 10^{-2} – 10^{-5} .

Time analysis of bacterial growth

In order to track the growth of the bacteria during the course of 4 hours and to establish the length of time it takes for the bacteria to reach the exponential phase of growth, the following experiment was performed. One loop of *S.epidermidis* was added to 5ml of TSB and this was incubated overnight with shaking. Different volumes (50µL, 250µL, 500µL) of the bacteria grown overnight was diluted into fresh glass flasks containing 5µL. The initial optical density (OD) of each concentration of bacteria was measured (neat) at time point 0 using a spectrophotometer. The bacteria were then incubated with shaking at 37°C and the OD was measured every hour. To prevent waste, the bacteria were diluted 1:10 in fresh TSB when the OD was measured.

2.10 Statistics

All statistics were performed on data using the SPSS software package. Statistics were performed within experiments as well as across experiments to check for consistency between individual experiments. Before testing validity of the null hypothesis in each experiment, tests for normality were performed on data using the Shapiro-Wilk test and equality of variance was measured using Levene's test for equal variance. Comparison of data between two data sets were analysed statistically using 2-tailed independent t-tests, where data was normally distributed, or Mann-whitney U tests where data was found to be not normally distributed. For comparison between multiple data sets (more than two), where normally distributed a One-Way ANOVA was performed using the Bonferri post-hoc test, otherwise an independent Kruskal Wallis test was performed.

Chapter 3: Human skin models- modulation of protein and gene expression results

3.0 Chapter 3 Introduction

Prior to this study a human skin explant model was established, mimicking inflammatory conditions (Bevan and Gavrilovic, personal communication). This data was analysed with a focus on the kynurenine pathway, as discussed in Chapter 1.

Chapter aims:

To analyse inflammation-regulated genes in existing microarray data from skin explant studies (Bevan and Gavrilovic data) combined with literature searches.

To assess the modulation of steady state mRNA levels in the human skin explant model system under different conditions. A series of qRT-PCR experiments were performed on RNA extracted from explants treated with various stimuli (See Appendix 2b for experiments summary). The change in gene expression between untreated and treated skin explants was quantified for the selected genes. Simulation of pathological conditions was accomplished through the use of IL-1/OSM inflammatory cytokines to mimic chronic inflammation; LPS to mimic bacterial infection and various glucose conditions to mimic hyperglycaemia, as described in Chapter 2.2.

3.1 Microarray and String analysis results

Prior to this study, a microarray experiment was performed on human skin explants (Bevan and Gavrilovic, unpublished data). Human skin explants were treated with inflammatory cytokines IL-1 and OSM alongside unstimulated control samples, a microarray was then performed on these explants, leading to the generation of a list of genes that were up/downregulated in response to stimulation with inflammatory cytokines. This was assessed by comparison of gene expression in the control skin explants to inflammatory cytokine-treated explants (See Chapter 2.3), from which a fold change was calculated. The data obtained from the microarray formed the basis of the current study. *TDO2* was selected as the main focus of this study due to the high fold change observed in both donors since it was the second most upregulated gene in both donors. String and gene ontology (GO analysis) was performed on genes that were up/downregulated with a fold change greater than 1.5. MCL clustering was then performed which revealed clusters of genes, indicating activation/deregulation of certain biological processes such as immune cell activation. Although TDO2 was not a part of any clusters in this string analysis, the large fold change was still perceived to be significant, thus it was chosen as the focus of this study. *IDO1* and other genes selected for investigation in this study were chosen based on literature analysis which revealed a connection to *TDO2*.

Upregulated genes

The largest cluster of genes obtained by string analysis of the upregulated genes from donor SPL003 were a group of 47 genes (Figure 3-2A). As expected, many of these genes are involved in immune cell regulation, including positive regulation of T cell costimulation and IL-1 receptor activity. (Table 3-1).

Similarly, the largest cluster (61 genes) obtained from the upregulated data from donor SPL004 contained genes involved in regulation of immune cells (Figure 3-2B)(Table 3-2).

Table 3-1: GO analysis of SPL003 upregulated largest cluster (only first three tables shown).

Biological Process (Gene Ontology)

GO-term	description	count in network	strength	false discovery rate
GO:2000525	Positive regulation of t cell costimulation	2 of 2	2.62	0.0016
GO:2000547	Regulation of dendritic cell dendrite assembly	2 of 3	2.44	0.0024
GO:0002408	Myeloid dendritic cell chemotaxis	2 of 3	2.44	0.0024
GO:0097029	Mature conventional dendritic cell differentiation	2 of 4	2.32	0.0034
GO:0001660	Fever generation	2 of 4	2.32	0.0034
				(more ...)

Molecular Function (Gene Ontology)

GO-term	description	count in network	strength	false discovery rate
GO:0031727	CCR2 chemokine receptor binding	2 of 6	2.14	0.0219
GO:0031726	CCR1 chemokine receptor binding	2 of 6	2.14	0.0219
GO:0004908	interleukin-1 receptor activity	2 of 7	2.08	0.0249
GO:0008009	Chemokine activity	11 of 48	1.98	4.41e-16
GO:0045236	CXCR chemokine receptor binding	4 of 18	1.97	4.15e-05
				(more ...)

Cellular Component (Gene Ontology)

GO-term	description	count in network	strength	false discovery rate
GO:1904724	Tertiary granule lumen	6 of 55	1.66	3.87e-06
GO:0035580	Specific granule lumen	4 of 62	1.43	0.0029
GO:0009897	External side of plasma membrane	8 of 331	1.0	0.00025
GO:0034774	Secretory granule lumen	6 of 324	0.89	0.0170
GO:0030141	Secretory granule	13 of 845	0.81	2.95e-05

Table 3-2: GO analysis of SPL004 upregulated largest cluster (only first three tables shown).

Biological Process (Gene Ontology)

GO-term	description	count in network	strength	false discovery rate
GO:0038172	interleukin-33-mediated signaling pathway	2 of 3	2.33	0.0036
GO:2000503	Positive regulation of natural killer cell chemotaxis	3 of 6	2.21	0.00014
GO:0060708	Spongiotrophoblast differentiation	2 of 4	2.21	0.0050
GO:0001660	Fever generation	2 of 4	2.21	0.0050
GO:2000501	Regulation of natural killer cell chemotaxis	4 of 9	2.15	4.63e-06
				(more ...)

Molecular Function (Gene Ontology)

GO-term	description	count in network	strength	false discovery rate
GO:0031726	CCR1 chemokine receptor binding	3 of 6	2.21	0.00036
GO:0004908	interleukin-1 receptor activity	3 of 7	2.14	0.00050
GO:0031731	CCR6 chemokine receptor binding	3 of 8	2.08	0.00062
GO:0031727	CCR2 chemokine receptor binding	2 of 6	2.03	0.0315
GO:0031730	CCR5 chemokine receptor binding	2 of 7	1.96	0.0376
				(more ...)

Cellular Component (Gene Ontology)

GO-term	description	count in network	strength	false discovery rate
GO:1904724	Tertiary granule lumen	6 of 55	1.54	1.93e-05
GO:0034364	High-density lipoprotein particle	3 of 29	1.52	0.0125
GO:0031093	Platelet alpha granule lumen	5 of 68	1.37	0.00059
GO:0035580	Specific granule lumen	4 of 62	1.32	0.0060
GO:0042581	Specific granule	5 of 159	1.0	0.0140

Downregulated genes

The largest cluster (32 genes) (Figure 3-2C) obtained from string analysis from the SPL003 microarray downregulated genes contained many genes involved in the structural integrity of the skin (Table 3-3). This implies that inflammatory cytokines could diminish the tensile strength of the skin. Previous studies have shown that OSM suppresses the expression of genes involved in epidermal differentiation, such as filaggrin, which is the second most significantly downregulated gene in this microarray with a fold change of 18.45 (p=0.00041) (Hänel et al., 2013).

The largest cluster (33 genes) (Figure 3-2D) in SPL004 downregulated genes also contained genes involved in cornification of stratum corneum, essentially implying disruption of the skin barrier in response to inflammatory cytokines (Table 3-4). The most downregulated gene in this microarray was filaggrin with a fold change of 23.37 (p=0.0000066).

Table 3-3: *SPL003 GO analysis of downregulated largest cluster (only first three tables shown).*

	Biological Process (Gene Ontology)			
GO-term	*description*	*count in network*	*strength*	*false discovery rate*
GO:0043163	Cell envelope organization	2 of 3	2.61	0.0158
GO:0018149	Peptide cross-linking	10 of 34	2.25	7.86e-17
GO:0070268	Cornification	17 of 113	1.96	2.63e-26
GO:0031424	Keratinization	30 of 226	1.91	3.29e-51
GO:0045104	Intermediate filament cytoskeleton organization	3 of 49	1.57	0.0462
	Molecular Function (Gene Ontology)			
GO-term	*description*	*count in network*	*strength*	*false discovery rate*
GO:0030280	Structural constituent of skin epidermis	4 of 14	2.24	5.70e-05
	Cellular Component (Gene Ontology)			
GO-term	*description*	*count in network*	*strength*	*false discovery rate*
GO:0001533	Cornified envelope	14 of 45	2.28	7.28e-25
GO:0045095	Keratin filament	4 of 92	1.42	0.0149
GO:0045111	Intermediate filament cytoskeleton	5 of 237	1.11	0.0239

Table 3-4: *SPL004 GO analysis of downregulated largest cluster (only first three tables shown).*

	Biological Process (Gene Ontology)			
GO-term	*description*	*count in network*	*strength*	*false discovery rate*
GO:0018149	Peptide cross-linking	8 of 34	2.14	2.89e-12
GO:0070268	Cornification	16 of 113	1.92	8.09e-24
GO:0031424	Keratinization	29 of 226	1.88	2.02e-47
	Molecular Function (Gene Ontology)			
GO-term	*description*	*count in network*	*strength*	*false discovery rate*
GO:0030280	Structural constituent of skin epidermis	4 of 14	2.23	6.49e-05
	Cellular Component (Gene Ontology)			
GO-term	*description*	*count in network*	*strength*	*false discovery rate*
GO:0001533	Cornified envelope	14 of 45	2.27	1.26e-24

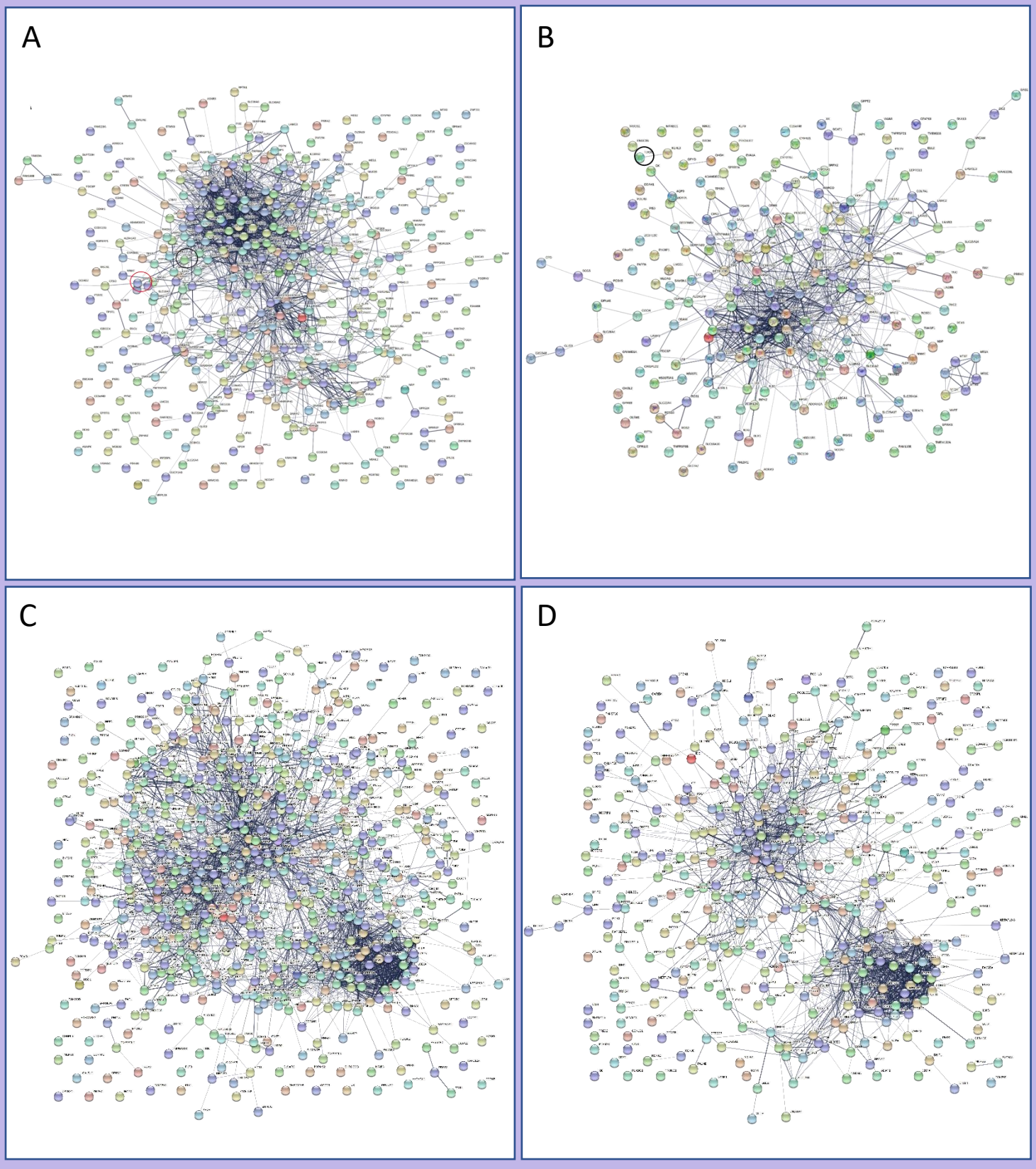

Figure 3-1: Differentially expressed microarray gene string network. *String analysis of data obtained from the microarray performed on explants from donors SPL003 (A&C) and SPL004 (B&D) consisting of genes which were upregulated (A&B) or downregulated (C&D) in response to inflammatory cytokine (IL-1/OSM) treatment by a fold change of >1.5X. Black circle =TDO2, red circle = IDO1.*

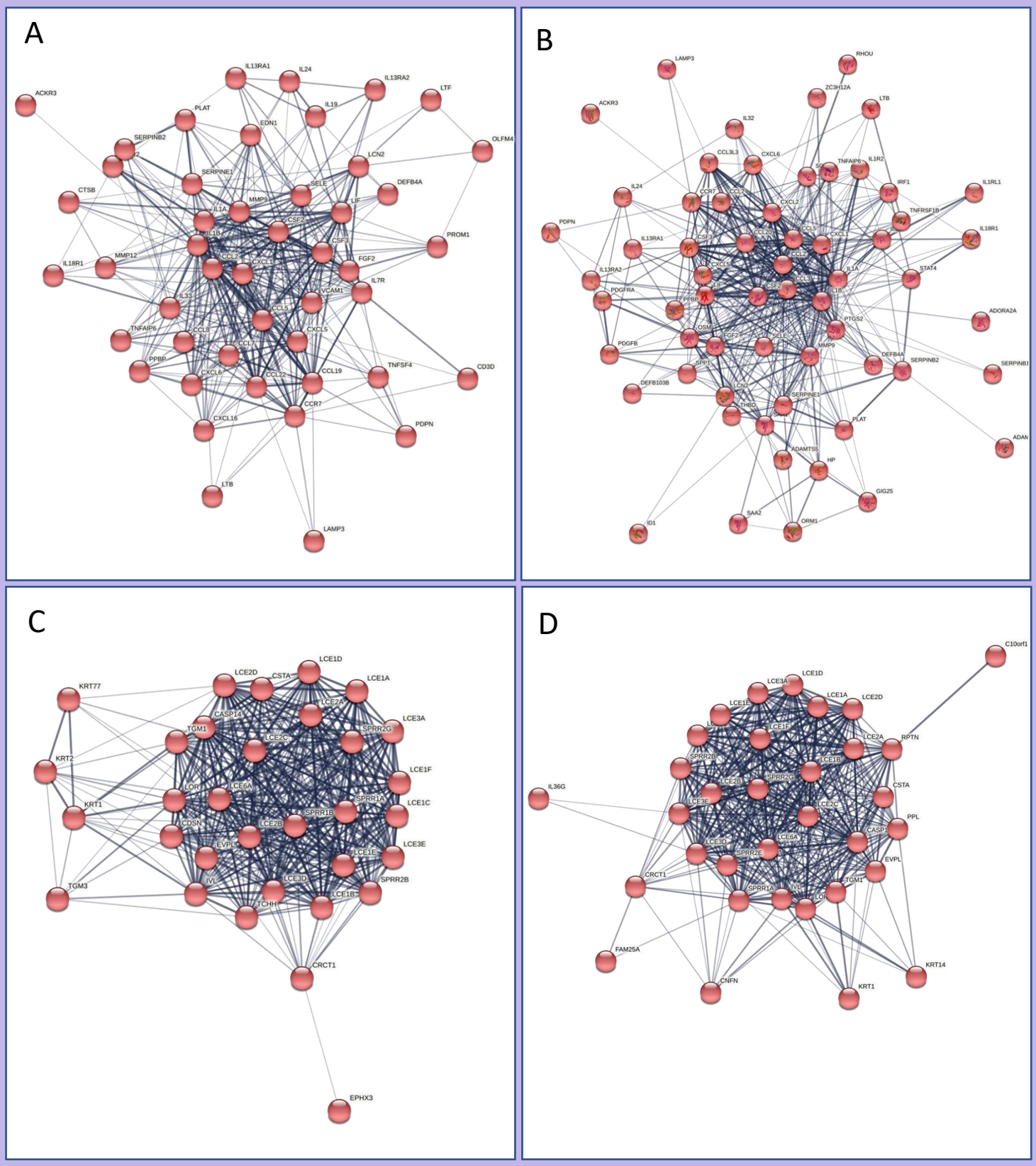

Figure 3-2: Largest cluster in each microarray network. *MCL clustering was used to find the largest cluster in each network from microarray data. (A) Largest cluster from SPL003 upregulated gene network containing 47 genes. (B) Largest cluster from SPL004 upregulated gene network containing 61 genes. (C) Largest cluster from SPL003 downregulated gene network containing 32 genes. (D) Largest cluster from SPL004*

Although the results of the string and GO analysis were interesting, due to the timeframe of this study, these genes were not studied further. Instead, specific genes were selected based on fold change and literature analysis, although these genes were not found to be in a cluster.

3.2 Microarray and Literature analysis results

In order to develop the analysis protocol, seven genes were identified as potential targets for therapy due to their involvement with the kynurenine pathway. *TDO2* was initially selected due to its significant upregulation in the human skin explant microarray (see Chapter 2.3) in response to IL-1/OSM (*TDO2* was the most highly upregulated gene expressed in one donor at approximately 20-fold) which inspired interest in the kynurenine pathway. The genes that were selected thereafter were chosen based on literature analysis of the TDO2 protein, to discover the interactions between the network of proteins that could possibly impact diabetic wound healing. This was decided based on background reading of TDO2; any gene that was mentioned to be involved with TDO2 in multiple studies was selected. A total of seven candidate genes were selected as a part of this study (Table 3-1). Parenthetically, use of the Genomatix software also revealed that TDO2 and IDO1 are connected in a larger pathway network (Appendix 1).

Table 3-5: Genes of interest and their respective functions

Gene	Function
TDO2	Metabolism of tryptophan
IDO1	Metabolism of tryptophan
AhR	Receptor to which TDO2 and IDO1 binds
IL-10	Anti-inflammatory effects
SOCS3	Promotes proteasomal degradation on IDO1
SLC7A7	Transports tryptophan into the cell
STAT3	Involved in IDO1 pathway

Expression of these genes was then investigated in the microarray data before further analysis by qRT-PCR and immunohistochemistry. Most of the genes were differentially expressed in the two conditions – unstimulated vs. IL-1/OSM treatment (Table 3-6). TDO2 was substantially upregulated in inflammatory conditions, with the greatest fold change among the two donors: 20.59 and 8.97. Both of these values had an extremely low p value, indicative of a high possibility of a direct link between inflammation and TDO2 expression. On the other hand, IDO1 had a very low fold change in both donors in comparison. AhR showed a trend towards downregulation in both donors, however this change was minimal

and only reached statistical significance in one of the donors. Of interest, SOCS3 was more than doubled in expression in inflammatory cytokine treated samples from both donors, and both of these results were statistically significant. This could be linked to the low expression of IDO1, since SOCS3 is an IDO1 inhibitor. IL-10, STAT3 and IL-6 showed no specific change in expression in response to the inflammatory cytokines.

Table 3-6: Genes of interest and their respective fold change in the microarray performed on donors SPL003 and SPL004 comparing gene expression in unstimulated skin samples to samples treated with inflammatory cytokines IL-1 and OSM

DONOR	SPL003		SPL004	
Gene	Fold change	P value	Fold change	P value
TDO2	20.59	3.25×10^{-11}	8.97	7.74×10^{-11}
IDO1	1.71	0.00051	1.28	0.02
AHR	-1.48	0.0053	-1.05	0.61
IL-10	-1.02	0.80	1.05	0.33
SOCS3	2.54	4.74×10^{-6}	2.76	2.06×10^{-8}
SLC7A7	1.58	0.0085	1.86	4.12×10^{-5}
STAT3	-1.22	0.012	1.16	0.0041
IL-6	1.04	0.81	1.32	0.038

Further analysis using STRING methodology revealed a number of interactions between the selected genes (Figure 3-3). All genes were connected to at least one other gene in the list by interactions that were derived from either; curated databases, experimentally determined, gene neighbourhood, gene co-concurrences, text mining, co-occurrence or protein homology. It also revealed possible connections to a few other genes, these included EGFR, EP300 and TCEB2. This provided a starting point for the following experiments, confirming a relationship between the proteins.

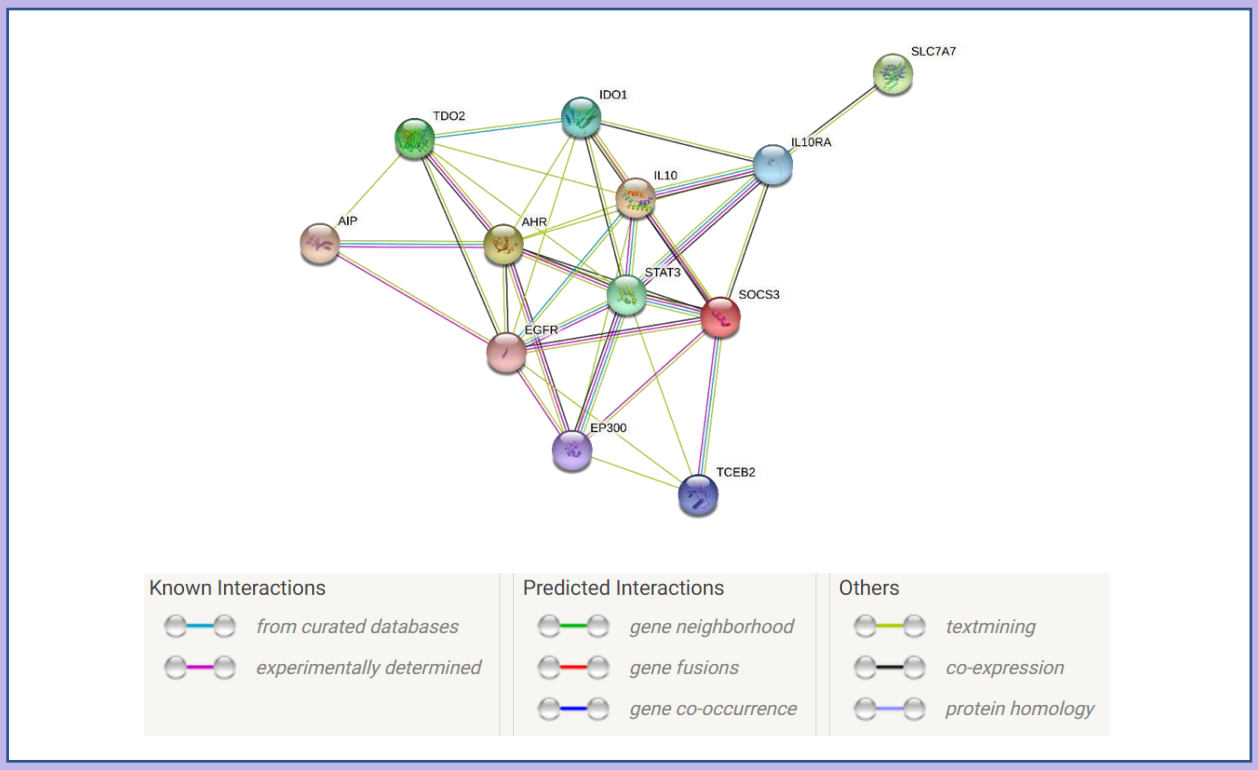

Figure 3-3: String network showing possible interactions between genes of interest based on previous research ("STRING: functional protein association networks", 2022).

3.3 Further analysis on selected genes – qRT-PCR results

In order to investigate the effects of different stimuli on the expression of the selected genes and confirm the results obtained from the microarray, qRT-PCR was performed on skin explants with the three different types of stimuli (inflammatory, bacterial and high glucose). The explants used in this investigation were the same donors used for the microarray experiment, SPL003 and SPL004, with the addition of several other donors. All data were obtained in triplicate from each donor at each condition and the RNA levels of TDO2 were quantified at day 1 and day 5 time points, although each skin explant was treated as an individual sample due to variations between dermal structures within each sample which could have an influence on gene expression i.e. no two explants are physiologically identical.

1. Chronic Inflammation

Inflammatory cytokines IL-1 and OSM (IL-1/OSM) were used to stimulate human skin explants over a 5-day period in order to partially mimic a more chronic inflammatory condition. Data is shown for individual donors and, where indicated results were combined across donors at each time point.

TDO2

Confirming the results obtained from the microarray, steady state levels for TDO2 mRNA showed a substantial increase in response the inflammatory cytokines IL-1/OSM, with almost a 200-fold upregulation in one particular donor - SPL003. All other samples also displayed the same pattern - significant increase in TDO2 expression in cytokine stimulated samples compared to unstimulated controls.

At day 1, each individual donor showed an increase in TDO2 expression in cytokine treated samples compared to unstimulated controls, though this change was not statistically significant for any of the within-donor comparisons. However, combined results from the donors did show a significant, 18-fold increase ($p < 0.001$) in TDO2 expression across all donors in the cytokine stimulated samples relative to unstimulated samples (Figure 3.4G).

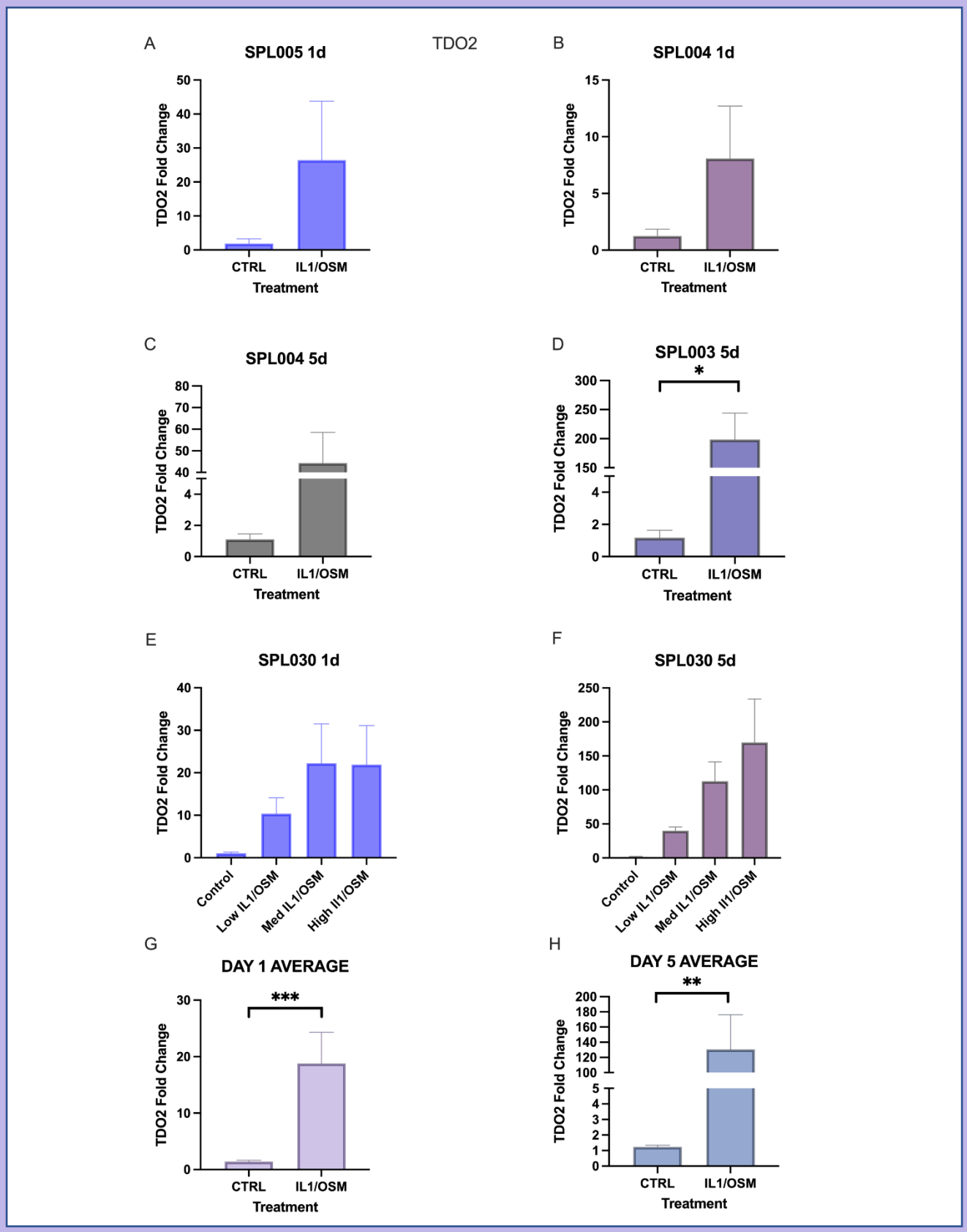

Figure 3-4: TDO2 gene expression is stimulated by IL-1/OSM. Relative fold change of TDO2 expression in inflammatory cytokine treated skin explants from four individual donors (A-F) and average values compared for 3 donors (G,H): (A) donor SPL003 at day 1, (B) SPL004 at day 1 and (C) day 5 (D) SPL005 at day 5. Dose response effect of cytokines was observed using 3 different concentrations of IL-1/OSM in donor SPL030 at day 1 (E) and day 5 (F). (G,H) All data was standardised to unstimulated control samples from each donor and mean values compared across donors at each day. Note that the data obtained from explants treated with the "high" concentration of IL-1/OSM from donor SPL030 was used in this combination of data as this was the same concentration used for other donors. n=3 donors 2-tailed independent t-test on all data where normal distribution was confirmed by Shapiro-wilk test. Mann-whitney U test performed on data that were not normally distributed. For multiple comparisons a One-way ANOVA was performed with Bonferri post-hoc test. (p<0.05, **p<0.01, ***p<0.001).*

This large increase in TDO2 steady state mRNA levels was then further elevated at day 5, with an average increase of 130-fold across all donors ($p < 0.01$). In the individual donors, although all showed an increase in expression, only the change in SPL003 was significantly different (Figure 3.4H; $p < 0.05$).

To conclude, TDO2 is highly responsive to inflammatory cytokines especially in SPL003, showing a large upregulation in all donors.

IDO1

IDO1 expression was upregulated in all donors upon stimulation with IL-1/OSM at least 3-fold (Figure 3-5). For SPL004, samples were taken at both 1 day and 5 days, although there was no significant difference between gene expression of IDO1 in the day 1 control and treated samples and their respective samples on day 5. This suggests that the effect of cytokines on IDO1 expression may be direct and sustained for a period of time.

In some donors, IDO1 could not be detected as some reached the 40-amplification cycle threshold and in many cases, the Ct values were greater than 35 cycles (data not shown). It

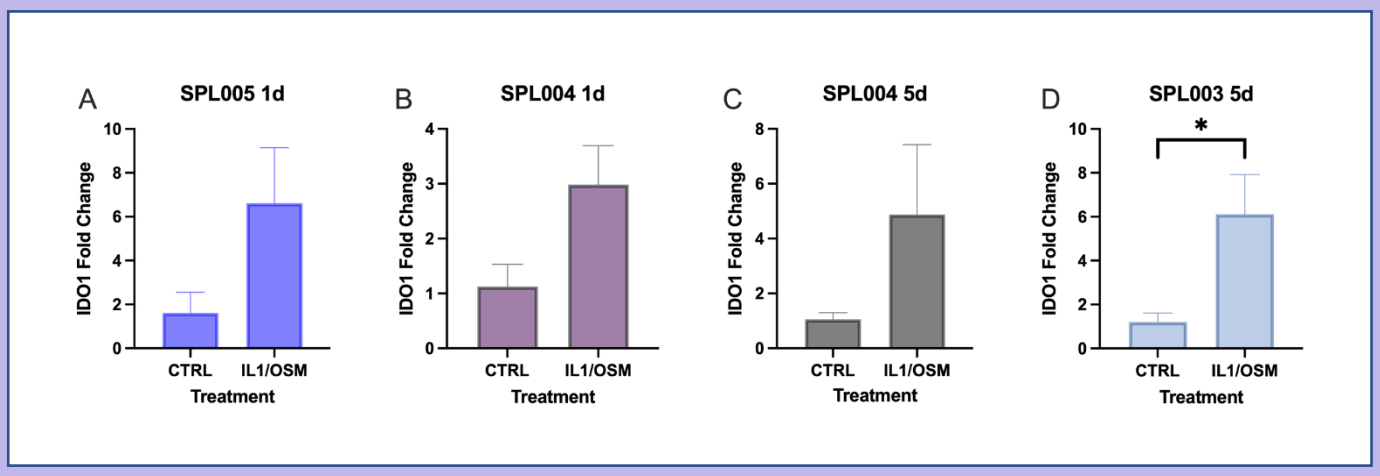

Figure 3-5: IDO1 is stimulated by IL-1/OSM, but to a lesser extent than TD02. *Relative fold change of IDO1 expression in inflammatory cytokine treated skin explants from four individual donors compared to unstimulated controls: (A) donor SPL003 at day 1, (B) SPL004 at day 1 and (C) day 5 (D) SPL003 at day 5. 2-tailed independent t-test on all data where normal distribution was confirmed by Shapiro-wilk test. Mann-whitney U test performed on data that were not normally distributed. For multiple comparisons a One-way ANOVA was performed with Bonferri post-hoc test. (* p<0.05, **p<0.01, ***p<0.001).*

was therefore possible that IDO1 is either very lowly expressed in the skin explants or possibly not expressed in some instances. Thus, it was not possible to plot all data, however some of the data was plotted to detect any minor changes in expression.

At day 1, both donors SPL005 and SPL004 showed an increase in expression of IDO1 upon stimulation with inflammatory cytokines IL-1/OSM however this was not a statistically significant change in either donors, so it was concluded that these inflammatory cytokines do not affect IDO1 expression at day 1 in skin (Figure 3-5 A & B).

Although IL-1/OSM treatment subjected to explants from the donors SPL004 and SPL003 at the day 5 time point also showed an increase in IDO1 expression, these changes were only found to be statistically significant in SPL003.

For SPL030, the samples were treated with three different concentrations of inflammatory cytokines. At day 1, no response to IL-1 and OSM was seen in donor SPL030, at all concentration levels. In addition, when standardised to day 5 control samples, there was no significant difference between the control group and any concentration of IL-1 and OSM in SPL030 treated samples. However, when standardised to day 1 control (unstimulated) group's average expression, the fold change at day 5 compared to day 1 samples were found to be significant at all concentration levels. However, this change seen was a downregulation in expression, which is the opposite of the expected result based on the results of the previous experiments.

The data from SPL004, SPL005 and SPL030 (Control and 'High' IL-1/OSM) at day 1 were collated to investigate the overall effect of IL-1/OSM treatment on the samples across all donors (data not shown due to high Ct values). The IL-1/OSM treated samples increased their expression of IDO1 by approximately 3.5-fold on average, which was a statistically significant different result with a p value of 0.031. Similarly, at day 5, the combined data from donors SPL003, SPL004 and SPL030 revealed that the inflammatory treated samples fold change reached statistical significance (p=0.004) (data not shown).

Ultimately, IDO1 mRNA expression in the skin samples was low, however, there was some induction seen in expression as a result of IL-1/OSM stimulation in some cases but this is a small immediate effect that, by day 5 is no longer observed and overall expression of IDO1 at this time point is even lower. This could be a result of inefficient probes and primers; future research could explore use of alternatives.

Other genes

Due to time restrictions, the remaining genes were only tested in donor SPL030. This donor was treated with varying concentrations of IL-1/OSM (high, medium and low) and gene expression was quantified at time points day 1 and day 5 (Table 3-7) (Figure 3-6).

Table 3-7: *Results obtained from qRT-PCR experiment on chronic inflammatory treated human skin explants compared to unstimulated controls (NS=not significant, ND=not determined). Average refers to the statistical significance of the difference between results of the combined mean results from each experiment.*

GENE	SPL003 5d IL-1/OSM	SPL004 5d IL-1/OSM	SPL004 1d IL-1/OSM	SPL005 1d IL-1/OSM	SPL030 IL-1/OSM	AVERAGE
IDO1	Upregulated (p=0.05)	Upregulated (NS)	Upregulated (NS)	Upregulated (NS)	Upregulated (NS)	Upregulated (1d p=0.031, 5d p=0.002)
TDO2	Upregulated (p=0.049)	Upregulated (NS)	Upregulated (NS)	Upregulated (NS)	Upregulated (NS)	Upregulated (1d p=0.000165, 5d p=0.003)
AhR	ND	ND	ND	ND	Upregulated (p=0.017)	ND
IL-10	ND	ND	ND	ND	Upregulated (p=0.01)	ND
SOCS3	ND	ND	ND	ND	Upregulated (1d)	ND
SLC7A7	ND	ND	ND	ND	Upregulated (5d)	ND
STAT3	ND	ND	ND	ND	ND	ND

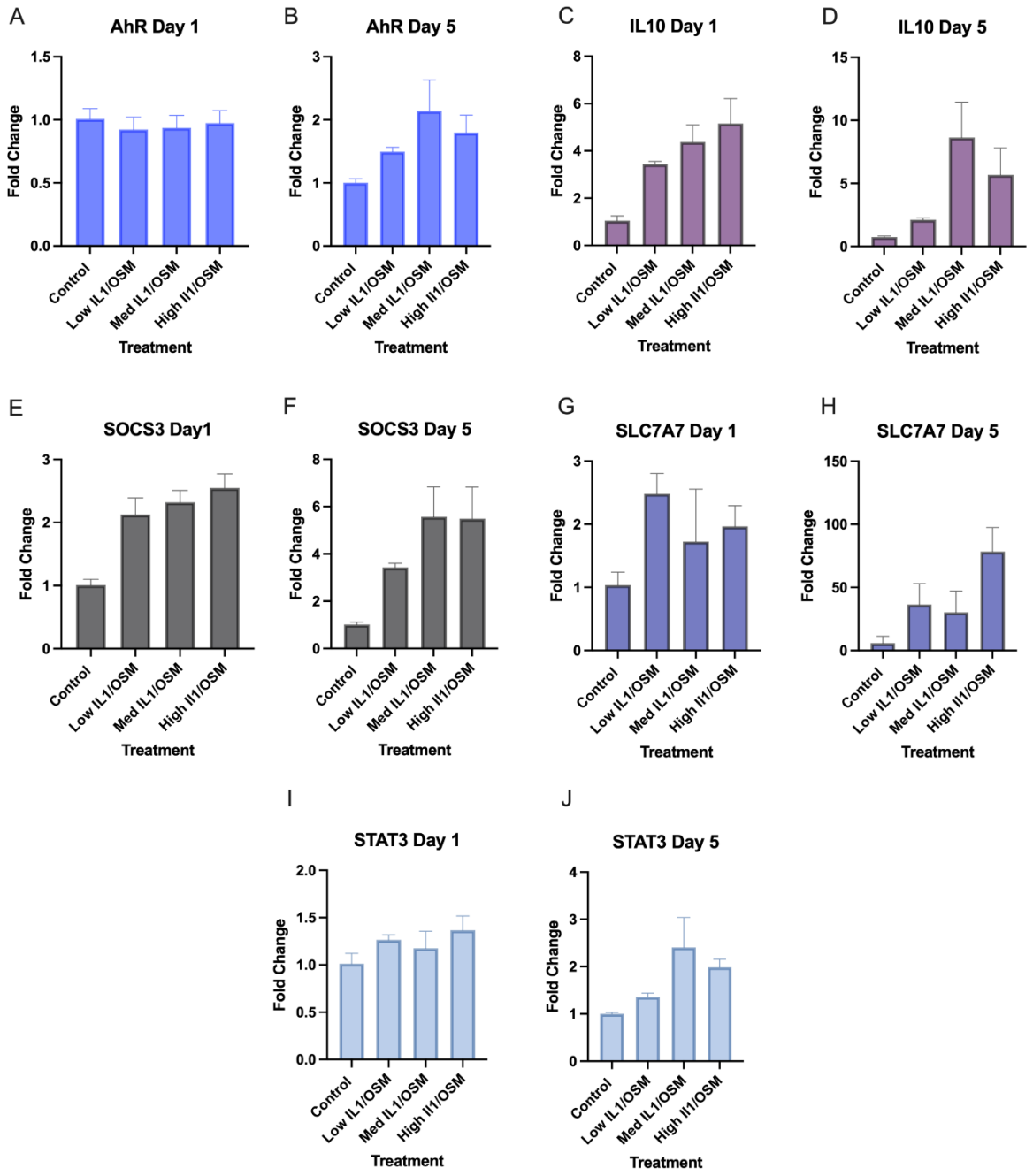

***Figure 3-6**: Genes is selected list showed varied responses to IL-1/OSM stimulants.* *Relative fold change of expression of candidate genes: (A-B) AhR, (B-C) IL-10, (E-F) SOCS3, (G-H) SLC7A7 and (I-J} STAT3 in donor SPL030 which was treated with 3 different levels of inflammatory cytokines IL-1/OSM.*

2. Hyperglycaemia and Wound Healing

DFUs are worsened due to hyperglycaemic conditions within the bloodstream of diabetic patients. This was mimicked in the "diabetic" experiment using varying levels of glucose, mannitol as an osmotic control and EGF as a positive control (Table 3-8) (Figure 3-7).

Table 3-8: Results obtained from qRT-PCR experiment on diabetic conditioned human skin explants compared to unstimulated controls (NS=not significant, ND=not determined). Average refers to the statistical significance of the difference between results of the combined mean results from each experiment.

GENE	SPL009	SPL010	SPL035	SPL011	AVERAGE
IDO1	ND	ND	ND	ND	ND
TDO2	NS	NS	Low glucose – Low glucose + EGF Upregulated (p=0.016)	NS	NS
AhR	NS	NS	NS	NS	NS
IL-10	NS	NS	NS	NS	Low glucose + Mannitol / Low glucose + Mannitol + EGF (p=0.031)
SOCS3	NS	NS	NS	NS	NS
SLC7A7	NS	NS	NS	NS	NS
STAT3	NS	NS	NS	NS	NS

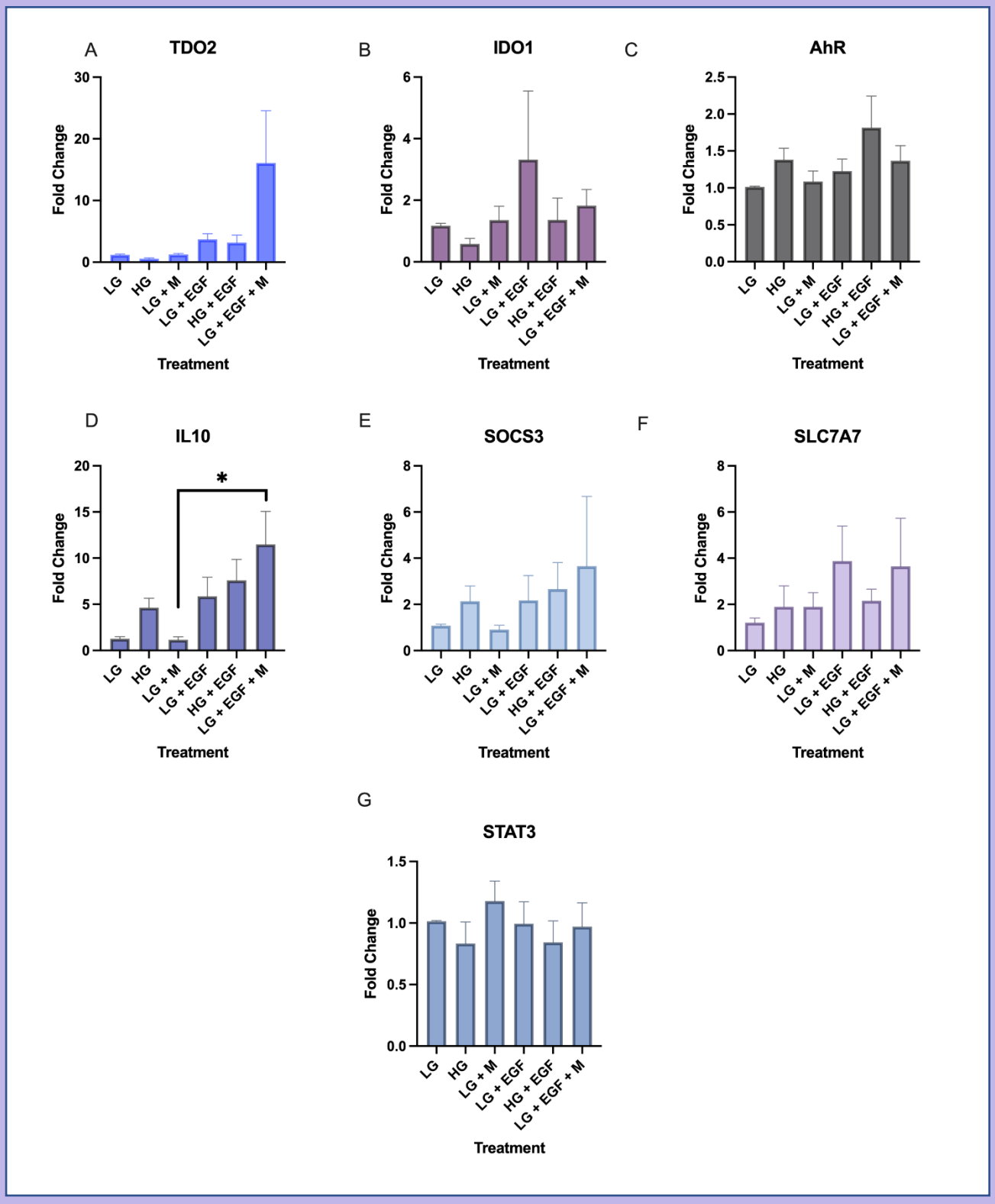

Figure 3-7: Hyperglycaemic conditions and EGF had little effect on gene expression. *Relative fold change of expression of candidate genes in conditions simulating the characteristic hyperglycaemia which is seen in diabetic patients and addition of EGF to investigate wound healing. Combined data from donors SPL009, SPL010, SPL035, SPL011. LG: low glucose (representative of a healthy level of glucose). HG: high glucose (representative of hyperglycaemic diabetic condition). LG + M: low glucose + mannitol (mannitol added as osmotic control). LG + EGF: low glucose + epidermal growth factor (EGF used as a positive control for wound healing). HG + EGF: high glucose + epidermal growth factor (hyperglycaemia + EGF used as a positive control for wound healing). LG + EGF + M: low glucose + epidermal growth factor ('healthy' glucose levels + EGF used as a positive control for wound healing + mannitol used as osmotic control). LG used to standardise all data in each gene i.e., fold change is change in gene expression in comparison to low glucose. (* $p<0.05$).*

3. Bacterial infection - LPS

TDO2

Data LPS treated skin explants showed no immediate effect on TDO2 expression as there was no significant difference in expression at day 1, with an overall slightly lower expression in the presence of LPS. However, the opposite was true at day 5, as LPS treated sample showed an average expression which was higher than that of the unstimulated samples. Although this difference did not reach statistical significance, a strong trend was observed (Table 3-9) (Figure 3-8).

IDO1

The data from SPL004 and SPL005 at day 1 were to investigate the effect of LPS treatment on the samples in both donors. LPS treated samples had a statistically significant increase in fold change of IDO1 compared to the controls at day 1. Conversely, at day 5, the combined data from donors SPL003 and SPL004 revealed that while LPS treatment still increased IDO1 expression, neither of them reach statistical significance (Table 3-9) (Figure 3-9).

Table 3-9: Results obtained from qRT-PCR experiment on LPS treated human skin explants compared to unstimulated controls (NS=not significant, ND=not determined).

GENE	SPL003 5d LPS	SPL004 5d LPS	SPL004 1d LPS	SPL005 1d LPS	AVERAGE
IDO1	Upregulated (p=0.026)	Upregulated	Upregulated (p=0.01)	Upregulated (p=0.05)	Upregulated (1d p=0.001, 5d p=0.068)
TDO2	Upregulated	Upregulated	Upregulated	Downregulated	Downregulated

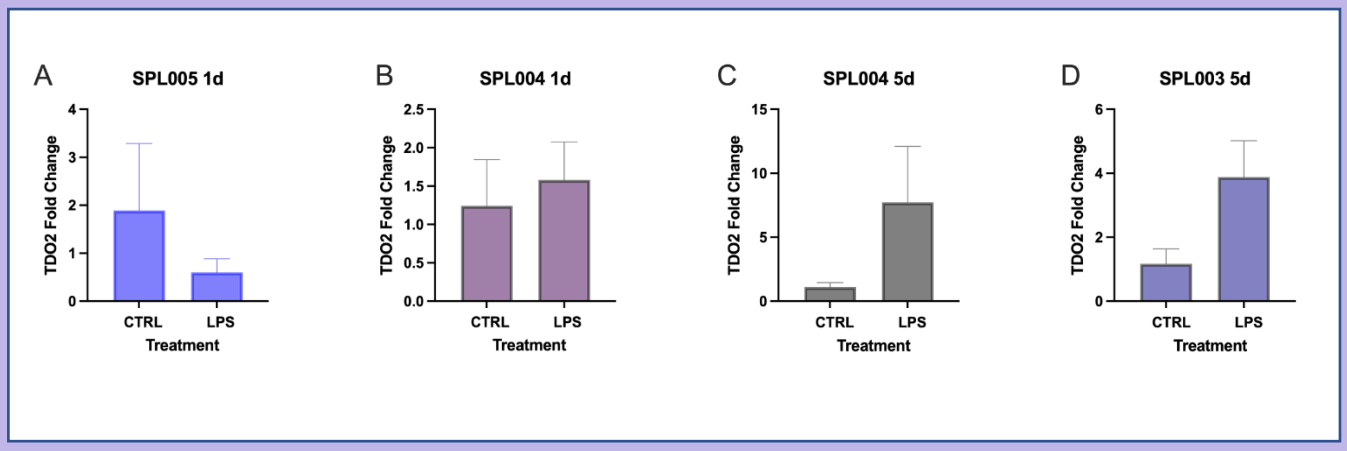

Figure 3-8: LPS displayed a delayed, minimal, upregulatory effect on TDO2 expression. *Fold change of TDO2 expression in LPS stimulated skin explants compared to unstimulated controls in donor (A) SPL005 and (B) SPL004 at 1 day time point, (C) SPL004 and (D) SPL003 at 5-day time point. Independent t-test performed on all data that were proven to be normally distributed by Shapiro-Wilk test. Where data was not normally distributed Mann Whitney test was performed instead. Levene's test was used to test for equal variance. No statistically significant results were obtained.*

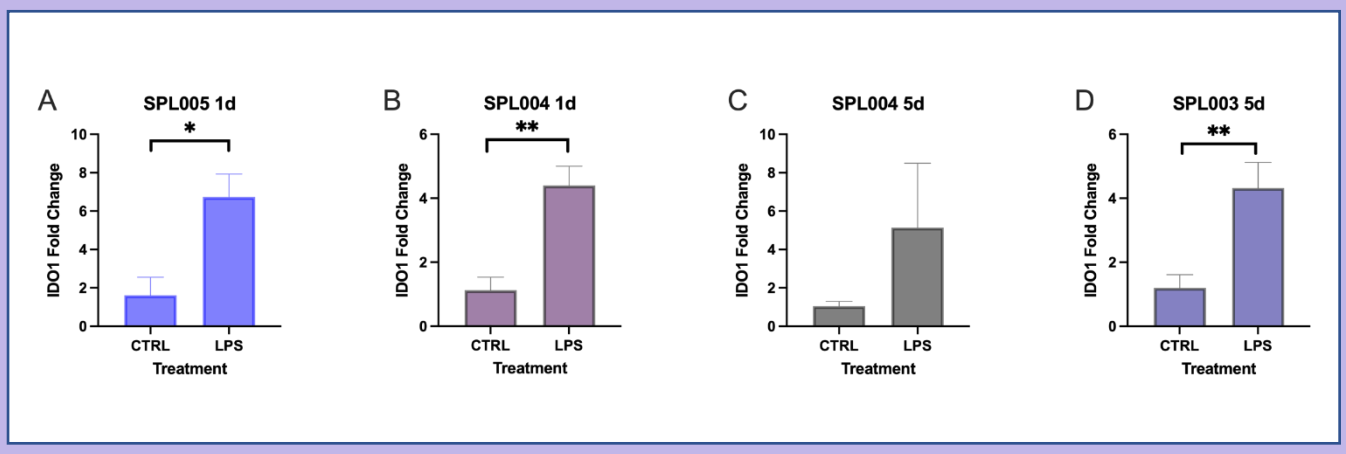

Figure 3-9: LPS significantly upregulates IDO1 expression. *Fold change of IDO1 expression in LPS stimulated skin explants compared to unstimulated controls in donor (A) SPL005 and (B) SPL004 at 1 day time point, (C) SPL004 and (D) SPL003 at 5-day time point. Independent t-test performed on all data that were proven to be normally distributed by Shapiro-Wilk test. Where data was not normally distributed Mann Whitney test was performed instead. Levene's test was used to test for equal variance. (* p<0.05, **p<0.01). LPS treatment caused a significant upregulation in IDO1 expression.*

3.4 Protein expression

In order to assess the protein expression of TDO2 and IDO1 in the skin, immunohistochemistry was performed on sections obtained from the human skin explants treated in different conditions – control (unstimulated), inflammatory (IL-1/OSM) and bacterial (LPS). Undertaking these experiments enabled further information about the localisation of the proteins within the skin, which would in turn reveal further functions of these proteins. Also, comparison of the intensity of the signal between different treatments indicates the behaviour of the proteins in response to different stimulants.

IDO1 and TDO2 protein expression in the skin

IDO1 was strongly expressed in the epidermis and some light expression was also observed in various dermal structures including sweat glands and hair follicles (Figure 3-10), highlighting potential roles for IDO1 in various essential metabolic processes. This was true for both inflammatory cytokine treated skin sections and unstimulated sections. Although it was predicted that the inflammatory cytokines would have an up-regulatory effect on IDO1, little to no effect was seen. A “no primary antibody” control revealed no detectable immunolabelling (data not shown) was observed in previous experiments, although this difference is relatively small. Staining of T_0 sections revealed expression of TDO2 in other structures of the skin (Figure 3-11).

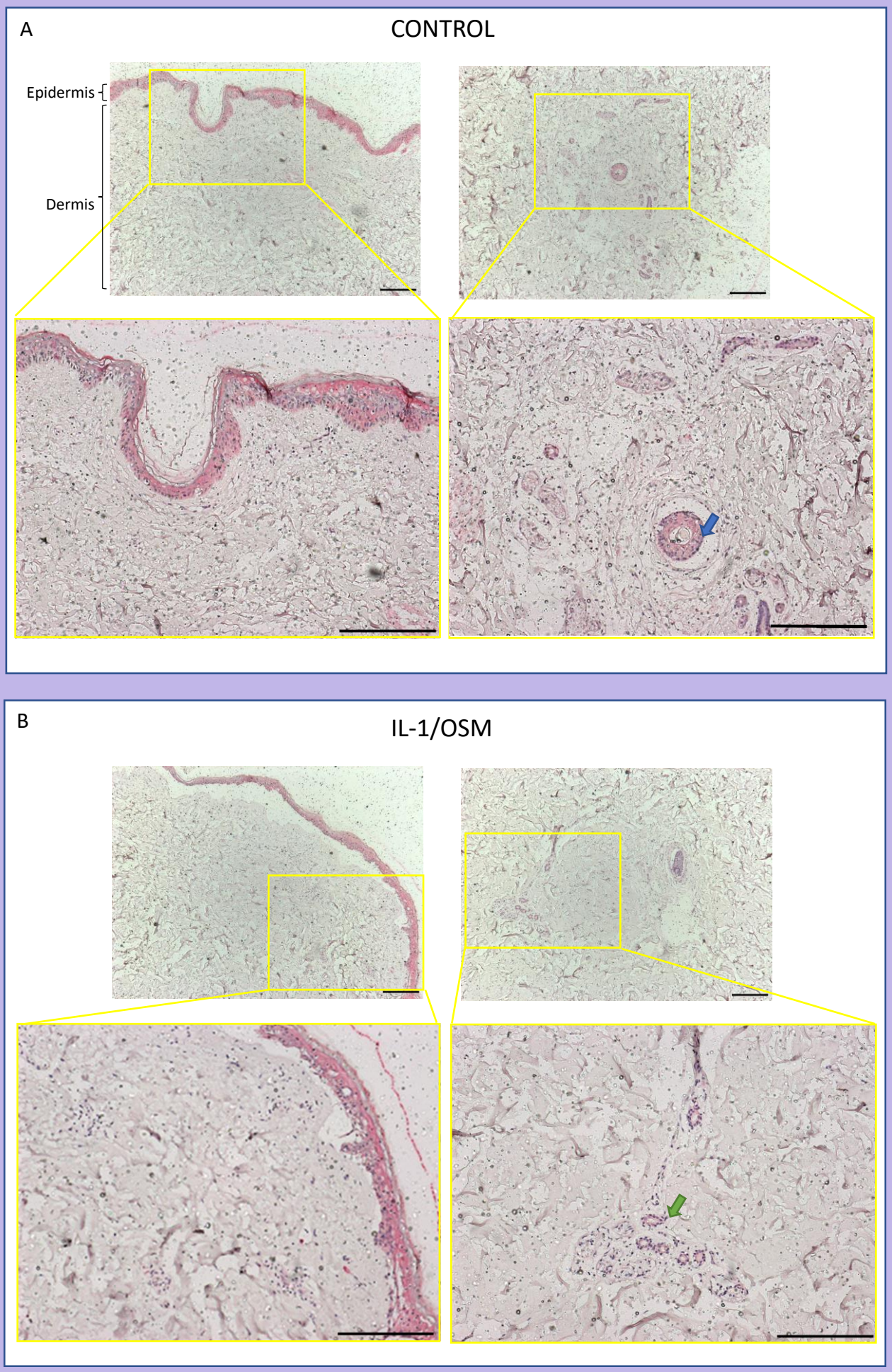

Figure 3-10: IDO1 is expressed to a slightly lesser extent in IL-1/OSM treated samples. *Immunohistochemistry performed on human skin explant sections obtained from donor SPL032 in different conditions. Control sections were obtained from unstimulated skin sections at day 5, IL-1/OSM sections treated with inflammatory cytokines IL-1 and OSM. Primary antibody at concentration 1:100. Scale bar is equal to 200µm. KEY: Blue arrow: hair follicle, Green arrow: sweat gland.*

TDO2 is strongly expressed in the epidermis and other structural dermal components

Immunolabelling for TDO2 in T_0 sections revealed expression of the protein in structural components of the dermis, which could suggest important roles for the enzyme.

Initially, TDO2 was immunolabelled for in T_0 sections which revealed strong expression in dermal structures such as hair follicles, sebaceous glands and sweat glands (Figure 3-11).

Next, the effect of the inflammatory cytokines IL-1 and OSM was analysed by comparison of TDO2 expression between these samples. TDO2 protein was highly expressed in the epidermis in all treatment conditions, with the unstimulated control sections possibly showing the strongest expression (Figure 3-12). This is the opposite of the effect that was expected since the microarray and qRT-PCR data showed that TDO2 was upregulated 20-fold in inflammatory conditions.

The same effect was also observed in the LPS treated skin samples, although to a lesser extent, TDO2 was downregulated in response to the bacterial product.

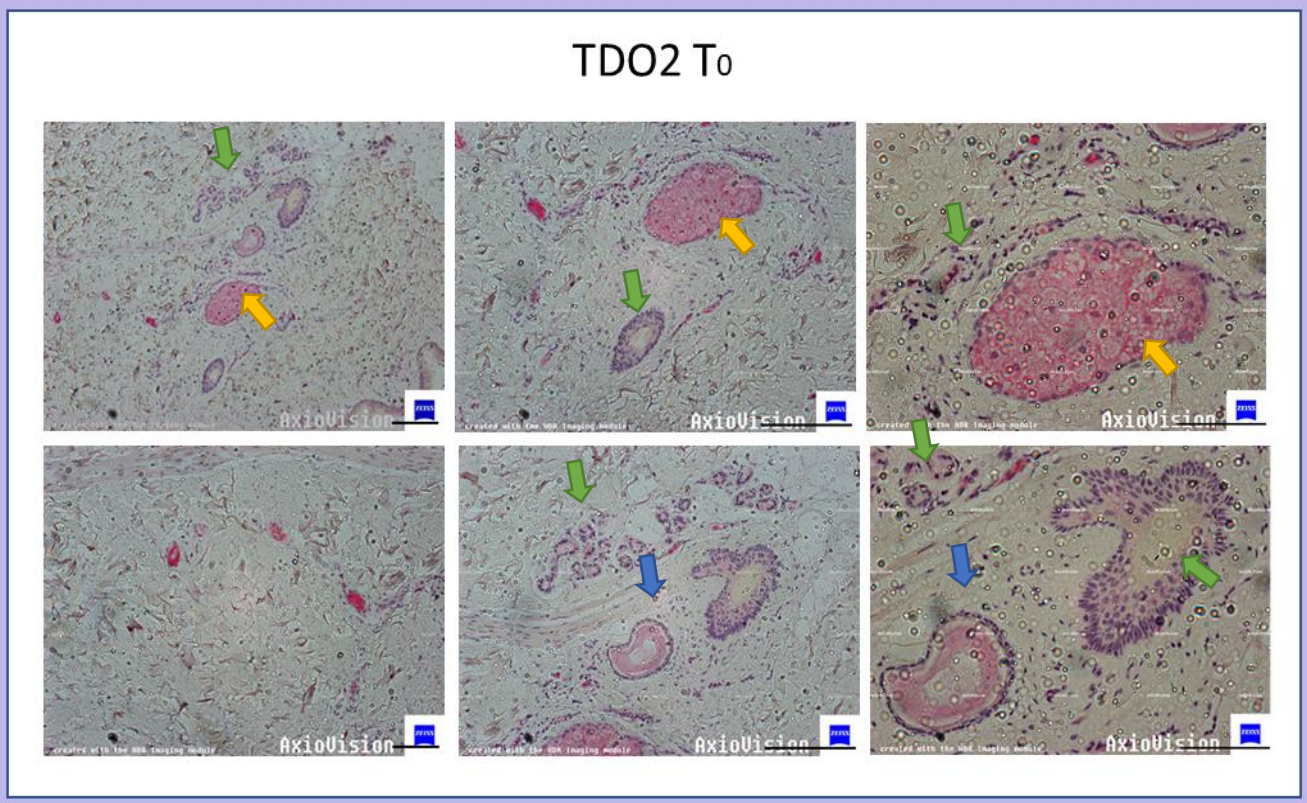

Figure 3-11: Expression of TDO2 in T_0 samples is strong in various dermal structures. *Immunohistochemistry performed on T_0 samples revealing high expression of TDO2 in sebaceous glands. KEY: Blue arrow: hair follicle, Green arrow: sweat gland, Yellow arrow: sebaceous gland.*

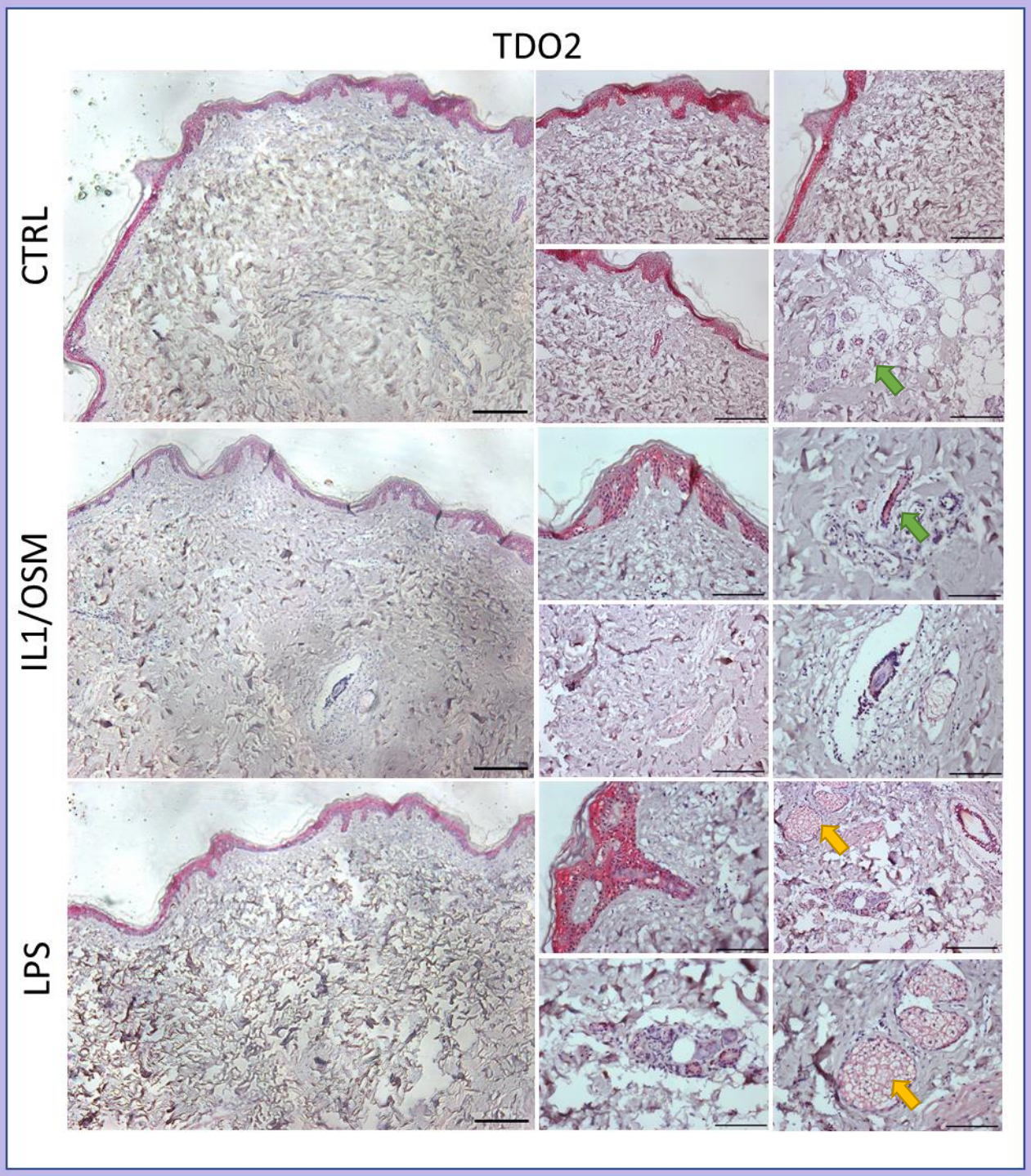

Figure 3-12: *Immunohistochemistry performed on human skin explant sections obtained from donor SPL004 in different conditions. CTRL sections were obtained from unstimulated skin sections at day 5, IL-1/OSM sections treated with inflammatory cytokines IL-1 and OSM and LPS-treated sections (a bacterial product).*

3.5 Chapter 3 Conclusion

Gene expression

TDO2

TDO2 responded drastically to stimulation with inflammatory cytokines. A number of previous studies have shown that TDO2 is stimulated by various inflammatory cytokines, and that the kynurenine pathway is upregulated in inflammatory conditions, therefore these results support this notion. The qRT-PCR experiments on human skin explants treated with inflammatory cytokines IL-1 and OSM at all time points expressed amounts of TDO2 that were hundreds times higher than that of their unstimulated counterparts, and a dose response was observed in donor SPL030, strongly indicating a correlation between IL-1/OSM and TDO2 expression. This data is also in line with data obtained from the previous microarray experiment.

On the other hand, in the qRT-PCR experiment which was performed on the "diabetic" conditioned samples, the expression of TDO2 was not so clearly regulated. Treating the skin samples with high glucose or the osmotic control mannitol had no effect on TDO2 expression, which is surprising since previous studies have shown that TDO2 is induced by the peptide hormone glucagon which is responsible for increasing systemic blood glucose levels (Munn et al., 1998). Theoretically, this would suggest that high glucose levels would decrease the expression of TDO2, as if TDO2 expression is upregulated in response to hypoglycaemia (as glucagon is elevated in hypoglycaemic conditions) the reverse effect would be seen in hyperglycaemic conditions. However, this response could be strictly hormonal, which is impossible to mimic with this *ex-vivo* model, as glucagon is produced and released by alpha cells in the pancreas.

TDO2 expression in response to LPS was minimally affected. Although the samples did express higher amounts of TDO2 in LPS stimulated samples at day 5, the fold change of mRNA expression was miniscule in comparison to that of samples treated with inflammatory cytokines. The fold change of TDO2 expression did not exceed 10-fold in any of the donor samples (SPL003, SPL004 and SPL005) at either time point – day 1 or 5. In fact, day 1 samples seemed to show no effect of LPS on TDO2 expression.

In summary, TDO2 expression was highly receptive to inflammatory cytokines, yet unresponsive to LPS.

IDO1

Overall, the CT values for many of the experiments when IDO1 was measured were above 35, indicating a low quantity of expression. Therefore, the results may be slightly inaccurate. However, despite high CT values, there was still a noticeable upregulation of 3-6 fold in inflammatory cytokine skin explants, which is indicative of some effect of the cytokines on IDO1 expression. Although this change only reached statistical significant in SPL003 at the day 5 time point.

The diabetic conditions and EGF had no effect on IDO1 expression.

Interestingly, unlike TDO2, the bacterial product LPS was able to increase IDO1 expression in all donors and time points, with statistical significance in most cases. This is in line with previous literature which states that IDO1 induces tryptophan catabolism in several tissues in response to bacterial products e.g. LPS and pro-inflammatory mediators e.g. TNF-α, IFN-γ (Bandeira et al., 2015).

The contrasting effects of the stimulants used in this study on the two enzymes IDO1 and TDO2 raises questions about the distinctive roles of the two enzymes, since they both have very different structures but supposedly perform the same function; there must be a biological explanation for the existence of two enzymes that perform the same function. Further research is required to elucidate this exact reason, but the results obtained from this study are one step in the right direction to answer this question.

AhR

AhR was largely unaffected by all stimulants. This was an unexpected result as the literature suggests that AhR is involved in inflammatory processes by producing a synergistic effect with the inflammatory cytokines, thus boosting inflammation in general (Hollingshead et al., 2008). The reason for this unresponsiveness could be the fact that qRT-PCR measures steady state mRNA and AhR may not be modulated at this timepoint or may not be regulated at the

mRNA level. In order to further investigate this effect, protein levels of AhR need to be investigated through techniques such as western blotting and immunohistochemistry in future studies which can be cross analysed with protein expression of TDO2 and IDO1.

Had there been enough time in this study, AhR levels in the LPS treated samples may have proven some change in expression of AhR, as it has been proven in previous studies that AhR is involved in LPS induced inflammatory responses (Nguyen et al., 2013).

IL-10

Although IL-1/OSM addition to the human skin explants had no statistically significant effect on expression of the inflammatory cytokine IL-10, there was a clear effect of the stimulants on IL-10 expression, as a dose response pattern was observed in the day 1 sample. However, at day 5 the pattern was slightly different, with the medium concentration of IL-1/OSM having the greatest effect on IL-10 expression. This could suggest that a certain amount of inflammatory cytokine produces a positive feedback effect, wherein other cytokines are also upregulated to boost the inflammatory effect, however once this crosses a threshold i.e. a certain amount and/or length of time, a negative feedback loop is activated, reducing cytokine expression in general to prevent chronic inflammation. This could be deregulated in diabetic conditions for various reasons, hence the characteristic chronic inflammation observed. This theory is supported by the results of the diabetic conditions on IL-10 expression, as there was a trend towards higher expression of IL-10 in high glucose conditions, indicating a general higher inflammatory grade in diabetic conditions, which is a widely accepted concept. EGF had a significant effect on IL-10 expression, with a higher expression in its presence. This could be due to the need for inflammation during the wound healing process.

SOCS3

IL-1/OSM seemed to have a small positive effect on SOCS3 expression in donor SPL030, although this was not proven to be statistically significantly different. The effect, albeit small was more evident at day 5, implying a slow, gradual effect on expression. Previous studies have shown that SOCS3 does have a major role in suppressing inflammation via its

involvement with the JAK kinase pathway (Carow and Rottenberg, 2014). Again, this may only be true for the steady-state mRNA expression, and further studies would be required to determine the differential protein expression of SOCS3.

SLC7A7

A substantial difference between day 1 samples and day 5 samples was observed. Despite no statistical significance. An 80-fold increase at day 5 in the "high IL-1/OSM" treated sample indicates that it is very likely that there is some effect of SOCS3 expression in inflammatory conditions. Since SLC7A7 is an amino acid transporter protein, a higher level of expression in inflammatory conditions would suggest a higher rate of transportation of amino acids i.e. tryptophan in/out of the cell. This could be evidence to support the theory that the kynurenine pathway is upregulated in inflammatory conditions, because if tryptophan is being transported more, it must be utilised to a higher degree, and also the rate of turnover/metabolism via the pathway would hence be upregulated. The diabetic and wound healing experiment, however, did not seem to have an effect on SLC7A7 expression.

STAT3

STAT3 expression was mostly unaffected by cytokines and diabetic conditions, as well as EGF. However, a slight change in expression was seen in the day 5 SPL030 sample, especially in the medium and high cytokine concentrations. This change was only around 2-3-fold and not statistically significant, therefore it is unlikely that there is a correlation between the stimulants and STAT3 mRNA expression. In terms of previous literature, STAT3 is known to be a component of the interleukin-6- (IL-6) activated acute phase response factor (APRF) complex, which is stimulated in inflammatory conditions (Hillmer et al., 2016).

For many of these experiments, statistical significance was not reached, however variations in structural components within samples from the same donor could lead to variations of gene expression in all cases. Although it was necessary to treat all samples from the same donor as the same, in reality, due to the biological nature of the skin the explants are never 100% identical. For example, one explant could contain a blood vessel and the gene in question could be highly expressed in blood vessels, but an explant from the same donor could have no blood vessels in the particular section cut. One way to overcome this issue is

to include a high number of samples to increase the likely hood of various structures to be included in all donors.

Protein expression

The initial microarray showed that IDO1 and TDO2 gene expression and qRT-PCR data were upregulated in response to inflammatory stimulants IL-1 and OSM. However, analysis of the protein expression in this immunohistochemistry experiment revealed that in the presence of inflammatory cytokines protein expression of TDO2 and IDO1 was similar (or slightly lower) than in unstimulated explants. The reason for these conflicting results could be due to the timing of tissue collection in experiments. This is because there would be a delay between upregulation of genes and upregulation of expression of the proteins and each experiment is a snapshot of the skin section at a given time point, not reflective of the dynamic process of altering protein expression. Future experiments could analyse the change in protein expression at multiple time points to test this theory.

Expression of TDO2 and IDO1 proteins in the epidermis indicates that topical treatments are a potential for clinical use, since the enzymes are near the surface of the skin so can be easily targeted. Additionally, TDO2 and IDO1 were strongly expressed in dermal structures, namely hair follicles, sweat glands and sebaceous glands. This could reveal more about the function of the proteins, for example sweat glands and hair follicles have been proven in previous literature to contribute to wound healing through maintenance and protection of the skin (Takeo et al., 2015). Sebaceous glands and sweat glands have also been shown to contribute to re-epithelialisation of the epidermis by forming keratinocyte outgrowths (Rittié et al., 2013). High expression of IDO1/TDO2 in these structures therefore present a possible link between the enzymes and these processes, although further research is required to confirm this.

TDO2 protein was also downregulated in LPS treated skin explants, revealing a possible role for the enzyme in the immune response, which several previous studies have also found (Opitz et al., 2020).

Overall, the results of these experiments reveal that TDO2 and IDO1 proteins are highly expressed in the skin in various locations. The qRT-PCR experiments revealed that TDO2 was

indeed strongly stimulated by inflammatory cytokines. The same result was expected when analysing the protein level however the inflammatory cytokines has the opposite effect. Although the expected result was not observed, the fact that TDO2 was noticeably downregulated in inflammatory conditions suggests that this mechanism is more complex and could be vital for potential discovery of novel therapeutics.

Chapter 4: Wound Healing Models

4.0 Chapter 4 Introduction

The results obtained in Chapter 3 suggested that TDO2 is expressed in human skin explants and its expression may change under conditions relevant to wound healing. Investigation of the impact of TDO2 on wound healing was performed through a scratch wound assay with the addition of 680C91, a TDO2 specific inhibitor that blocks activity of the enzyme. In total, four experiments were completed with slightly different treatments in each experiment (as described in Chapter 2.7). Time-lapse imaging was used to observe the rate of scratch wound closure in the different conditions; control conditions where cells were cultured in DMEM and 2% FCS only, vehicle controls with added DMSO, and inhibitor treated cells with the addition of 680C91 at different concentrations. Subjecting the cells to low glucose conditions was also used in the latter two experiments to investigate the effects of glucose in wound closure. It was concluded that addition of the inhibitor had a significant negative impact on rate of wound closure, and low glucose decreased wound closure rate in the presence of the inhibitor (See Appendix 3 for timelapse videos).

To create diabetic wound models, human skin explants were used, creating an *ex-vivo* wound healing model as described in Chapter 2.8. Utilisation of immunohistochemistry was implemented to observe the histological changes in wound closure upon stimulation with EGF and in differing levels of glucose. Changes in re-epithelialisation revealed that high glucose levels do impact wound healing, but only in the presence of EGF.

4.1 Cell culture experiments - TDO2 inhibitor 680C91

Cell migration decreased in presence of inhibitor

Changes in cell morphology between the different treatments gives an indication as to which cells are actively dividing and which are failing to do so. The DMEM control cells appear to be actively proliferating and filling the space made by the scratch, the cells are spindle like in shape indicating cells undergoing migration. Although the vehicle control healed as efficiently as the control cells in terms of overall percentage closure, a small number of cells appear more rounded and the cells do not appear quite as active as DMEM control cells, but still there are cells with the distinct spindle-like shape present in abundance. However, addition of the inhibitor at all three concentrations appears to have severely affected cell morphology and behaviour. The number of migrating cells diminishes as the concentration of the inhibitor increases and instead of spindle-like structure, the cells look more rounded and less active. At the highest concentration, the cells appear granulated and there is a very small number of cells migrating towards the centre of the wound (Figure 4-1A).

Percentage closure of wounds decreased in presence of *TDO2 inhibitor 680C91*

In Experiment 1 (Figure 4-1), the scratch wound cells were observed using timelapse microscopy over a 16-hour time frame in 5 different conditions (control, vehicle control, 10µM inhibitor, 20µM inhibitor and 40µM inhibitor). This experiment revealed that higher concentrations of the inhibitor impacted the total percentage closure of the scratch wounds. The control treatment cells that were in DMEM only + 2% FCS healed effectively, reaching an average percentage closure of approximately 80% (Figure 4-1B). Reduced wound closure was observed in the vehicle control which used the highest concentration of the DMSO solvent, reaching 60% closure at 16h (Figure 4-1B). Whereas the cells that were treated with the inhibitor showed a slowed rate of wound closure and a lower percentage closure by the end of the experiment. At 10 µm concentration, the cells appeared more rounded and less active. At the highest concentration, the cells appear granulated and there is a very small number of cells migrating towards the centre of the wound (Figure 4-1A).

The same conditions as Experiment 1 were used for Experiment 2, however a 24-hour time frame was used instead. Again, control and vehicle control wounds healed effectively, and percentage closure was inversely correlated with concentration of 680C91 (Figure 4-2).

Low glucose levels further decreased rate of wound closure

The latter 2 experiments – Experiments 3 and 4 incorporated a subset of cells treated in low glucose levels as opposed to commonly used higher levels of glucose in DMEM media. This significantly decreased the percentage closure of the wounds at the end of the 24-hour period in both experiments (Figure 4-3, 4-4). Although interestingly, in experiment 4, the rate of wound closure in the low glucose control was faster than that of the control and vehicle control cells in the early stages. The same pattern of percentage wound closure and rate of healing was seen in these two experiments, with higher concentrations of inhibitor yielding slower rates of wound closure. The low glucose treatment seemed to accentuate the effect of the inhibitor, as the cells that were treated with both the inhibitor and low glucose conditions healed the worst, with a dose response observed inversely with higher concentrations of the inhibitor. This effect was not seen in the control samples, indicating a possible interaction between 680C91 and glucose.

Scratch wounds of 3T3 cells treated with the highest concentration (40 µM) of the TDO2 inhibitor, 680C91, showed more impaired wound healing compared to the vehicle control. The cells treated with the highest concentration of vehicle alone showed no significant difference in wound closure, with a percentage closure similar to that of the DMEM only controls.

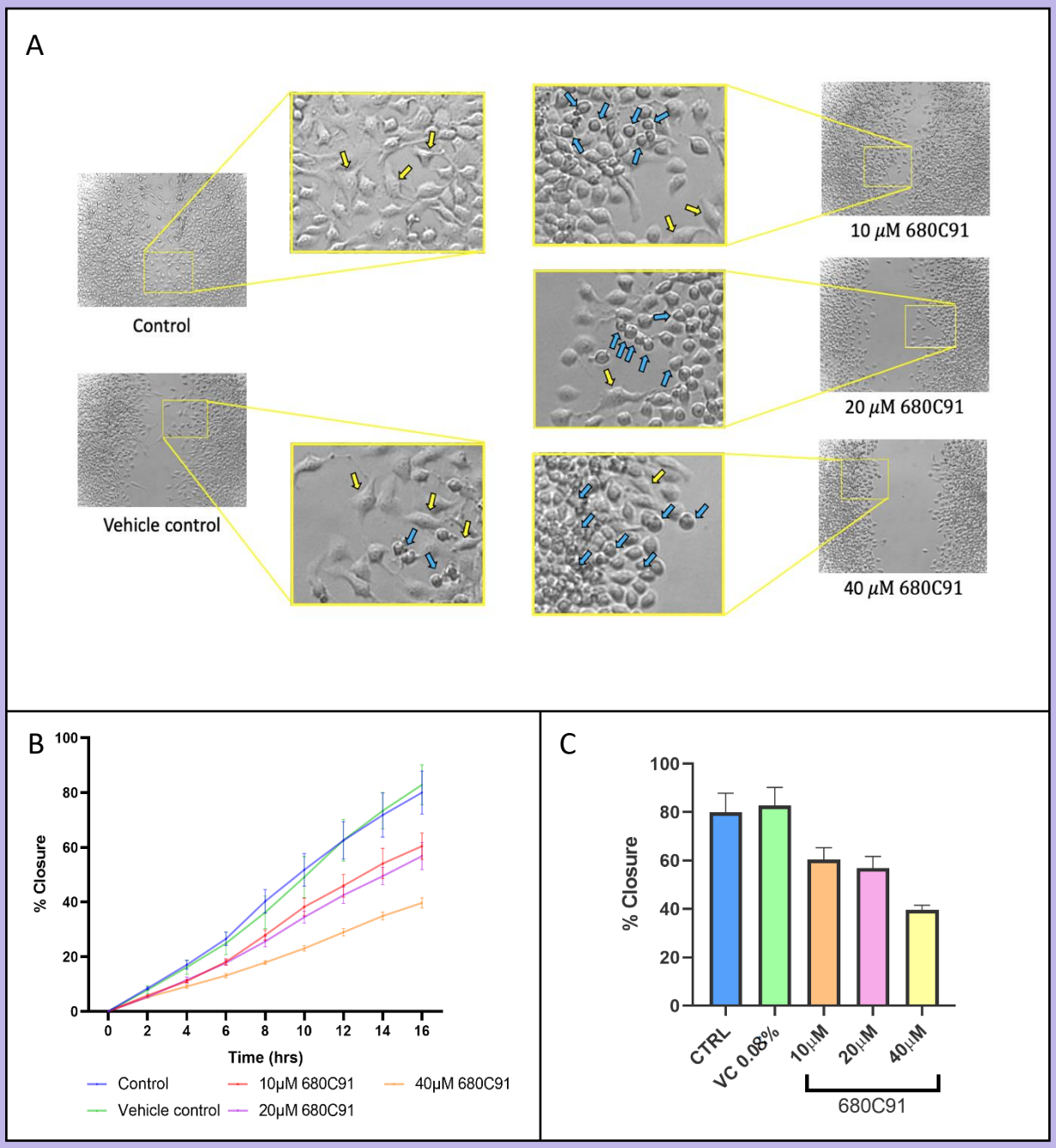

Figure 4-1: TDO2 inhibitor decreased the rate of scratch wound closure. *Experiment 1. Scratch wounds healed slower with Cells treated in 5 different conditions- control: DMEM + 2% FCS only, vehicle control: DMEM + 2% FCS only. 680C91 (inhibitor TDO2) was dissolved in DMSO and 3 different concentrations were used to treat the cells. Scratch wound closure observed over 16-hour period to assess rate of 'wound' healing. (A) Timelapse images of cells at 16-hour time point in the 5 different conditions. Differences in cell morphology seen between control and treated cells. Yellow arrows indicate cells undergoing cell migration with spindle-like morphology. Blue arrows indicate rounded cells which are more numerous in higher concentrations of inhibitor. (B) Percentage closure of cells over time during the 16-hour period. (C) Overall percentage closure of scratch wounds by the end of 16 hours. Mean of triplicate data with SEM bars on all graphs. One way ANOVA performed on all data using SPSS. *p<0.05, **p<0.01, ***p<0.001.*

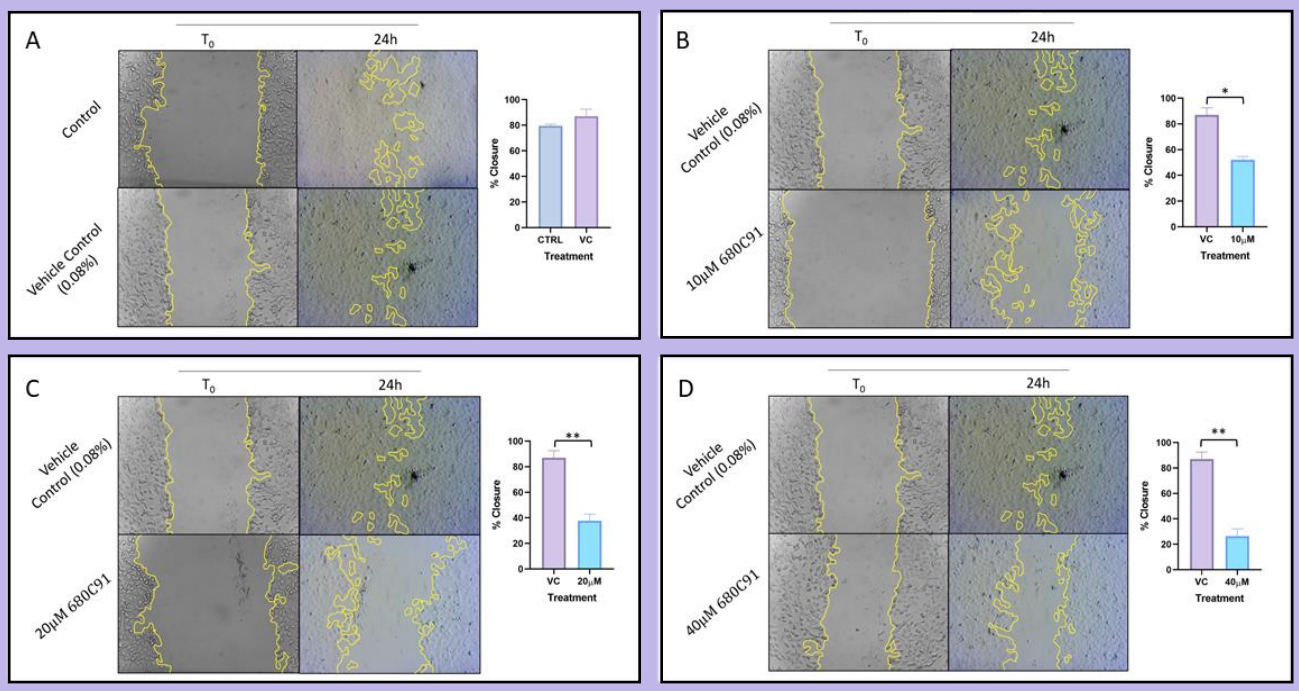

Figure 4-2: Cells treated with TDO2 inhibitor displayed morphological changes as well as slowed healing rate. *Percentage closure of scratch wound assay on cells treated with and without addition of TDO2 680C91. (A) DMEM + 2% FCS control cells vs. DMEM + 2% FCS + 0.08% DMSO vehicle control cells (equivalent to amount of solvent used in highest concentration of inhibitor. (B) vehicle control cells vs. cells treated with 10 μM inhibitor 680C91. (C) vehicle control vs. 20 μM inhibitor cells. (D) vehicle control vs. 40 μM inhibitor cells. Images analysed on ImageJ software to measure 'wound' area. One way ANOVA performed on all data using SPSS. *p<0.05, **p<0.01, ***p<0.001.*

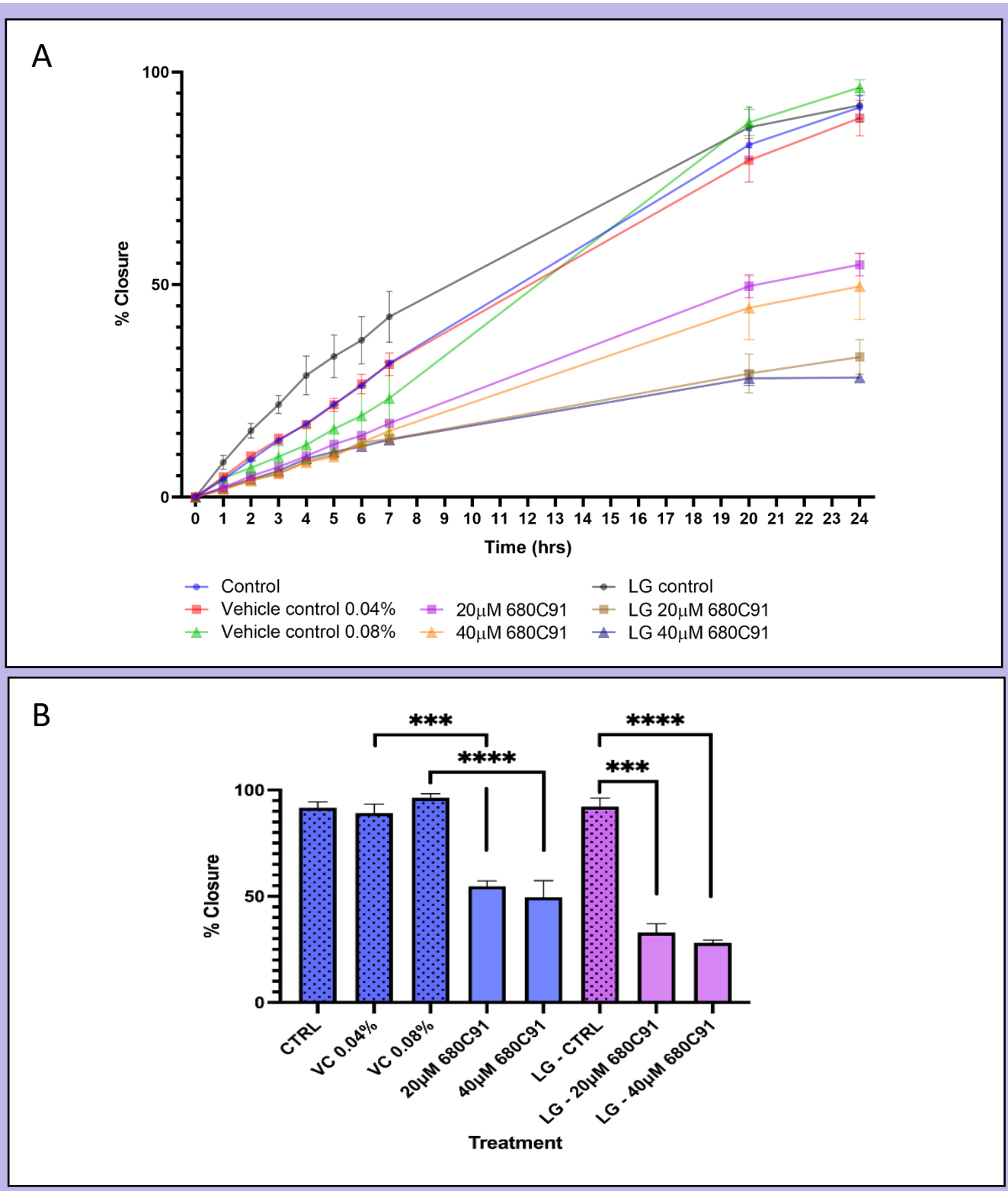

Figure 4-3: Low glucose increased wound closure rate in absence of 680C91 TDO2 inhibitor but further delayed wound healing in presence of inhibitor. *Experiment 3 – 3T3 cells scratch wound assay experiment. (A) Controls – DMEM + 2% FCS only control (blue), and Low glucose DMEM+ 2% FCS control (black). DMSO vehicle controls at 0.04% (red) and 0.08% (green), these were the concentrations of DMSO equivalent to the amount of solvent used to dissolve the inhibitor at 20uM (pink) and 40uM (yellow), respectively. Shape of marker corresponds to equivalent concentrations of DMSO. All cells were cultured with DMEM + 2% FCS (B) Average total percentage closure of scratch wounds at t=24 hours. (VC 0.08% = DMSO vehicle controls. LG = low glucose samples).*

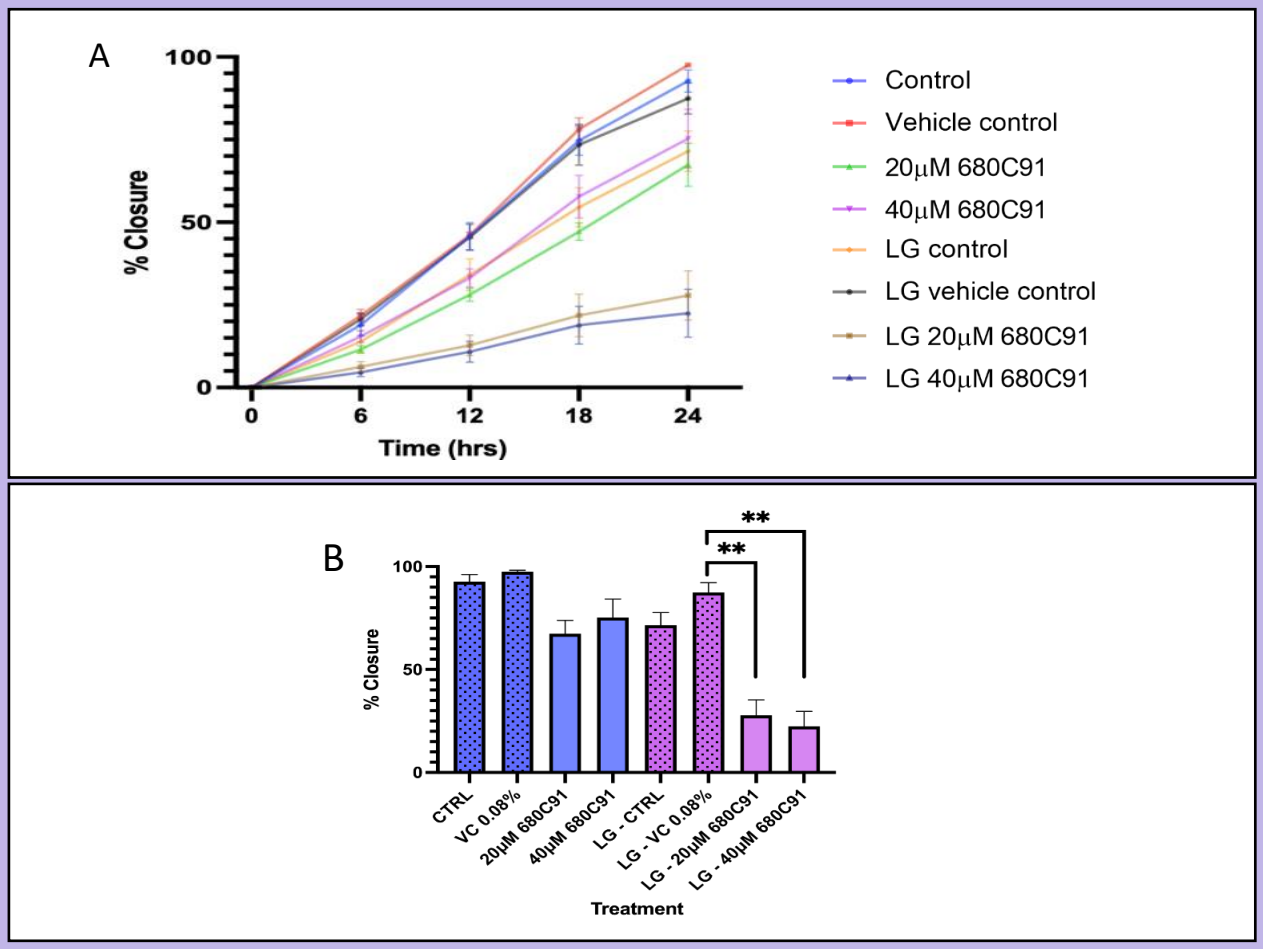

Figure 4-4: Low glucose and high 680C91 - TDO2 inhibitor was the worst conditions for scratch wound closure. (A) Experiment 4- percentage closure of mouse 3T3 cells in scratch wound assay with different treatments over 24-hour period. Control cells were treated with DMEM + 2% FCS only. Vehicle control cells were DMSO at 0.08% - equivalent to the highest concentration of solvent used to dissolve the inhibitor at 40μM. (B) Average total percentage

Data from all experiments were averaged and combined where the same treatment was used at least three times – control, 0.08% DMSO control, 20uM inhibitor and 40uM inhibitor (Figure 4-5). The strong trends seen , whilst not reaching significance, support the hypothesis that inhibition of TDO2 reduces the rate of wound healing likely through a combination of reduced cell migration and proliferation.

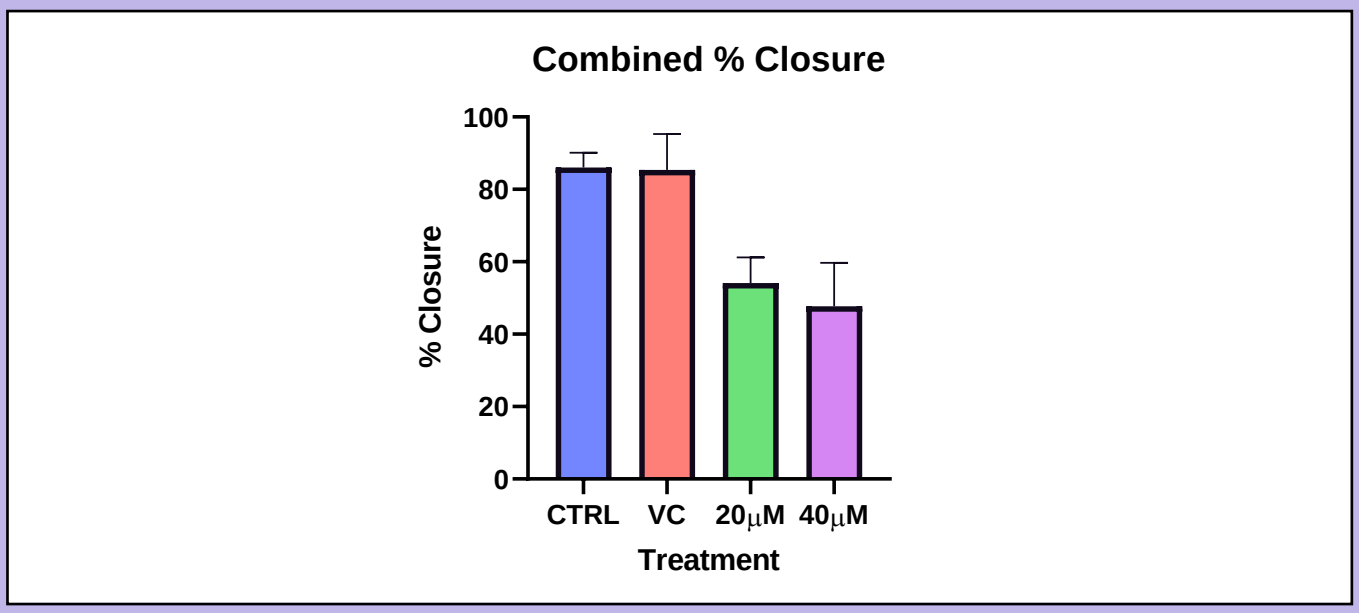

Figure 4-5: Overall, TDO2 inhibitor 680C91 was found to decrease wound healing rate across all experiments. *Combined percentage closure of scratch wound assay performed on mouse 3T3 cells across all 4 experiments by the end of each experiment.*

4.2 Diabetic Wound Healing Experiments – Human explant model

The human skin explant wound experiment described in Chapter 2 was sectioned and H&E staining performed as described in Chapter 2.8. Image J analysis was then used to measure the area, length and average thickness of the re-epithelisation of the wounds at day 8 so this could be cross-analysed in the different conditions.

In the individually measured explant samples from donor SPL032, there is a trend of decreased area comparing high glucose + EGF samples with low glucose + EGF samples (Figure 4-6B). The length of the re-epithelialisation is apparently higher in the low glucose samples in the presence of EGF, compared to high glucose + EGF. Although mannitol may have had a small effect, this change was not significant so it can be concluded that the decrease in rate of wound closure was due to high glucose rather than any changes in osmotic gradient. On the contrary, the wounds treated with high glucose + EGF appeared to have a higher average thickness, the H&E-stained images show a clear difference in histology of the HG+EGF wounds in comparison to much of the other treatments (Figure 4-6D). The area of epithelialisation appears truncated and thicker, as if the cells have multiplied too quickly, spreading laterally rather than longitudinally, and in a more disorderly manner. This is also true for the high mannitol + EGF treated wounds. There is no clear difference between any of the treatments in the absence of EGF.

Analysis of the above experimental data was performed together with data collected from two previous experiments with other donor samples (data provided by Drs Bevan and Gavrilovic, personal communication). Combined results of the area of each wound in four of the conditions (low glucose, high glucose, low glucose + EGF, high glucose + EGF) revealed a similar area of re-epithelialisation in the low- or high-glucose treated samples in the absence of EGF. However, in the high glucose + EGF samples, a trend towards a decrease in the area of re-epithelialisation observed when compared to low glucose + EGF treatment (Figure 4-7).

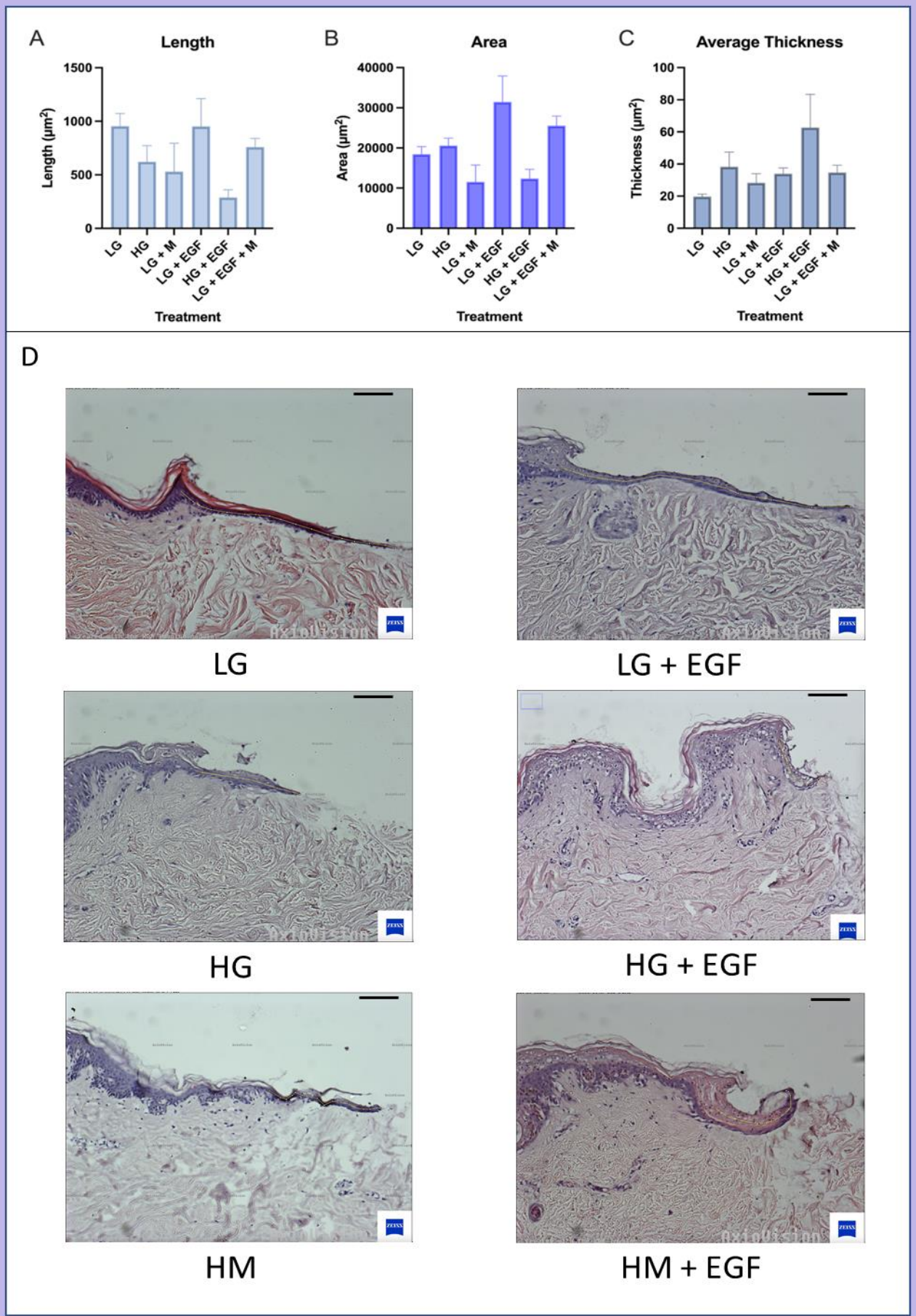

Figure 4-6: Addition of glucose and EGF to wounds altered wound closure and morphology. *Individual measurements for wound re-epithelialisation of diabetic treated wounds from donor SPL032. Total average length (A), area (B) and average thickness (C) of right-hand side and left-hand side re-epithelisation of explants treated in 'diabetic' conditions in triplicate. (D) Diabetic wound treated sample H&E staining with marked length measured and used in data. Analysed in Image J software FIJI. Scale bars are 200 µm.*

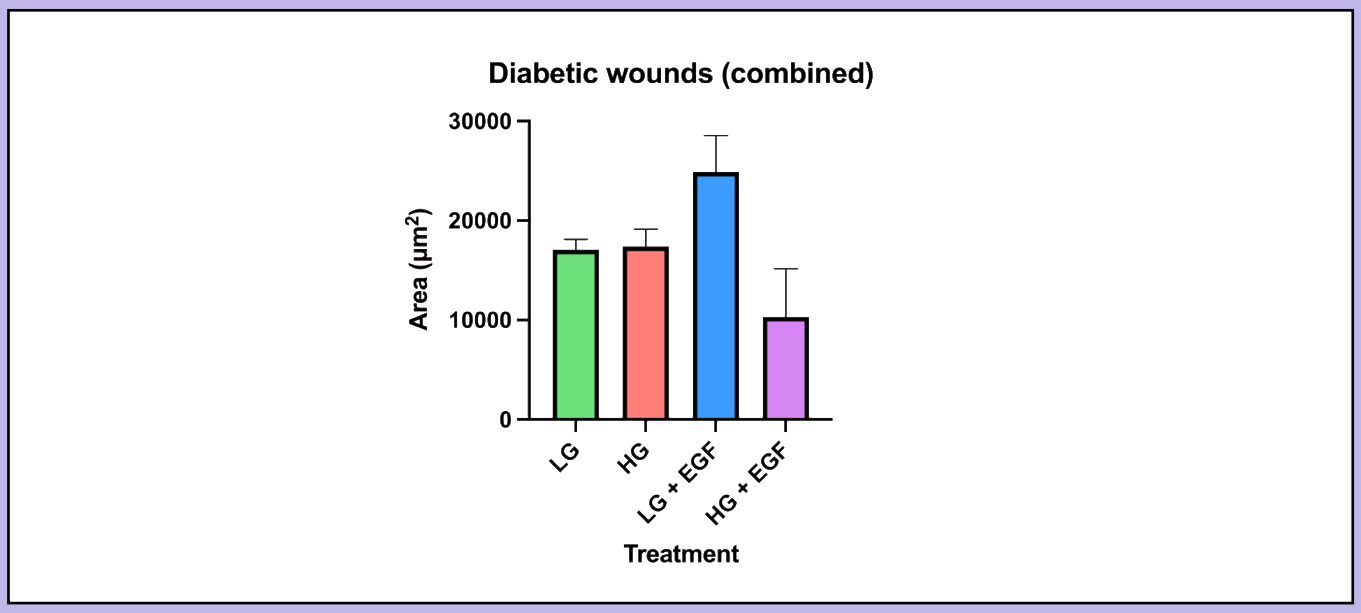

Figure 4-7: High glucose decreased wound healing in presence of EGF. *Combined data from "diabetic" conditioned skin explants which were wounded and allowed heal. Area of re-epithelialisation was measured using ImageJ and data from donors SPL035, SPL019 and SPL009 were combined and plotted in this graph.*

4.3 Chapter 4 Conclusion

Overall, from the scratch wound experiments it can be concluded that TDO2 is likely to play an important role in wound closure. This is the opposite of the known effect of IDO1, as shown by a previous study by Ito et al. who demonstrated accelerated wound healing in IDO1 knock out mice due to upregulation of pro-inflammatory cytokines IL-6 and TNFα (Ito et al., 2015). These authors also explored scratch wound closure in mouse embryo fibroblasts (MEFs) derive from wild type or Ido-/- mice and observed that depletion of tryptophan in the culture medium resulted in delayed wound closure. This theory is in line with results obtained from several other studies suggesting that a higher presence of tryptophan increases rate of wound closure (Bandeira et al., 2015). Since TDO2 and IDO1 are involved in tryptophan's metabolism, absence of one of these enzymes would result in a higher presence of the amino acid, and there have been previous studies linking tryptophan to wound healing in a positive manner. For example, NHK cells were used in a scratch wound assay which showed that addition of tryptophan was able to increase wound closure from 20% (vehicle) to 70% closure (Barouti et al., 2015). Thus, data obtained from this study opposes the original hypothesis, suggesting an alternative mechanism of action that perhaps doesn't involve the levels of circulating tryptophan. The current study did not assess tryptophan levels therefore future studies should incorporate analysis of tryptophan in correlation with IDO1/TDO2 expression and the corresponding effects on wound healing.

Alteration of glucose levels only had an effect on wound closure in the presence of the inhibitor. This is indicative of a connection between glucose and TDO2. Interestingly, one previous study analysed the effects of a glucocorticoid named dexamethasone on IDO1/TDO2 expression, and concluded that administration of dexamethasone upregulates TDO2, whilst having no effect on IDO1 expression (Cecchi et al., 2021). This is interesting due to the fact that the results of the present study imply that there is a positive correlation between TDO2 and wound healing, whereas previous research has suggested a negative correlation between IDO1 and wound healing (Ito et al., 2015). Additionally, dexamethasone has been proven to increase blood glucose levels in adults, which provides some evidence for a link between the two (Abdelmannan et al., 2010).

The diabetic wound healing human skin explant experiments revealed that in the presence of EGF, high glucose had a negative effect on re-epithelialisation, slowing down the rate of wound healing in the samples. The explanation for these results can be linked to a connection between high glucose levels and the EGFR. A previous study concluded that high glucose interferes with the EGFR–phosphatidylinositol 3-kinase/Akt pathway, resulting in delayed wound healing (Xu et al., 2009). Consequently, in the presence of high glucose, EGF cannot exert its effect due to lack of EGFR. This would explain why EGF increased wound closure in low glucose levels, as the glucose is not present in sufficient levels to affect EGF, therefore EGF can exert it's proliferative effect and aid wound closure. In the high glucose treated samples, EGFR is affected so the added EGF has no effect, and any existing EGF within the sample also cannot bind to promote wound closure, as a result, the rate of wound closure is even slower than the samples without added EGF. This could also be a potential link between high glucose levels in diabetic patients and the onset of DFUs due to delayed wound healing.

Chapter 5 – NSPinfex

Proof of Concept (PoC) experiment

5.0 Chapter 5 Introduction

This PoC experiment was performed to assess the viability of the human skin explants as a model for bacterial growth for future experiments. Bacteria were grown on the surface of human skin explants overnight, retrieved by different methods and regrown on agar to determine the best method of retrieval through counting colony forming units (cfu) on the agar. qRT-PCR of certain genes involved in inflammation and cell proliferation was then performed on the skin explants on which the bacteria were grown.

5.1 Retrieval of bacteria

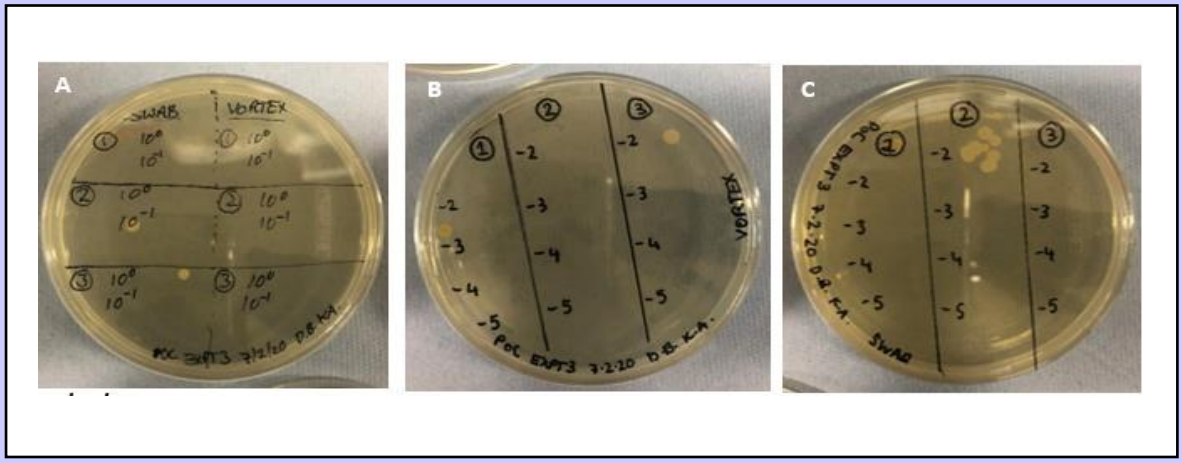

Figure 5-1: Initial attempts to recover bacteria from skin explants. *Following S.epidermidis culture on human skin explants overnight, bacteria were retrieved from the surface of the explants via two methods – 'swab' or 'vortex'. Images of serial dilutions of recovered bacteria in agar culture, (37°C, 24 hrs) are depicted: (A) no bacteria controls; samples recovered from (B) vortexed explants and (C) swabbed explants. Bacterial colonies did not grow on any dilution of recovered samples though contamination was present on all plates (blue arrows).*

Following culture of *S.epidermidis* on human skin explants overnight, bacteria were retrieved from the surface of the explants via two methods – 'swab' or 'vortex'. Initially, no colonies grew in the expected areas and there were signs of contamination (Figure 5-1). Due to the apparent lack of recovery of bacteria, the recovered samples were plated onto agar plates without dilution and incubated for 24 hours to determine if there were low numbers

of bacterial cells present in the samples (Figure 5-2). These bacteria successfully grew colonies in the expected area; the colonies were counted by hand where visible, however the results were inconsistent and no specific pattern was observed with respect to method of bacterial retrieval (vortex or swab). (Table 5-1, Table 5-2).

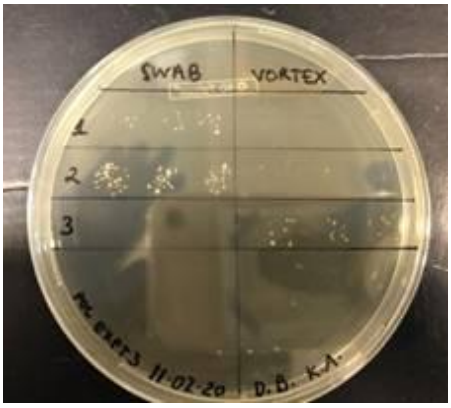

Figure 5-2: Undiluted bacteria successfully grown on agar, with variable results. Undiluted S.epidermidis transferred from surface of human skin explants to agar via two methods – "swab" and "vortex", in triplicate and grown overnight at 37°C. Bacteria successfully grew in 2/3 repeats for "swab" method and 1/3 repeats for "vortex" method.

Table 5-1: Number of cfus counted from the swabbed explants after 24hrs.

	Cfus counted (triplicate)	**Average cfu per 5µL**	**Average cfu per 500 µL**	**Average cfu/ml**
SWAB 1	7, 8, 8	7.67	766.67	1533.33
SWAB 2	40, 24, 30	31.3	3133.33	6266.67
SWAB 3	0, 0, 0	0	0	0

Table 5-2: Number of cfus counted from the vortexed explants after 24hrs.

	Cfus counted (triplicate)	Average cfu per 5µL	Average cfu per 500 µL	Average cfu/ml
VORTEX 1	0,0,0	0	0	0
VORTEX 2	0,1,0	0.33	33.33	66.67
VORTEX 3	9,10,12	10.33	1033.33	2066.67

5.2 Altering growth media

Upon re-evaluation of the method, it was decided that the reason for the unsuccessful growth of the bacteria could have been due to a lack of nutrients present on the surface of the skin explants, which would therefore lead to death of the bacteria. This theory was tested by altering the media in which the bacteria were diluted i.e. replacing PBS with tryptic soy broth (TSB) where previously mentioned. After repeating the whole experiment with this difference, more consistent results were obtained (Figure 5-3).

Table 5-3: Counted number of colonies per 5 µL and calculated amount per 500 µL

Dilution	Cfus counted	Average	Cfu per 500 µL	Average cfu/ml
10^{-5}	205, 172, 255	210.67	$210.67 \times 10^5 \times 100 = 2.11 \times 10^9$	4.22×10^9
10^{-6}	55, 75, 68	66	$66 \times 10^6 \times 100 = 6.6 \times 10^9$	1.32×10^{10}
10^{-7}	12, 21, 12	15	$15 \times 10^7 \times 100 = 1.5 \times 10^{10}$	3×10^{10}
10^{-8}	6, 7, 3	5.33	$5.33 \times 10^8 \times 100 = 5.3 \times 10^{10}$	1.06×10^{11}

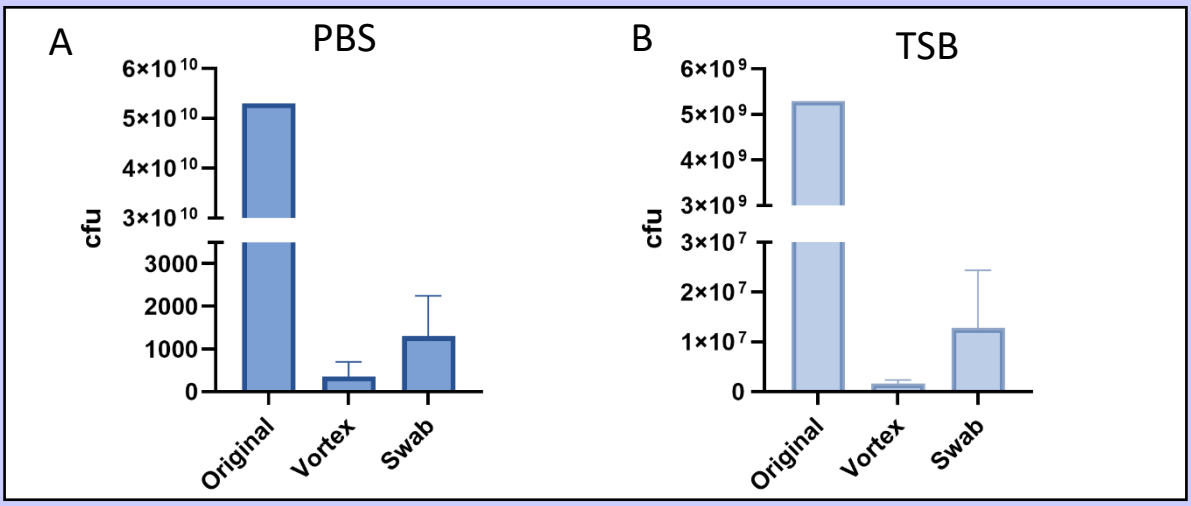

Figure 5-3: Bacteria recovered in TSB survived better. Average cfu/ml recovered from vortexed and swabbed samples compared to the original culture of bacteria when grown in (A) PBS and (B) TSB.

A much larger number of bacteria was obtained using TSB as the medium. However, the total number of bacteria obtained using both methods (swab and vortex) were a very small percentage of the total that was originally placed on the explant (10^7). This could suggest that either both methods are inefficient ways of retrieving bacteria from the samples, or that the bacteria simply could not survive on the explants overnight. A possible explanation for this could be due to the antiseptic that is used during the initial surgery performed on the donor, which could remain present on the skin explants leading to death of the bacteria.

5.3 Time analysis of bacterial growth

The aims of this experiment were to identify the cause of the previous experiments where bacteria failed to grow, and to monitor growth of bacteria during the day to determine the optimum time for retrieval of the bacteria in future experiments.

Upon analysis, it was concluded that 500 µL of bacteria in TSB reached the exponential phase the quickest, as expected (Figure 5-4). The 250 µL of bacteria did not grow at all – possibly due to contamination although the exact cause is unknown, especially since the 50 µL did start to multiply at around 3 hours.

Table 5-4: Number of colonies measured throughout 4 hours in differing concentrations of TSB.

Time (hrs)	Volume of bacteria in 5 ml TSB (µL)	OD	Calculated cfu/ml
0	50	0.297	2.97×10^7
	250	0.393	3.93×10^7
	500	0.715	7.15×10^7
1	50	0.020	2.00×10^7
	250	0.070	7.00×10^7
	500	0.156	1.56×10^8
2	50	0.065	6.50×10^7
	250	0.070	7.00×10^7
	500	0.495	4.95×10^8
3	50	0.150	1.50×10^8
	250	0.089	8.90×10^7
	500	0.850	8.50×10^8
4	50	0.307	3.07×10^8
	250	0.096	9.60×10^7
	500	1.253	1.25×10^9

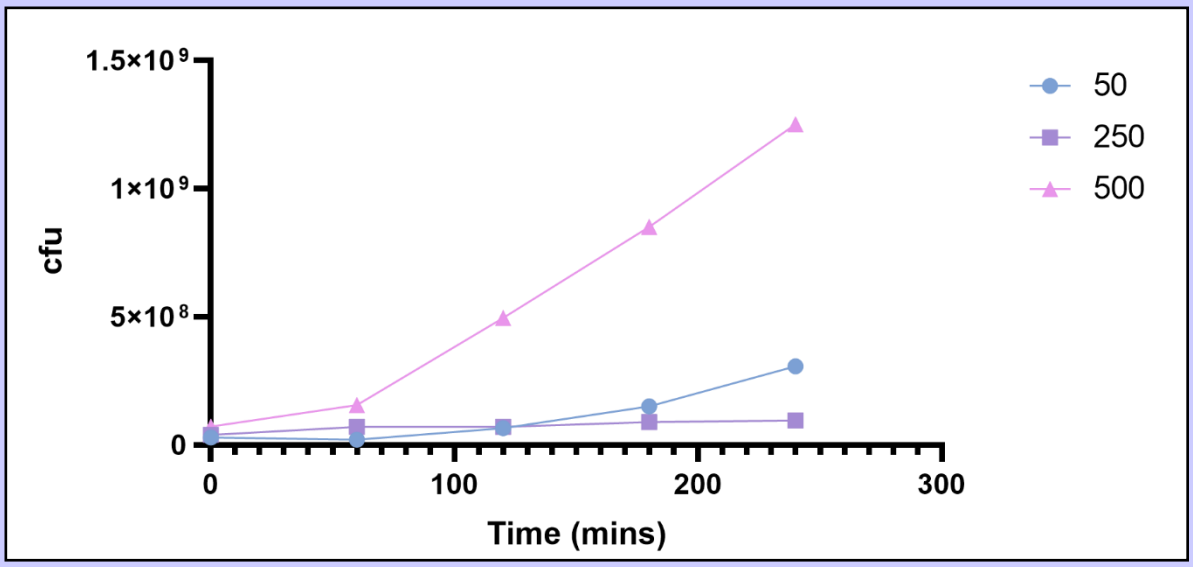

Figure 5-4: Higher concentrations of bacteria grow exponentially faster. *Growth of bacteria was measured over time at different concentrations, 50uL, 250uL and 500uL per 5ml TSB.*

5.4 qRT-PCR – S.epidermidis

PoC experiments (Chapter 2.9) were performed to investigate the effects of bacteria on the surface of the skin on expression of four other genes which were selected based on previous literature and their involvement in wound healing and *S.epidermidis* was added to the surface of the skin explants and RNA was subsequently extracted from the explants, comparing gene expression in the skin treated with (+BAC) and without (-BAC) bacteria for 4 genes; TNFα, IL-6, IL-8 and PCNA (Figure 5-5). Two individual experiments named "PoC3" and "PoC4" using the same methodology as outlined in Chapter 2.9; to grow bacteria on the skin explants, and these explants were used as subjects for this portion of the study.

TNFα

The expression of the cytokine TNFα was quantified by qRT-PCR in the -BAC and +BAC skin explants in the NSPinfex experiments. A trend towards higher expression of TNFα was observed in the +BAC samples, although this didn't reach statistical significance. However, this difference was more noticeable in the PoC3 skin samples, with a fold change of around 2.5.

IL-6

Quantification of the steady state mRNA levels of cytokine IL-6 in the skin explants treated with and without *S.epidermidis* revealed a significant upregulation of 6-fold in both PoC3 ($p=0.003251$) and PoC4 ($p=0.002616$). Due to high statistical significance and consistency of fold change between the two experiments, the data suggests a possible direct correlation between the bacterial stimulus and internal expression of IL-6.

IL-8

IL-8 expression was unchanged upon stimulation with the bacteria in PoC4, however a downregulation of the cytokine mRNA was observed in PoC4. Since neither of these results were of statistical significance it is unlikely that the addition of the bacteria had an effect on IL-8 expression.

PCNA

This marker of proliferation, PCNA was also measured in the explants from PoC3 and PoC4, however, other than a small increase in expression in PoC4 +BAC compared to its corresponding -BAC, which was not statistically significant, there was no difference seen in the expression of this gene as a result of addition of *S.epidermidis*.

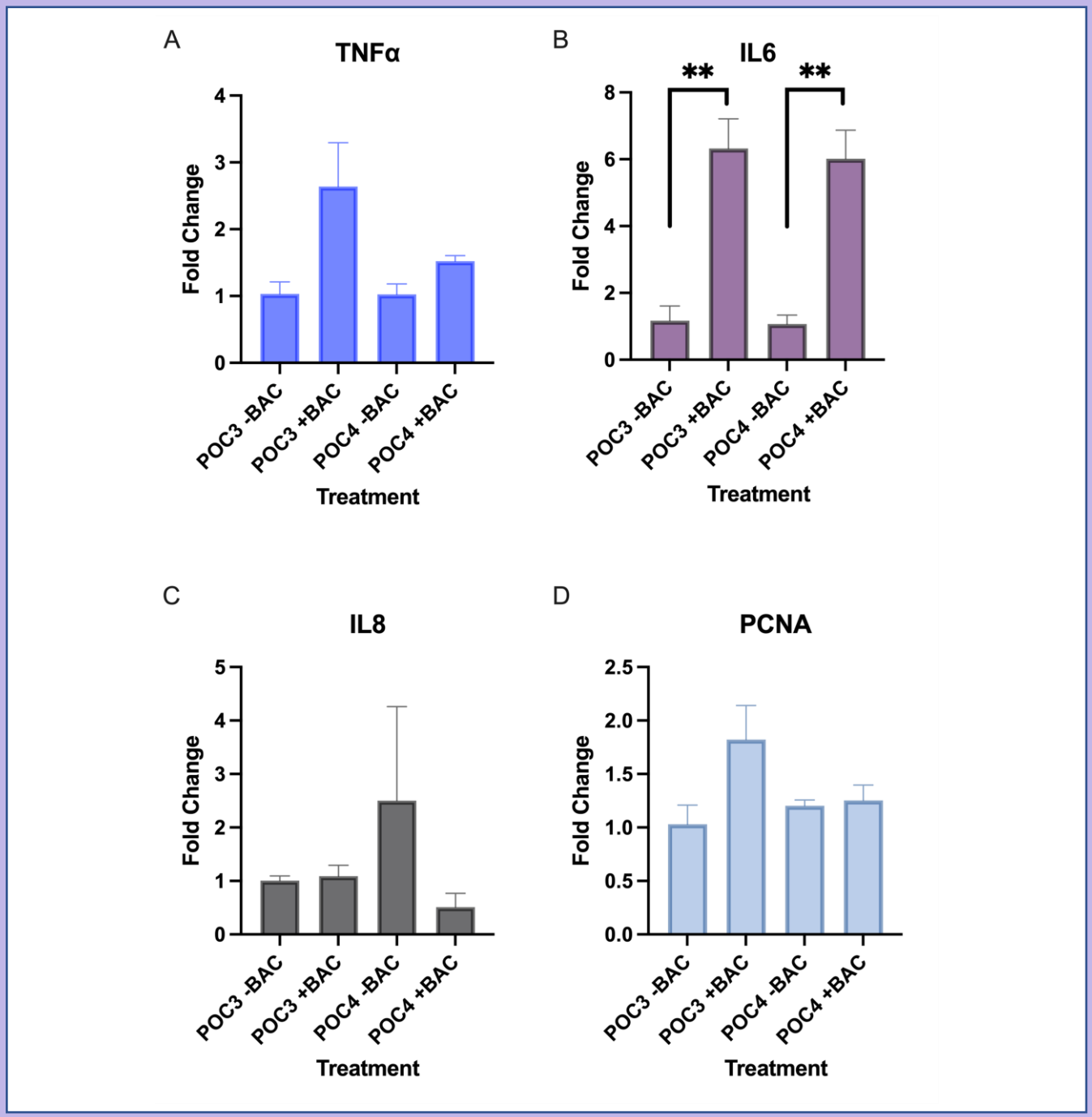

Figure 5-5: Bacteria addition to skin explants increases expression of interleukin 6. *Steady state mRNA levels of (A) TNFα (B) IL6, (C) IL8 and (D) PCNA in human skin explants taken from two proof of concept experiments – PoC3 and PoC4 each treated with and without S.epidermidis (-BAC and +BAC, respectively). Shapiro Wilk test of normality performed on all data proved all data normally distributed, subsequent One-way ANOVA performed to test null-hypothesis. **p<0.01.*

5.5 Chapter 5 Conclusion

Ultimately, this PoC experiment proved to lack precision in a few areas, and a lot more work is needed to streamline this method before it can be used as a method for future analysis of differential growth of bacteria under different conditions. On the other hand, some bacteria did survive and was successfully retrieved and counted, so these are promising results for future studies.

The qRT-PCR experiment assessing the effects of the addition of bacteria *S.epidermidis* to the skin revealed a significant upregulation in IL-6 expression. This could occur due to the role for IL-6 in acute-phase response during bacterial infection (Wu et al., 2016).

Chapter 6: Discussion

6.0 Chapter 6 Introduction

The present study tested the hypothesis that the kynurenine pathway may exert effects on wound healing in diabetes and/or chronic inflammation through related pathways and mechanisms. Previous literature on the pathway is limited and further research is required in order to fully comprehend the role of the pathway in diabetic wound healing. Possible conclusions may be drawn linking tryptophan catabolism to inflammatory wound healing which involves the kynurenine pathway, IDO1 and TDO2.

The initial hypothesis suggested that high levels of the enzymes IDO1 and TDO2 would have a negative impact on wound healing and therefore would contribute to formation of DFUs due to elevated levels of the proteins in the characteristic chronic inflammatory state of diabetic patients. However, results from this study suggest the opposite is true, and that upon inhibition of TDO2, wound healing is impeded, therefore a positive correlation between TDO2 levels and rate of wound healing was observed. This could imply that the higher levels of TDO2 in a diabetic patient with chronic inflammation could have a positive effect on wound healing and that patients with higher levels of TDO2 have better wound healing capabilities, therefore may be less likely to develop DFUs. Further research is needed to confirm this possibility, as the present study did not perform any *in-vivo* tests. Additionally, while the IDO1 protein was not analysed as part of this study, based on evidence from previous literature, a mechanism for the relation between the kynurenine pathway and chronic wound healing was proposed (Figure 6-1). This chapter will summarise the proposed mechanism for the delayed wound healing and chronic inflammatory effects of TDO2, IDO1 and associated proteins based on results obtained from this study and previous literature.

6.1 Discussion of experiment results

Analysis of the expression of TDO2 in this study highlighted the highly stimulative effect of cytokines on TDO2 gene expression. Firstly, in the microarray, TDO2 was the most second most highly upregulated gene in inflammatory conditions, this effect was confirmed in the results of the qRT-PCR experiments. However, when protein expression was analysed via immunohistochemistry, this cytokine-mediated upregulation of TDO2 was not observed. This suggests that time may be an important aspect in the function of TDO2. Speculation that TDO2 may be involved in the process of wound healing led to the scratch wound assay experiments that incorporated the inhibitor 680C91 which blocked the effects of TDO2. The results of this experiment unexpectedly had the opposite effect of the original hypothesis, as blockade of TDO2 decreased the rate of wound closure. Since tryptophan has been shown in previous studies to increase wound healing, it was predicted that inhibition of the enzymes that break down tryptophan would lead to an increased rate of wound closure due to the subsequent higher level of residual tryptophan.

One theory of the effects seen during this study is that the heightened levels of TDO2/IDO1 as seen in the initial microarray and in the qRT-PCR experiments could be the physiological response to increased inflammation, and that in normal conditions this has a positive effect. However, these effects can be detrimental in chronic inflammatory conditions and also have a negative impact on wound healing. This provides a potential new link between chronic inflammation and delayed wound healing, presenting a potential new target for therapeutics.

A study by Asp et al. investigated the RNA expression of IDO1, TDO2 and other kynurenine metabolites in human dermal fibroblast cell cultures, comparing the untreated cells with cells treated with inflammatory cytokines IFN-γ and TNFα (Asp et al., 2011). They found that IDO1 was significantly upregulated (>105-fold; $p < 0.001$) upon cytokine stimulation, whereas TDO2 was significantly downregulated (20-fold; $p < 0.001$)(Asp et al., 2011). This inflammatory cytokine-induced upregulation of IDO1 supports the findings of previous literature and results of this project. The downregulation of TDO2 observed by Asp and

colleagues (2011) opposes the results of the microarray and the qRT-PCR obtained in this project, however it does partially agree with the results of the IHC.

Moreover, there is increasing evidence of the involvement of TDO2 in cancer, and emerging research suggests that presence of this enzyme is indicative of poor prognosis. Decades of research have proven cancer cells to be highly proliferative and resilient. However, in a non-cancer setting, where cells are failing to survive and proliferate, the phenotype of cancer cells could be emulated in order to prevent cell death and failure of wound healing such as in diabetic ulcers. Thus, upregulation of TDO2 in treatment of DFUs could be advantageous to wound healing. Nevertheless, targeting the enzyme directly may not be the best method due to this possibility of cancer development, and decreased lifespan; as knockdown of TDO2 was shown in Caenorhabditis elegans to increase lifespan by ~15% (Sorgdrager et al., 2019). Further research is required in order to confirm the correct theory.

6.2 Proposed Mechanism

One of the main activators of TDO2 and IDO1 expression is the transcription factor AhR. A feed forward activation loop is formed between the interactions of the kynurenine pathway with AhR leading to more transcription of IDO1 and TDO2 as well as genes involved in cell migration.

The number labels in Figure 6-1 will be discussed in further detail below.

① *The Kynurenine Pathway*

The kynurenine pathway is the metabolic pathway through which the amino acid tryptophan is catabolised. The first rate-limiting step of the pathway is catalysed by either IDO1 or TDO2, depending on circumstance and/or location. For example, in the liver, TDO2 is the main enzyme performing this function. The kynurenine pathway is activated in inflammatory, infectious, and stressful circumstances (Mándi et al., 2022). Over 95% of tryptophan is metabolized into kynurenine and its products, leading to the production of one molecule of NAD+ per tryptophan molecule metabolised (Savitz, 2020)(Yu et al., 2018). This catabolism of tryptophan primarily occurs in healthy individuals in the liver via TDO2 activation (Bandeira et al., 2015). The pathway undergoes various steps (not shown) eventually producing kynurenine as the final product. Kynurenine then leads to activation of the transcription factor AhR (Seok et al., 2018).

② *The Aryl hydrocarbon receptor*

The aryl hydrocarbon receptor (AhR) is a ligand-activated transcription factor that acts as a sensitive sensor for xenobiotics and is abundantly expressed in the skin (Furue et al., 2019). AhR effects are complex and recent evidence suggests that AhR is also a sensor for maintaining haemostatis under healthy physiological conditions (reviewed in Murray and Perdew, 2020) AhR senses products of the kynurenine pathway and may have an important role in the IDO1/TDO2 pathway that implicates wound healing. It is involved in activation of expression of the IDO1 and TDO2 genes, as well as direct activation of the IDO1 protein

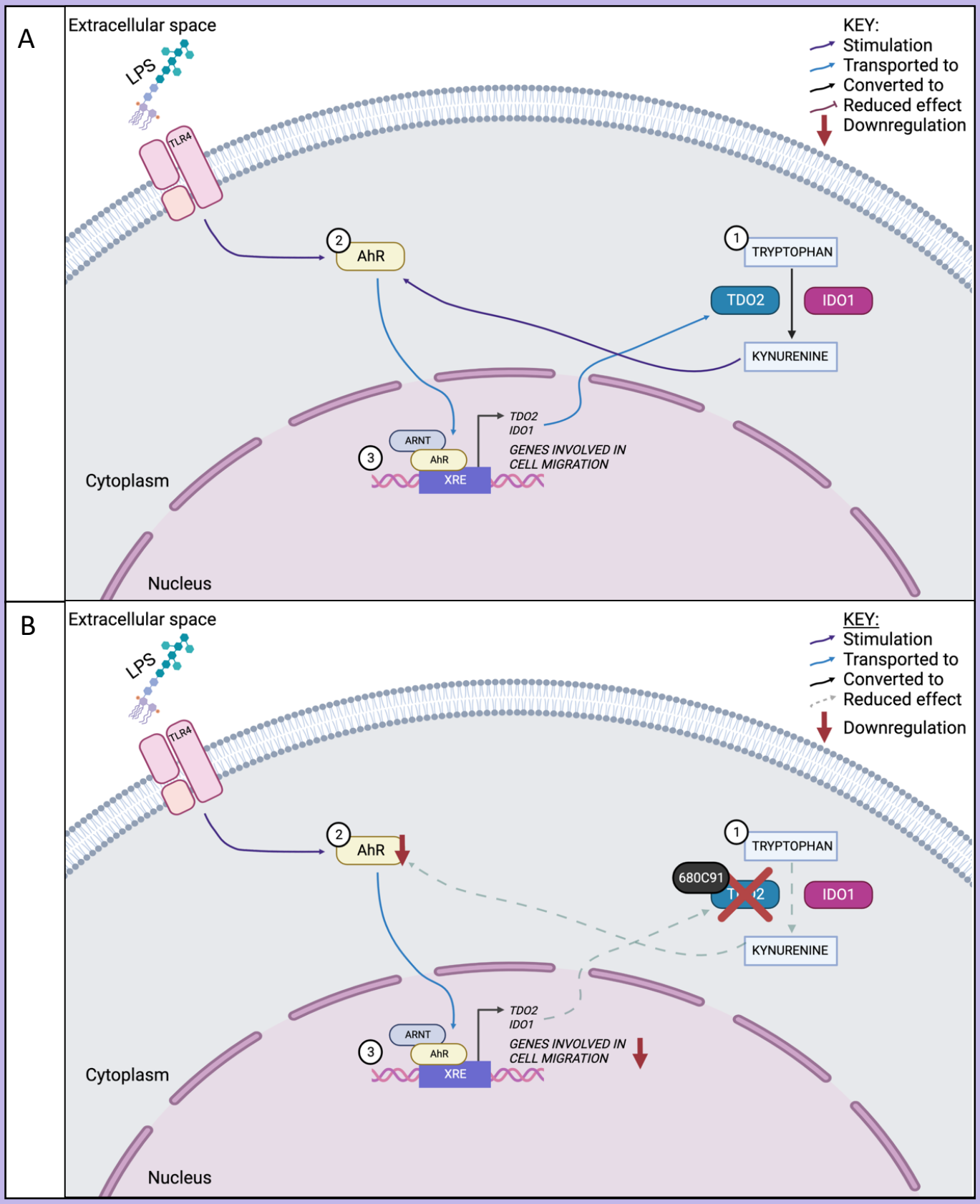

Figure 6-1: Feed-forward activation loop between AhR and the kynurenine pathway. *(A) The proteins IDO1 and TDO2 catalyse formation of kynurenine through a cascade of events (not shown). Kynurenine then feeds back to AhR, further activating it, as well as bacterial products such as LPS. Activation of AhR leads to translocation to the cell nucleus and transcription of genes involved in cell migration (aiding wound healing) as well as TDO2 and IDO1, which further increases activity of kynurenine pathway. (B) Addition of the TDO2 inhibitor 680C91 causes reduced effect of kynurenine on AhR therefore less TDO2, IDO1 and cell migration gene expression, leading to impeded wound healing effect.*

itself. In the absence of ligands, AhR exists in the cytoplasm as an inactive complex made up of 90kDa heatshock protein (HSP90), AhR interacting protein (AIP- otherwise known as XAP2), the protein kinase SRC and co-chaperone p23 (Rothhammer and Quintana, 2019). This complex stabilises the protein, preventing proteasomal degradation and localising it to the cytoplasm, and also allows it to have high affinity for its ligands. Once an AhR agonist binds, AIP dissociates from the complex which results in shuttling of the complex to nucleus. AhR then dissociates and binds to a protein called ARNT (also known as hypoxia inducible factor 1β). This AhR-ARNT complex then translocates to xenobiotic response elements (XREs) to promote expression of target genes, including TDO2 and IDO1.

Some studies have shown a role for AhR in wound healing of the skin. For example, a study by Barouti et al found that AhR is expressed in the leading edge of *in vitro* wounds. They also found that patients with acute dioxin intoxication caused by environmental pollutant 2,3,7,8-tetrachlorobenzo-p-dioxin (TCDD) had faster healing wounds. TCDD is a member of the dioxin family and an activator of AhR, and this was thought to be the reason behind faster wound healing caused by TCDD accelerating wound healing. Previous studies have also reported that TCDD-driven AhR activation results in a significant upregulation of IL-10 (Zhu et al., 2018). Since tryptophan has a shorter half-life than TCDD and is also an activating AhR agonist, it could have the same effect and would be more useful for use in clinical treatment. Furthermore, bacterial metabolism of tryptophan can produce metabolites which can act as AhR agonists, this can lead to an increased efficiency of wound healing of the skin, especially in wounds where there is a high degree of bacterial infection such as in DFUs (Barouti et al., 2015). This would suggest an internal response to LPS in which presence of the bacterial product is indicative of infection, therefore the response would be to upregulate genes involved in wound healing to prevent further infiltration of pathogens into the wound.

③ *AhR and cell migration*

Previous studies have shown links between AhR and epithelial mesenchymal transition (EMT), highlighting an important role of this transcription factor in cell migration. A study by Ikuta et al. found that AhR expression is induced by loss of cell-cell contact, and

subsequently acts as a transcription factor for Slug; a protein involved in reduced level of cytokeratin 18, an epithelial marker, and with increased fibronectin, a mesenchymal marker (Belguise et al., 2007). These data suggest that activation of AhR could aid in wound healing by encouraging the important process of EMT in cell migration.

On the other hand, other studies such as Carvajal-Gonzalez et al. reveal that AhR-/- mice exhibit accelerated wound healing. Wounds in these mice had a higher collagen content and enhanced re-epithelialisation through activation of TGF-β. The difference in AhR function could lie in the nature of the inflammatory phase of wound healing. Interestingly, it is beneficial to have an absence of AhR in the later phases of wound healing, i.e. collagen formation and proliferation/migration of keratinocytes, when inflammation is resolved. In a chronic inflammatory state, however, AhR has a beneficial effect on wound healing. There are currently no mouse studies incorporating diabetic wounds in analysis of AhR on wound healing. It would be useful to compare the role of AhR in chronic inflammatory conditions and normal wound healing where inflammation still occurs but resolves itself accordingly. In contrast Cecchi et al also found inhibition of TDO2 with 680C91 decreased dexamethasone induced cell migration and proliferation, indicating a potential link between the TDO2-AhR pathway and glucocorticoids.

Summary

In summary, AhR is an important factor in the involvement of TDO2 and IDO1 in skin wound healing, with links to oxidative stress, bacterial infection and inflammation and immunity and could be fundamental in the link between the kynurenine pathway and wound healing. Chronic inflammation (for example in diabetes) causes upregulation of TDO2, which activates the kynurenine pathway, leading to larger amounts of kynurenine production. Kynurenine then activates AhR, in addition to LPS from an infected wound, leading to upregulation of expression of genes involved in cell migration.

Topical treatment of Tapinarof, a natural AhR agonist has previously been shown to resolve skin inflammation in mice and humans, aiding in the treatment of psoriasis and atopic dermatitis (Smith et al., 2017). A similar treatment could be used to treat DFUs, as activation

of AhR could have anti-inflammatory and positive wound healing effects, based on this data from previous research.

In the microarray data analysed as part of this study, the expression of the gene IDO1 was found to be upregulated upon stimulation with inflammatory cytokines (1.7-fold) but not modulated in the other donor and qRT-PCR validation showed very low levels of detectable expression of IDO1. However, immunohistochemistry revealed that the protein IDO1 was slightly downregulated upon stimulation with the same cytokines. This result was unexpected initially, however upon further research, the non-redundant roles of TDO2 and IDO1 became clear (Puccetti, 2014). That is, in inflammatory conditions, the catalysis of the first step of the kynurenine pathway switches from being performed by IDO1 to TDO2, due to the presence of IL-6 which is necessary for the inflammatory response but also drives the proteasomal degradation of IDO1. Therefore, although the RNA expression of IDO1 may marginally increase, the protein level may be depleted, while TDO2 RNA expression will increase along with the protein expression and activity. This theory corresponds with the results of the microarray where TDO2 was very strongly up-regulated (up to 20-fold) and in immunohistochemistry by inflammatory cytokines in this project.

6.3 Experimental limitations and future experiments.

Though the current study highlighted certain effects of TDO2 on skin wound healing, much of the proposed mechanism is speculative in nature. This is due to lack of sufficient time and fresh skin tissue supply (as a result of the COVID-19 pandemic) to clarify the roles of the various compounds in wound healing of the skin.

Although the effects of IDO1 were not elucidated during this study, much of the previous literature on IDO1 has proven that this enzyme is a key component in chronic inflammation. This role mainly involves immune cells which were difficult to implicate in this study as *ex-vivo* models were used where there is no blood supply i.e. no immune cells present in the model. Thus, the exerted effect of IDO1 could not have been observed or analysed. Therefore, future studies should examine the alternative expression of IDO1 in inflammatory vs normal conditions in-vivo. This could involve an IDO1 knock-out experiment in *Mus Musculus*, where wound healing could be analysed in the knock-out mice compared to the wild-type mice. There have been a few previous studies that have used a similar model to this, however none yet with regards to the effects of wound healing (Hirata et al., 2018).

Since the model system used in this study were human skin explants, there were some limitations, especially with regards to inflammation. While the skin explants do contain resident immune cells, any recruitment of additional immune cells is not possible due to the absence of a blood supply and other organ systems. This is where *in-vivo* mouse models systems would be of more value.

Recently, a Ido1/Tdo2 knockout mouse model was characterised and shown to display various features although a good rate of survival (Aslamkhan et al., 2020). This suggests that these enzymes are a potential target for therapy. Future studies could incorporate an experiment which compares the wound healing rates of these knock out mice compared to wildtype mice, also comparing single knock-out to double knock-out. This would elucidate the question of whether the two enzymes are synonymous or whether one is more important than the other.

In addition, the microarray results highlighted a key factor. The donor SPL003 had a fold change of 20.59, whist the donor SPL004 only had a fold change of 8.97. Whilst this is still a significant fold change, it is vastly divergent to the fold change of SPL003. This implies variability in the levels of initial TDO2 within each patient and/or variability in the responsiveness of the enzyme to stimuli. Future studies could explore whether these variabilities impact the rate of wound healing i.e., testing if patients with naturally higher levels of TDO2 have a higher wound healing ability or vice versa.

6.4 Conclusion

Ultimately, the findings of this study point to a potential role for TDO2 in inflammatory wound healing, especially with relation to AhR. The entire pathway may be implemented in deregulation of normal wound healing in diabetic patients or in other chronic inflammatory diseases based on previous literature. However further research is still needed to fully understand the mechanisms explored in this project.

Current data on the enzymes TDO2 and IDO1 is lacking, especially with regards to wound healing. Since some studies have implied a role for TDO2 in cancer, there is also its potential use in wound healing in a non-cancer state. On the other hand, upregulation of these proteins in an effort to treat patients could present adverse effects due to the correlation between the kynurenine metabolites and oxidative stress. A potential solution could be to target the AhR protein instead since it is more well-known and therefore potentially safer due to its proven roles in promotion of wound healing and inflammation resolution. Alternatively, antioxidants could be used in combination with compounds targeting TDO2 or IDO1 when used in therapy to prevent the harmful effects of the oxidative kynurenines.

The qRT-PCR experiment showed a dramatic increase in TDO2 expression followed by inflammatory cytokine addition, consistent with the findings from the initial microarray experiment. However, it was not possible to explain the significance of this change due to the lack of previous research on the TDO2 protein. It is clear that TDO2 is preferentially utilised for tryptophan catabolism in inflammatory conditions, but what difference does this make? Could it be due to the structural component of TDO2 and its higher affinity for tryptophan? Perhaps the existence of the two proteins is required for the same reasons two types of well-known oxygen carrying proteins of the blood exist – haemoglobin and myoglobin. Haemoglobin, like TDO2, is a homotetramer containing four heme groups. Myoglobin, like IDO1, is a monomer containing one heme group. The answers to these questions will only be found through years of further research.

References

Scientific Journals and Reviews

Abdelmannan, D., Tahboub, R., Genuth, S., Ismail-Beigi, F., n.d. Effect of dexamethasone on oral glucose tolerance in healthy adults. Endocr Pract 16, 770–7. https://doi.org/10.4158/EP09373.OR

Alexiadou, K., Doupis, J., 2012. Management of Diabetic Foot Ulcers. Diabetes Therapy 3. https://doi.org/10.1007/s13300-012-0004-9

Aslamkhan, A.G., Xu, Q., Loughlin, A., Vu, H., Pacchione, S., Bhatt, B., Garfinkel, I., Styring, T.G., LaFranco-Scheuch, L., Pearson, K., Reynolds, S., Li, N., Zhou, H., Miller, J.R., Solban, N., Bass, A., Glaab, W.E., 2020. Characterization of indoleamine-2,3-dioxygenase 1, tryptophan-2,3-dioxygenase, and Ido1/Tdo2 knockout mice. Toxicology and Applied Pharmacology 406, 115216. https://doi.org/10.1016/J.TAAP.2020.115216

Asp, L., Johansson, A.-S., Mann, A., Owe-Larsson, B., Urbanska, E.M., Kocki, T., Kegel, M., Engberg, G., Lundkvist, G.B., Karlsson, H., 2011. Effects of pro-inflammatory cytokines on expression of kynurenine pathway enzymes in human dermal fibroblasts. Journal of Inflammation 8, 25. https://doi.org/10.1186/1476-9255-8-25

Baltzis, D., Eleftheriadou, I., Veves, A., 2014. Pathogenesis and Treatment of Impaired Wound Healing in Diabetes Mellitus: New Insights. Advances in Therapy 31, 817–836. https://doi.org/10.1007/s12325-014-0140-x

Bandeira, L.G., Bortolot, B.S., Cecatto, M.J., Monte-Alto-Costa, A., Romana-Souza, B., 2015. Exogenous Tryptophan Promotes Cutaneous Wound Healing of Chronically Stressed Mice through Inhibition of TNF-alpha and IDO Activation. PLoS One 10, e0128439. https://doi.org/10.1371/journal.pone.0128439

Barouti, N., Mainetti, C., Fontao, L., Sorg, O., 2015. L-Tryptophan as a Novel Potential Pharmacological Treatment for Wound Healing via Aryl Hydrocarbon Receptor Activation. Dermatology 230, 332–339. https://doi.org/10.1159/000371876

Bass, R., Ellis, V., 2002. Cellular mechanisms regulating non-haemostatic plasmin generation. Biochem Soc Trans 30, 189–194. https://doi.org/10.1042/0300-5127:0300189

Belguise, K., Guo, S., Yang, S., Rogers, A.E., Seldin, D.C., Sherr, D.H., Sonenshein, G.E., 2007. Green Tea Polyphenols Reverse Cooperation between c-Rel and CK2 that Induces the Aryl Hydrocarbon Receptor, Slug, and an Invasive Phenotype. Cancer Res 67, 11742–11750. https://doi.org/10.1158/0008-5472.can-07-2730

Bertani, B., Ruiz, N., 2018. Function and Biogenesis of Lipopolysaccharides. EcoSal Plus 8. https://doi.org/10.1128/ecosalplus.esp-0001-2018

Birner, A., Platzer, M., Bengesser, S.A., Dalkner, N., Fellendorf, F.T., Queissner, R., Pilz, R., Rauch, P., Maget, A., Hamm, C., Herzog-Eberhard, S., Mangge, H., Fuchs, D., Moll, N., Zelzer, S., Schütze, G., Schwarz, M., Reininghaus, B., Kapfhammer, H.P., Reininghaus, E.Z., 2017. Increased breakdown of kynurenine towards its neurotoxic branch in bipolar disorder. PLoS ONE 12. https://doi.org/10.1371/JOURNAL.PONE.0172699

Bishop, A., 2008. Role of oxygen in wound healing. J Wound Care 17, 399–402. https://doi.org/10.12968/JOWC.2008.17.9.30937

Boer, M., Duchnik, E., Maleszka, R., Marchlewicz, M., 2016. Structural and biophysical characteristics of human skin in maintaining proper epidermal barrier function. Adv Dermatol Allergol 1, 1–5. https://doi.org/10.5114/pdia.2015.48037

Brem, H., Tomic-Canic, M., 2007. Cellular and molecular basis of wound healing in diabetes. Journal of Clinical Investigation 117, 1219–1222. https://doi.org/10.1172/jci32169
Carow, B., Rottenberg, M.E., 2014. SOCS3, a Major Regulator of Infection and Inflammation. Frontiers in Immunology 5, 58. https://doi.org/10.3389/fimmu.2014.00058
Cecchi, M., Paccosi, S., Silvano, A., Eid, A.H., Parenti, A., 2021. Dexamethasone Induces the Expression and Function of Tryptophan-2-3-Dioxygenase in SK-MEL-28 Melanoma Cells. Pharmaceuticals 14, 211. https://doi.org/10.3390/PH14030211
Chen, L., Deng, H., Cui, H., Fang, J., Zuo, Z., Deng, J., Li, Y., Wang, X., Zhao, L., 2018. Inflammatory responses and inflammation-associated diseases in organs. Oncotarget 9, 7204–7218. https://doi.org/10.18632/oncotarget.23208
Cristina De Oliveira Gonzalez, A., Fortuna Costa, T., De, Z., Andrade, A., Alves, A.R., Medrado, P., 2016. Wound healing-A literature review *. An Bras Dermatol 91, 614–634. https://doi.org/10.1590/abd1806-4841.20164741
Dąbrowska, A.K., Spano, | F, Derler, | S, Adlhart, | C, Spencer, | N D, Rossi, | R M, 2018. The relationship between skin function, barrier properties, and body-dependent factors. Skin Res Technol 24, 165–174. https://doi.org/10.1111/srt.12424
Davis, I., Liu, A., 2015. What is the tryptophan kynurenine pathway and why is it important to neurotherapeutics? Expert Review of Neurotherapeutics 15, 719–721. https://doi.org/10.1586/14737175.2015.1049999
Demidova-Rice, T.N., Hamblin, M.R., Herman, I.M., 2012. Acute and impaired wound healing: pathophysiology and current methods for drug delivery, part 1: normal and chronic wounds: biology, causes, and approaches to care. Adv Skin Wound Care 25, 304–314. https://doi.org/10.1097/01.ASW.0000416006.55218.d0
Dunnill, C., Patton, T., Brennan, J., Barrett, J., Dryden, M., Cooke, J., Leaper, D., Georgopoulos, N.T., 2015. Reactive oxygen species (ROS) and wound healing: the functional role of ROS and emerging ROS-modulating technologies for augmentation of the healing process. International Wound Journal. https://doi.org/10.1111/iwj.12557
Fallarino, F., Grohmann, U., Hwang, K.W., Orabona, C., Vacca, C., Bianchi, R., Belladonna, M.L., Fioretti, M.C., Alegre, M.L., Puccetti, P., 2003. Modulation of tryptophan catabolism by regulatory T cells. Nat Immunol 4, 1206–1212. https://doi.org/10.1038/ni1003
Feksa, L.R., Latini, A., Rech, V.C., Feksa, P.B., Koch, G.D.W., Amaral, M.F.A., Leipnitz, G., Dutra-Filho, C.S., Wajner, M., Wannmacher, C.M.D., 2008. Tryptophan administration induces oxidative stress in brain cortex of rats. Metabolic Brain Disease 23, 221–233. https://doi.org/10.1007/s11011-008-9087-4
Frykberg, R.G., Banks, J., 2015. Challenges in the Treatment of Chronic Wounds. Advances in Wound Care 4, 560. https://doi.org/10.1089/WOUND.2015.0635
Furue, K., Ito, T., Tsuji, G., Ulzii, D., Vu, Y.H., Kido-Nakahara, M., Nakahara, T., Furue, M., 2019. The IL-13–OVOL1–FLG axis in atopic dermatitis. Immunology 158, 281–286. https://doi.org/10.1111/imm.13120
Furuya, F., Ishii, T., Kitamura, K., 2019. Chronic Inflammation and Progression of Diabetic Kidney Disease. Contributions to Nephrology 198, 33–39. https://doi.org/10.1159/000496526
Gao, M., Nguyen, T.T., Suckow, M.A., Wolter, W.R., Gooyit, M., Mobashery, S., Chang, M., 2015. Acceleration of diabetic wound healing using a novel protease–anti-protease combination therapy. Proceedings of the National Academy of Sciences 112, 15226–15231. https://doi.org/10.1073/pnas.1517847112

Gordon, R., 2013. Skin Cancer: An Overview of Epidemiology and Risk Factors. Seminars in Oncology Nursing 29, 160–169. https://doi.org/10.1016/j.soncn.2013.06.002
Guo, S., Dipietro, L.A., 2010. Factors Affecting Wound Healing. J Dent Res 89, 219–229. https://doi.org/10.1177/0022034509359125
Gurtner, G.C., Werner, S., Barrandon, Y., Longaker, M.T., 2008. Wound repair and regeneration. Nature 453, 314–321. https://doi.org/10.1038/nature07039
Hayaishi, O., 1993. My life with tryptophan--never a dull moment. Protein Sci 2, 472–475. https://doi.org/10.1002/pro.5560020320
Hillmer, E.J., Zhang, H., Li, H.S., Watowich, S.S., 2016. STAT3 signaling in immunity. Cytokine Growth Factor Rev 31, 1–15. https://doi.org/10.1016/j.cytogfr.2016.05.001
Hirata, N., Hattori, S., Shoji, H., Funakoshi, H., Miyakawa, T., 2018. Comprehensive behavioral analysis of indoleamine 2,3-dioxygenase knockout mice. Neuropsychopharmacol Rep 38, 133–144. https://doi.org/10.1002/NPR2.12019
Hollingshead, B.D., Beischlag, T. v, Dinatale, B.C., Ramadoss, P., Perdew, G.H., 2008. Inflammatory signaling and aryl hydrocarbon receptor mediate synergistic induction of interleukin 6 in MCF-7 cells. Cancer Res 68, 3609–3617. https://doi.org/10.1158/0008-5472.CAN-07-6168
Ito, H., Ando, T., Arioka, Y., Saito, K., Seishima, M., 2015. Inhibition of indoleamine 2,3-dioxygenase activity enhances the anti-tumour effects of a Toll-like receptor 7 agonist in an established cancer model. Immunology 144, 621–630. https://doi.org/10.1111/imm.12413
Kanitakis, J., 2002. Anatomy, histology and immunohistochemistry of normal human skin. Eur J Dermatol 12, 390–9; quiz 400–1.
Khalil, C., 2018. Human skin explants an in vitro approach for assessing UVB induced damage. Toxicol In Vitro 53, 193–199. https://doi.org/10.1016/J.TIV.2018.08.013
Kobayashi, T., Naik, S., Nagao, K., 2019. Choreographing Immunity in the Skin Epithelial Barrier. Immunity 50, 552–565. https://doi.org/10.1016/j.immuni.2019.02.023
Koh, T.J., DiPietro, L.A., 2011. Inflammation and wound healing: the role of the macrophage. Expert Rev Mol Med 13, e23–e23. https://doi.org/10.1017/S1462399411001943
Kolarsick, P.A.J., Kolarsick, M.A., Goodwin, C., 2011. Anatomy and Physiology of the Skin. J Dermatol Nurses Assoc 3, 203–213. https://doi.org/10.1097/jdn.0b013e3182274a98
Krishna Kolluru, G., Bir, S.C., Kevil, C.G., Calvert, J.W., 2012. Endothelial Dysfunction and Diabetes: Effects on Angiogenesis, Vascular Remodeling, and Wound Healing. International Journal of Vascular Medicine 2012, 30. https://doi.org/10.1155/2012/918267
Krzyszczyk, P., Schloss, R., Palmer, A., Berthiaume, F., 2018. The Role of Macrophages in Acute and Chronic Wound Healing and Interventions to Promote Pro-wound Healing Phenotypes. Front Physiol 9, 419. https://doi.org/10.3389/fphys.2018.00419
Lawton, S., 2019. Skin 1: the structure and functions of the skin. Nursing Times [online]; 115, 12, 30-33.
Mándi, Y., Stone, T.W., Guillemin, G.J., Vécsei, L., Williams, R.O., 2022. Editorial: Multiple Implications of the Kynurenine Pathway in Inflammatory Diseases: Diagnostic and Therapeutic Applications. Frontiers in Immunology 13, 427. https://doi.org/10.3389/FIMMU.2022.860867/BIBTEX
Martinotti, S., Ranzato, E., 2020. Scratch Wound Healing Assay. Methods Mol Biol 2109, 225–229. https://doi.org/10.1007/7651_2019_259

Mirza, R.E., Fang, M.M., Ennis, W.J., Koh, T.J., n.d. Blocking Interleukin-1b Induces a Healing-Associated Wound Macrophage Phenotype and Improves Healing in Type 2 Diabetes. https://doi.org/10.2337/db12-1450

Munn, D.H., Zhou, M., Attwood, J.T., Bondarev, I., Conway, S.J., Marshall, B., Brown, C., Mellor, A.L., 1998. Prevention of Allogeneic Fetal Rejection by Tryptophan Catabolism. Science (1979) 281, 1191–1193. https://doi.org/10.1126/science.281.5380.1191

Murakami, Y., Hoshi, M., Imamura, Y., Arioka, Y., Yamamoto, Y., Saito, K., 2013. Remarkable Role of Indoleamine 2,3-Dioxygenase and Tryptophan Metabolites in Infectious Diseases: Potential Role in Macrophage-Mediated Inflammatory Diseases. Mediators of Inflammation 2013, 1–9. https://doi.org/10.1155/2013/391984

Murray, I.A., Perdew, G.H., 2020. How Ah Receptor Ligand Specificity Became Important in Understanding Its Physiological Function. Int J Mol Sci 21, 1–19. https://doi.org/10.3390/IJMS21249614

Nguyen, N.T., Hanieh, H., Nakahama, T., Kishimoto, T., 2013. The roles of aryl hydrocarbon receptor in immune responses. Int Immunol 25, 335–343. https://doi.org/10.1093/intimm/dxt011

Nguyen, A. v, Soulika, A.M., 2019. Molecular Sciences The Dynamics of the Skin's Immune System. https://doi.org/10.3390/ijms20081811

Novikov, O., Wang, Z., Stanford, E.A., Parks, A.J., Ramirez-Cardenas, A., Landesman, E., Laklouk, I., Sarita-Reyes, C., Gusenleitner, D., Li, A., Monti, S., Manteiga, S., Lee, K., Sherr, D.H., 2016. An aryl hydrocarbon receptor-mediated amplification loop that enforces cell migration in ER-/PR-/Her2- human breast cancer cells. Molecular Pharmacology 90, 674–688. https://doi.org/10.1124/MOL.116.105361/-/DC1

Nowak, C., Hetty, S., Salihovic, S., Castillejo-Lopez, C., Ganna, A., Cook, N.L., Broeckling, C.D., Prenni, J.E., Shen, X., Giedraitis, V., Ärnlöv, J., Lind, L., Berne, C., Sundström, J., Fall, T., Ingelsson, E., n.d. Glucose challenge metabolomics implicates medium-chain acylcarnitines in insulin resistance OPEN. https://doi.org/10.1038/s41598-018-26701-0

Opitz, C.A., Somarribas Patterson, L.F., Mohapatra, S.R., Dewi, D.L., Sadik, A., Platten, M., Trump, S., 2020. The therapeutic potential of targeting tryptophan catabolism in cancer. British Journal of Cancer 122, 30–44. https://doi.org/10.1038/s41416-019-0664-6

Orabona, C., Pallotta, M.T., Grohmann, U., 2012. Different partners, opposite outcomes: a new perspective of the immunobiology of indoleamine 2,3-dioxygenase. Mol Med 18, 834–842. https://doi.org/10.2119/molmed.2012.00029

Orzalli, M.H., 2019. Human Skin Explants Recapitulate Key Features of HSV-1 Infections. Journal of Investigative Dermatology 139, 519–521. https://doi.org/10.1016/J.JID.2018.09.015

Pahwa, R., Goyal, A., Jialal, I., 2021. Chronic Inflammation. Pathobiology of Human Disease: A Dynamic Encyclopedia of Disease Mechanisms 300–314. https://doi.org/10.1016/B978-0-12-386456-7.01808-6

Pakyari, M., Farokhi, A., Jalili, R.B., Kilani, R.T., Brown, E., Ghahary, A., 2019. Local Expression of Indoleamine 2,3, Dioxygenase Prolongs Allogenic Skin Graft Take in a Mouse Model. Adv Wound Care (New Rochelle) 8, 58–70. https://doi.org/10.1089/wound.2018.0811

Park, S., Kang, H.J., Jeon, J.H., Kim, M.J., Lee, I.K., 2019. Recent advances in the pathogenesis of microvascular complications in diabetes. Arch Pharm Res 42, 252–262. https://doi.org/10.1007/S12272-019-01130-3

Patel, S., Srivastava, S., Singh, M.R., Singh, D., 2019. Mechanistic insight into diabetic wounds: Pathogenesis, molecular targets and treatment strategies to pace wound healing. Biomedicine and Pharmacotherapy 112. https://doi.org/10.1016/J.BIOPHA.2019.108615

Phillips, S.J., 2000. Physiology of Wound Healing and Surgical Wound Care. ASAIO Journal 46.

Pierce, G.F., 2001. Inflammation in nonhealing diabetic wounds: the space-time continuum does matter. Am J Pathol 159, 399–403. https://doi.org/10.1016/S0002-9440(10)61709-9

Powell, J., 2006. Skin physiology. Women's Health Medicine 3, 130–133. https://doi.org/10.1383/wohm.2006.3.3.130

Puccetti, P., 2014. On the Non-Redundant Roles of TDO2 and IDO1. Frontiers in Immunology 5, 522. https://doi.org/10.3389/fimmu.2014.00522

Reaven, E.P., Cox, A.J., 1965. ORGAN CULTURE OF HUMAN SKIN*. Journal of Investigative Dermatology 44, 151–156. https://doi.org/10.1038/jid.1965.29

Richards, C.D., 2013. The Enigmatic Cytokine Oncostatin M and Roles in Disease. ISRN Inflammation 2013, 1–23. https://doi.org/10.1155/2013/512103

Rittié, L., Sachs, D.L., Orringer, J.S., Voorhees, J.J., Fisher, G.J., 2013. Eccrine Sweat Glands are Major Contributors to Reepithelialization of Human Wounds. The American Journal of Pathology 182, 163–171. https://doi.org/10.1016/j.ajpath.2012.09.019

Rothhammer, V., Quintana, F.J., 2019. The aryl hydrocarbon receptor: an environmental sensor integrating immune responses in health and disease. Nature Reviews Immunology 19, 184–197. https://doi.org/10.1038/s41577-019-0125-8

Sahle, F.F., Gebre-Mariam, T., Dobner, B., Wohlrab, J., Neubert, R.H., 2015. Skin diseases associated with the depletion of stratum corneum lipids and stratum corneum lipid substitution therapy. Skin Pharmacol Physiol 28, 42–55. https://doi.org/10.1159/000360009

Sari, S., Tomek, P., Leung, E., Reynisson, J., 2019. Discovery and Characterisation of Dual Inhibitors of Tryptophan 2,3-Dioxygenase (TDO2) and Indoleamine 2,3-Dioxygenase 1 (IDO1) Using Virtual Screening. Molecules 24. https://doi.org/10.3390/molecules24234346

Savitz, J., 2020. The kynurenine pathway: a finger in every pie. Mol Psychiatry 25, 131–147. https://doi.org/10.1038/s41380-019-0414-4

Seok, S.H., Ma, Z.X., Feltenberger, J.B., Chen, Hongbo, Chen, Hui, Scarlett, C., Lin, Z., Satyshur, K.A., Cortopassi, M., Jefcoate, C.R., Ge, Y., Tang, W., Bradfield, C.A., Xing, Y., 2018. Trace derivatives of kynurenine potently activate the aryl hydrocarbon receptor (AHR). The Journal of Biological Chemistry 293, 1994. https://doi.org/10.1074/JBC.RA117.000631

Simonneau, M., Frouin, E., Huguier, V., Jermidi, C., Jégou, J.F., Godet, J., Barra, A., Paris, I., Levillain, P., Cordier-Dirikoc, S., Pedretti, N., Bernard, F.X., Lecron, J.C., Morel, F., Favot, L., 2018. Oncostatin M is overexpressed in skin squamous-cell carcinoma and promotes tumor progression. Oncotarget 9, 36457–36473. https://doi.org/10.18632/ONCOTARGET.26355

Smith, S.H., Jayawickreme, C., Rickard, D.J., Nicodeme, E., Bui, T., Simmons, C., Coquery, C.M., Neil, J., Pryor, W.M., Mayhew, D., Rajpal, D.K., Creech, K., Furst, S., Lee, J., Wu, D., Rastinejad, F., Willson, T.M., Viviani, F., Morris, D.C., Moore, J.T., Cote-Sierra, J., 2017. Tapinarof Is a Natural AhR Agonist that Resolves Skin Inflammation in

Mice and Humans. Journal of Investigative Dermatology 137, 2110–2119. https://doi.org/10.1016/j.jid.2017.05.004
Song, X., Zhang, Y., Zhang, L., Song, W., Shi, L., 2018. Hypoxia enhances indoleamine 2,3-dioxygenase production in dendritic cells. Oncotarget 9, 11572–11580. https://doi.org/10.18632/oncotarget.24098
Sorgdrager, F.J.H., Naude, P.J.W., Kema, I.P., Nollen, E.A., Deyn, P.P., 2019. Tryptophan Metabolism in Inflammaging: From Biomarker to Therapeutic Target. Front Immunol 10, 2565. https://doi.org/10.3389/fimmu.2019.02565
Strbo, N., Yin, N., Stojadinovic, O., 2014. Innate and Adaptive Immune Responses in Wound Epithelialization. Adv Wound Care (New Rochelle) 3, 492–501. https://doi.org/10.1089/WOUND.2012.0435
Sun, Q., Li, J., Gao, F., 2014. New insights into insulin: The anti-inflammatory effect and its clinical relevance. World Journal of Diabetes 5, 89. https://doi.org/10.4239/WJD.V5.I2.89
Takeo, M., Lee, W., Ito, M., 2015. Wound Healing and Skin Regeneration. Cold Spring Harbor Perspectives in Medicine 5, a023267–a023267. https://doi.org/10.1101/cshperspect.a023267
Terness, P., Bauer, T.M., RöSe, L., Dufter, C., Watzlik, A., Simon, H., Opelz, G., 2002. Inhibition of Allogeneic T Cell Proliferation by Indoleamine 2,3-Dioxygenase–expressing Dendritic Cells. Journal of Experimental Medicine 196, 447–457. https://doi.org/10.1084/jem.20020052
Tsalamandris, S., Antonopoulos, A.S., Oikonomou, E., Papamikroulis, G.-A., Vogiatzi, G., Papaioannou, S., Deftereos, S., Tousoulis, D., 2019. The Role of Inflammation in Diabetes: Current Concepts and Future Perspectives. European Cardiology Review 14, 50–59. https://doi.org/10.15420/ecr.2018.33.1
Velnar, T., Bailey, T., Smrkolj, V., 2009. The wound healing process: an overview of the cellular and molecular mechanisms. J Int Med Res 37, 1528–1542. https://doi.org/10.1177/147323000903700531
Walton, B.L., Byrnes, J.R., Wolberg, A.S., 2015. Fibrinogen, red blood cells, and factor XIII in venous thrombosis. J Thromb Haemost 13 Suppl 1, S208-15. https://doi.org/10.1111/jth.12918
Watkins, J., 2013. Skin rashes, part 1: Skin structure and taking a dermatological history. undefined 24, 30–33. https://doi.org/10.12968/PNUR.2013.24.1.30
Wu, Y., Ding, Y., Tanaka, Y., Zhang, W., 2014. Risk Factors Contributing to Type 2 Diabetes and Recent Advances in the Treatment and Prevention. Int. J. Med. Sci 11, 1185–1200. https://doi.org/10.7150/ijms.10001
Wu, Y., Wang, M., Zhu, Y., Lin, S., 2016. Serum interleukin-6 in the diagnosis of bacterial infection in cirrhotic patients A meta-analysis. https://doi.org/10.1097/MD.0000000000005127
Xu, K.P., Li, Y., Ljubimov, A. v, Yu, F.S.X., 2009. High Glucose Suppresses Epidermal Growth Factor Receptor/Phosphatidylinositol 3-Kinase/Akt Signaling Pathway and Attenuates Corneal Epithelial Wound Healing. Diabetes 58, 1077–1085. https://doi.org/10.2337/db08-0997
Xue, M., Jackson, C.J., 2015. Extracellular Matrix Reorganization During Wound Healing and Its Impact on Abnormal Scarring. Advances in Wound Care 4, 119–136. https://doi.org/10.1089/WOUND.2013.0485/ASSET/IMAGES/LARGE/FIGURE4.JPEG

Ye, Z., Yue, L., Shi, J., Shao, M., Wu, T., 2019. Role of IDO and TDO in cancers and related diseases and the therapeutic implications. J Cancer 10, 2771–2782. https://doi.org/10.7150/JCA.31727

Young, A., McNaught, C.-E., 2011. The physiology of wound healing. Surgery (Oxford) 29, 475–479. https://doi.org/https://doi.org/10.1016/j.mpsur.2011.06.011

Yousef, H., Alhajj, M., Sharma, S., 2020. Anatomy, Skin (Integument), Epidermis, in: StatPearls. Treasure Island (FL).

Yu, E., Papandreou, C., Ruiz-Canela, M., Guasch-Ferre, M., Clish, C.B., Dennis, C., Liang, L., Corella, D., Fitó, M., Razquin, C., Lapetra, J., Estruch, R., Ros, E., Cofán, M., Arós, F., Toledo, E., Serra-Majem, L., Sorlí, J. v, Hu, F.B., Martinez-Gonzalez, M.A., Salas-Salvado, J., 2018. Association of Tryptophan Metabolites with Incident Type 2 Diabetes in the PREDIMED Trial: A Case–Cohort Study. Clinical Chemistry 64, 1211–1220. https://doi.org/10.1373/clinchem.2018.288720

Zhang, Z., Cui, T., Cui, M., Kong, X., 2020. High prevalence of chronic kidney disease among patients with diabetic foot: A cross-sectional study at a tertiary hospital in China. Nephrology 25, 150–155. https://doi.org/10.1111/nep.13596

Zhao, R., Liang, H., Clarke, E., Jackson, C., Xue, M., 2016. Inflammation in Chronic Wounds. International Journal of Molecular Sciences 17, 2085. https://doi.org/10.3390/ijms17122085

Zhu, J., Luo, L., Tian, L., Yin, S., Ma, X., Cheng, S., Tang, W., Yu, J., Ma, W., Zhou, X., Fan, X., Yang, X., Yan, J., Xu, X., Lv, C., Liang, H., 2018. Aryl Hydrocarbon Receptor Promotes IL-10 Expression in Inflammatory Macrophages Through Src-STAT3 Signaling Pathway. Front Immunol 9, 2033. https://doi.org/10.3389/fimmu.2018.02033

Websites and Programmes

Genomatix Software Suite - Scientific Analysis of genomic data, 2022. Genomatix.de. URL https://www.genomatix.de/solutions/genomatix-software-suite.html (accessed 7. 22. 21).

NICE [WWW Document], 2022. NICE. URL https://www.nice.org.uk/ (accessed 1. 21. 20).

Rasband, W.S., ImageJ, U. S. National Institutes of Health, Bethesda, Maryland, USA, https://imagej.nih.gov/ij/, 1997-2018.

STRING: functional protein association networks, 2022. String-db.org. URL https://string-db.org/cgi/input?sessionId=bfbiiApToEu8&input_page_show_search=on (accessed 6. 22. 22).

Thermo Fisher Scientific - UK 2022. Thermofisher.com. URL https://www.thermofisher.com/order/catalog/product/S0125> (accessed 7. 20. 22).

Appendix 1 – Genomatix maps (Genomatix.de, 2022).

a. TDO2 Network

Key:

- - - - - -	2 genes are associated by experimental validation.
——▷	Gene A activates Gene B.
——⊣	Gene A inhibits Gene B.
——◇	Gene A regulates Gene B.
——	2 genes are associated by expert-curation.

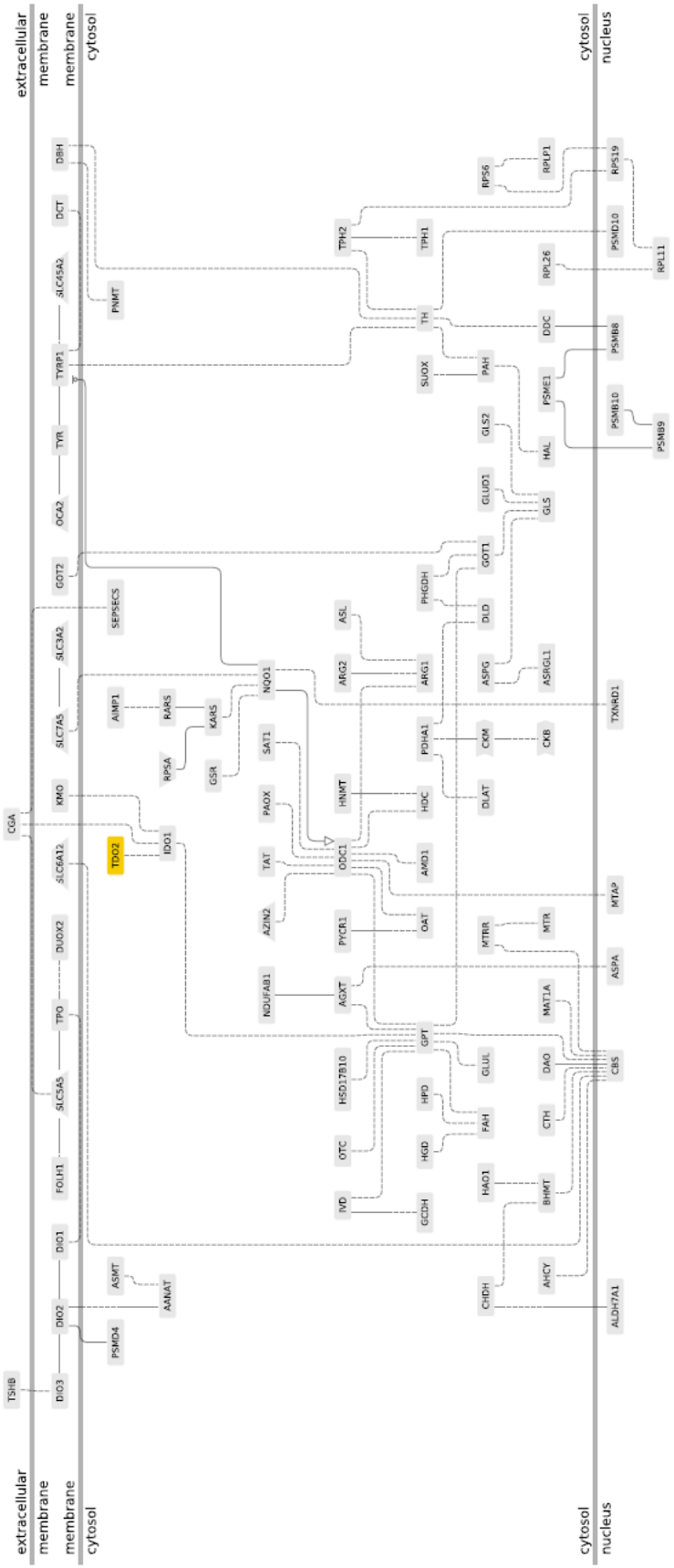

b. Cytokine signalling in Immune system

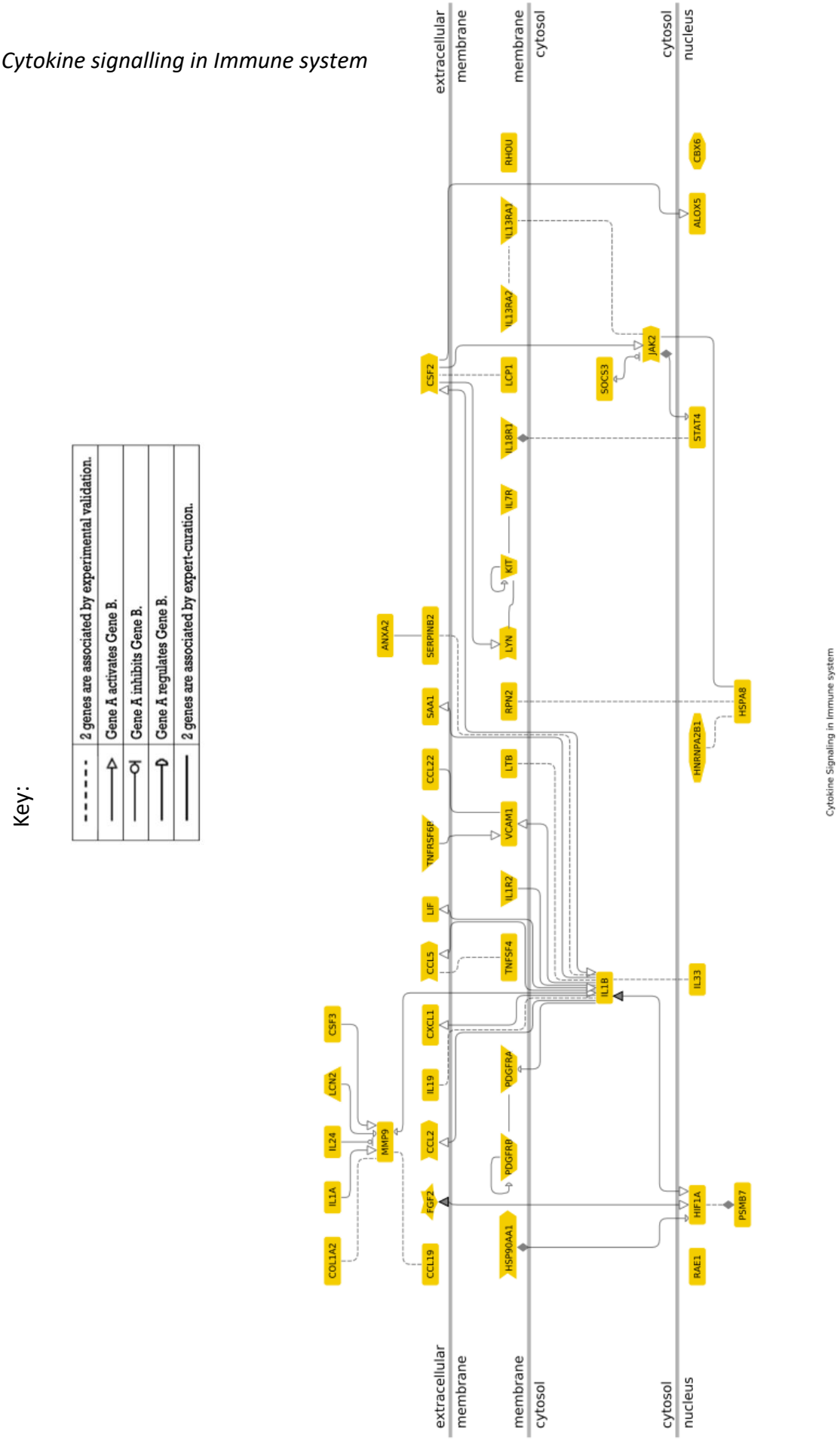

c. Inflammatory network

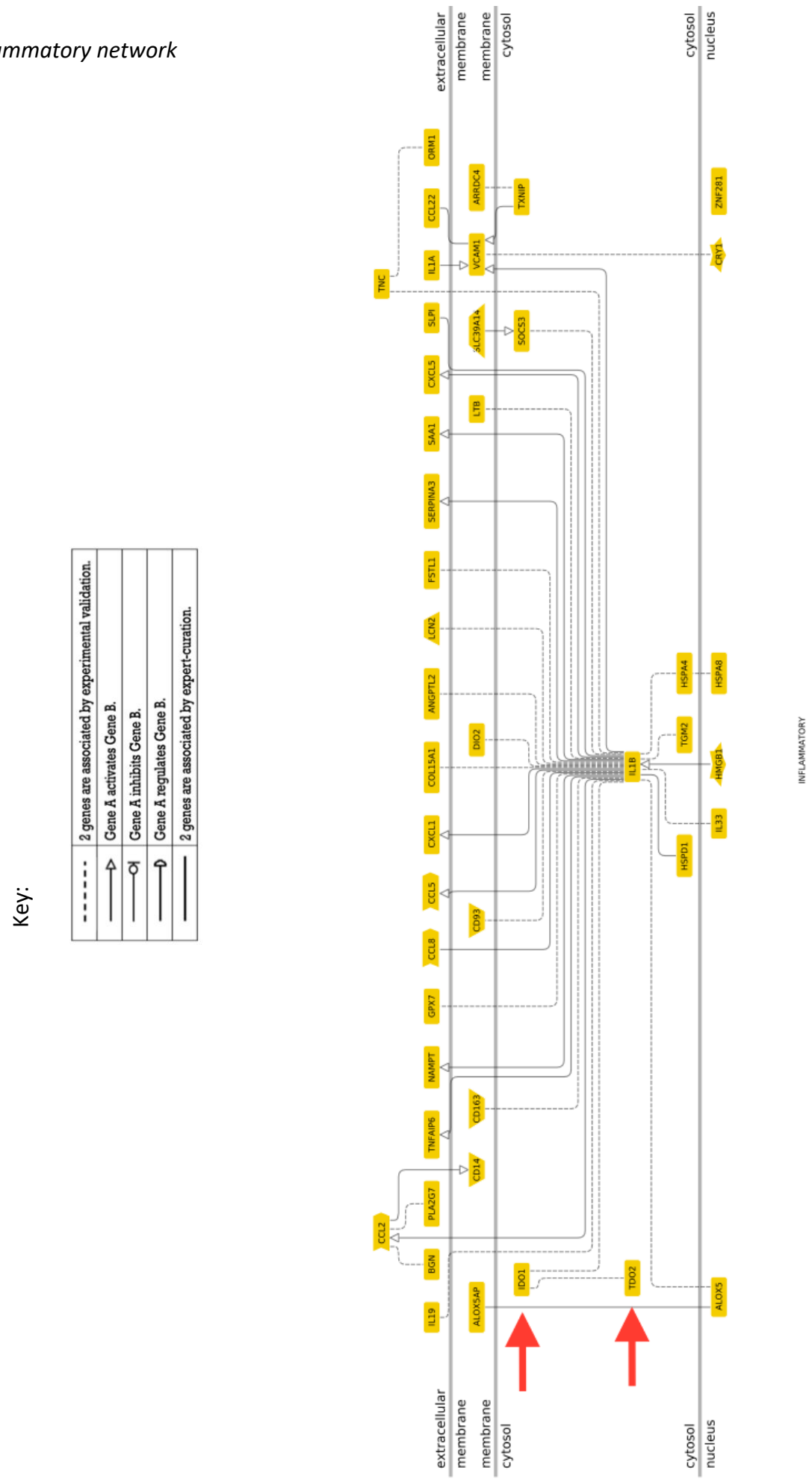

Appendix 2 – Donor and Experiment Information

a. Donor ages

Donor Code	Age
SPL003	69
SPL004	50
SPL005	69
SPL009	N/A
SPL010	48
SPL011	N/A
SPL029	N/A
SPL030	51
SPL032	N/A
SPL035	N/A

b. Chapter 3 experiments summary

Figure reference	Gene(s)	Donor	Time point	Treatment	Method
3-4	TDO2	SPL003, SPL004	Day 1, Day 5	IL-1/OSM	qRT-PCR
3-5	IDO1	SPL003, SPL004	Day1, Day 5	IL-1/OSM	qRT-PCR
3-6	AhR, IL-10, SOCS3, SLC7A7, STAT3	SPL030	Day 1, Day 5	IL-1/OSM	qRT-PCR
3-7	AhR, IL-10, SOCS3, SLC7A7, STAT3	SPL030	Day 5	High Glucose	qRT-PCR
3-8	TDO2	SPL004, SPL005	Day 1, Day 5	LPS	qRT-PCR
3-9	IDO1	SPL004, SPL005	Day 1, Day 5	LPS	qRT-PCR
3-10	IDO1	SPL004	Day 5	IL-1/OSM	IHC
3-11	TDO2	SPL004	T0	None	IHC
3-12	TDO2	SPL004	Day 5	IL-1/OSM	IHC

Appendix 3 – Timelapse videos of cell culture scratch wound healing experiments.

a. Scratch Wound Healing Assay EXPT 1
https://youtu.be/TUANyJ89hn8

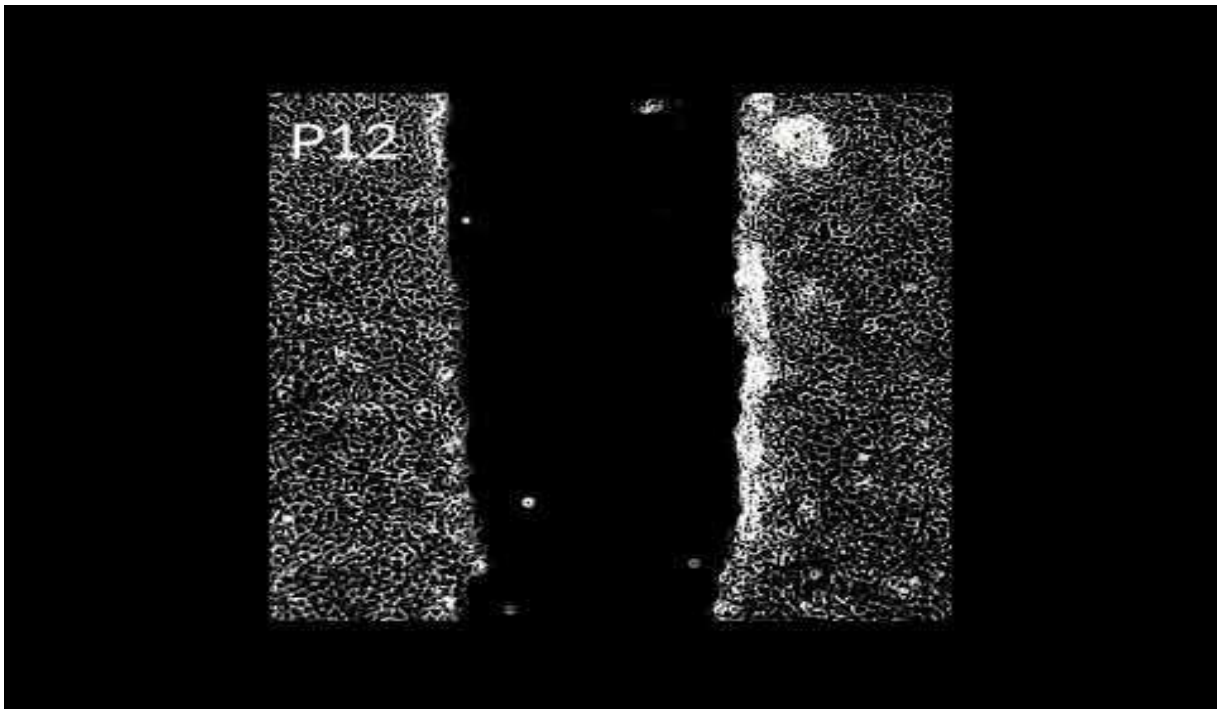

b. Scratch Wound Healing Assay EXPT 4
https://youtu.be/0JFVeOFoH8I